**US Army Corps
of Engineers**
Los Angeles District

COAST OF CALIFORNIA
STORM AND TIDAL WAVES STUDY

FOURIER GRAIN-SHAPE AND MINERALOGIC ANALYSIS OF COASTAL AND INNER SHELF SAND SAMPLES: DANA POINT TO THE UNITED STATES-MEXICO BORDER

CCSTWS 90-1
OCTOBER 1989

FOURIER GRAIN-SHAPE AND MINERALOGIC ANALYSES OF COASTAL AND INNER SHELF SAND SAMPLES: DANA POINT TO THE UNITED STATES-MEXICO BORDER

Coast of California Storm and Tidal Wave Study

Final Geologic Report

May 1989

prepared by

Robert H. Osborne, Kelly S. Ahlschwede, Sean D. Broadhead, Kyung H. Cho, Eleanor A. Compton and Chia-Chen Yeh

Sedimentary Petrology Laboratory
Department of Geological Sciences
University of Southern California
Los Angeles, CA 90089-0740

SUMMARY

The identification of local sand sources and the volumetric contribution of each during a given time interval is essential to our understanding of coastal processes and the computation of meaningful sediment budgets for the littoral zone. Fourier grain-shape analysis (FGSA) of fluvial, sea cliff, beach and inner shelf samples was performed to identify and quantify the local sand sources for littoral sediment within the coastal reach extending from Dana Point to the United States-Mexico Border.

Three major segments have been identified within this coastal region since the 1960's; namely, the Oceanside, Mission Beach and Silver Strand Littoral Cells. The Oceanside Cell may be informally divided into five segments. These are, from north to south, the Capistrano subcell (Dana Point to San Mateo Point), the San Onofre subcell (San Mateo Point to the North Jetty at Oceanside Harbor), the Oceanside-Carlsbad subcell (Oceanside Harbor to the onshore projection of Carlsbad Submarine Canyon), the Encinitas subcell (from Carlsbad Submarine Canyon to La Jolla Submarine Canyon), and the La Jolla Cove Subcell (La Jolla Submarine Canyon to Point La Jolla). These subcells are based on the physiography of the coast and adjacent continental shelf, which, in turn, affects the distribution of sediment and energy inpinging along the coast.

In addition to the identification and quantification of fluvial, sea cliff and longshore sand sources for each cell or subcell, FGSA indicated that an average of 35 percent of the medium-grained sand in the foreshore samples was derived from inner shelf sources. The mechanisms responsible and pathway for transporting shelf sand to the foreshore are not known at this time, but it seems likely that storm activity perhaps coupled with transport through ridge and runnel systems may be involved.

Although FGSA identified important shape-compositional differences between and among littoral subdivisions, the shape composition within each cell or subcell is rather uniform. This relationship may reflect sediment mixing as a result of seasonally-related, bidirectional longshore and perhaps onshore transport during a relatively recent but undefined time interval.

Mineralogic data from river, cliff and upcoast and downcoast littoral sources were useful in defining petrofacies (mineral assemblages) within each cell or subcell. The observed petrofacies changes often are associated with river mouths. These petrofacies data served to help define cell and subcell boundaries as well as net longshore transport directions.

The boundaries between the Oceanside, Mission Beach and Silver Strand Littoral Cells are known to be effective barriers to littoral sand transport. Fourier grain-shape and mineralogic data for 1986 beach sample sets indicate some sand exchange between the Capistrano and San Onofre subcells, and considerable exchange between the Oceanside-Carlsbad and Encinitas subcells. Except for beach nourishment projects, Oceanside Harbor is a littoral sediment sink, therefore little sand is exchanged naturally between the San Onofre and Oceanside-Carlsbad subcells. Sampling in the La Jolla Cove subcell was inadequate to examine the littoral exchange between the Encinitas and La Jolla Cove subcells.

CONTENTS

vi

vii

PLATES

1. INTRODUCTION

1.01   The principal purpose of this report is to determine the local sediment sources of beach sand samples from the Oceanside, Mission Beach and Silver Strand littoral cells (Figure 1). The Oceanside Littoral Cell is divided into five subcells, which are, from north to south: (1) the Capistrano Subcell (from Dana Point to San Mateo Point), (2) the San Onofre Subcell (from San Mateo Point to the north breakwater at Oceanside Harbor), (3) the Oceanside-Carlsbad Subcell (from the south jetty at Oceanside Harbor to Carlsbad Submarine Canyon), (4) the Encinitas Subcell (from Carlsbad Submarine Canyon to La Jolla Submarine Canyon), and (5) the La Jolla Cove Subcell (from La Jolla Submarine Canyon to Point La Jolla). Fourier shape analysis of medium-grained sand was used to estimate the percent each potential local source has contributed to a given set of beach samples. The results obtained from the Fourier grain-shape and associated mineralogic analyses comprise important input for future sediment budget and littoral transport studies.

Purpose and Scope

1.02   The purpose of the Coast of California Storm and Tidal Waves Study is to collect, reduce and interpret oceanographic, meteorologic, hydrologic, geologic and sedimentologic information. Task 6 includes the collection, analysis and interpretation of sedimentologic data from the littoral zone. Results of Task 1D will be integrated with Task 9, River Sediment Discharge Study Task 8, River Sediments, and Task 7, Bluff Sediment Study to locate ultimate and local source areas and to determine the volumetric contribution of each potential source area to each beach segment.

Authority

1.03   This storm and tidal wave study is being undertaken pursuant to Section 208 of the Flood Control Act of 1965, Public Law 89-298.

Report Preparation

1.04   This report was prepared by personnel of the Sedimentary Petrology Laboratory at the University of Southern California. The contract was administered by Noble Consultants, Inc., Irvine, California.

1.05   The study was initially funded by the House Appropriation Committee in its Report No. 97-177, 97th Congress, 1st Session (page 23). The Corps of Engineers has been directed to concentrate on the Dana Point to Mexican border segment of the study (House Report No. 97-177, page 23).

1.06   The following are related reports prepared by the Los Angeles District which contain significant data on littoral zone sediments in the study area.
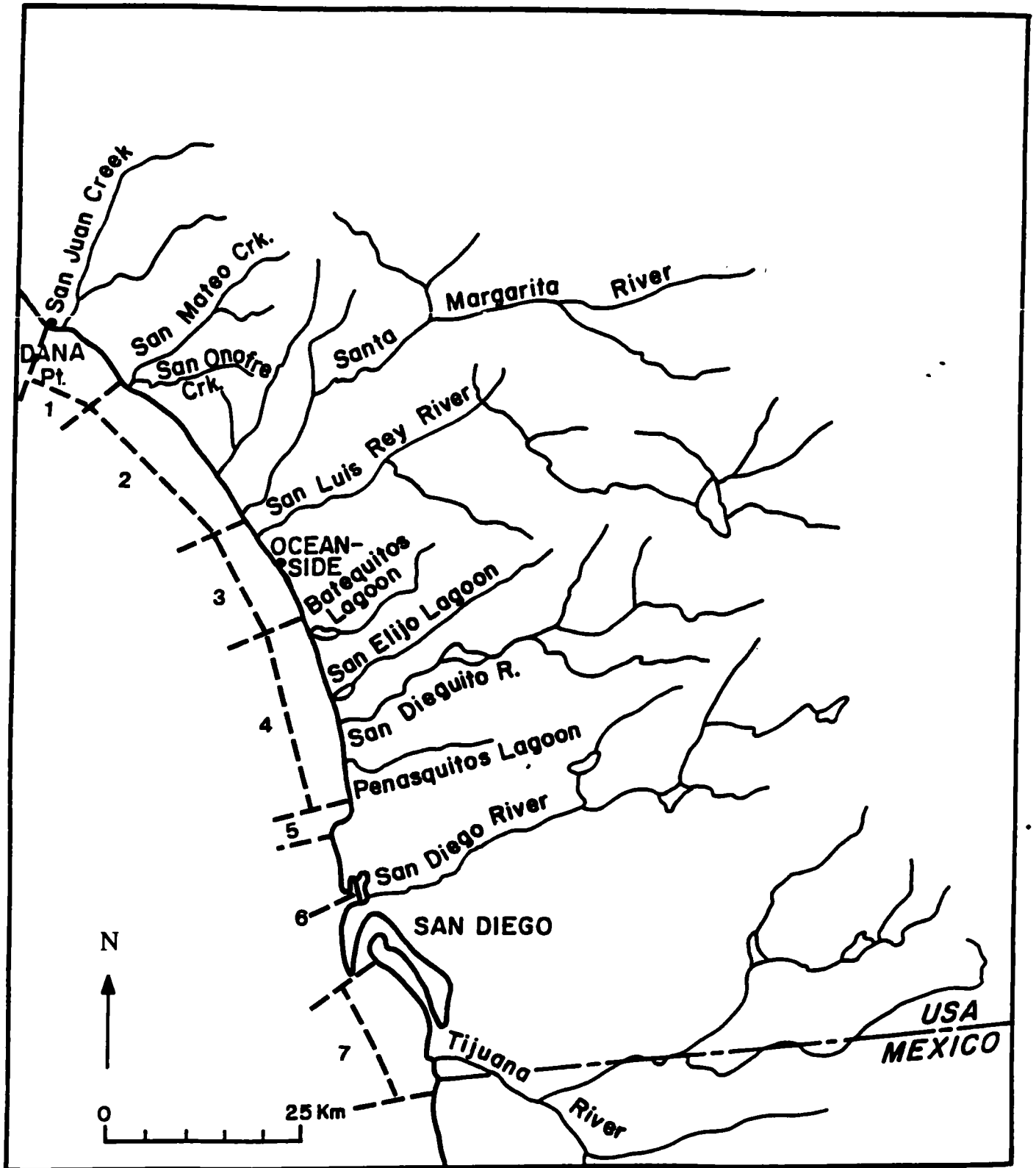
Figure 1. Location map showing the Oceanside, Mission Beach and Silver Strand Littoral Cells as well as the five divisions of the Oceanside Cell. Subdivisions 1 through 5 are assigned to the Oceanside Littoral Cell: 1=Capistrano subcell, 2=San Onofre subcell, 3=Oceanside-Carlsbad subcell, 4=Encinitas subcell and 5=La Jolla Cove subcell. Subdivision 6 is the Mission Beach Littoral Cell and 7 is the Silver Strand Littoral Cell.

Title	Date
Beach Erosion Control Report on Cooperative Study of Orange County, California. Appendix V, Phase 1.	June, 1959
Beach Erosion Control Report on Cooperative Study of San Diego County, California, Appendix IV, Phase 2.	March, 1960
Beach Erosion Control Report Cooperative Research and Data Collection Program of Southern California, Cape San Martin to Mexican Boundary. Three Year Report 1964-1966. Three Year Report, 1967-1969 Cooperative Research and Data Collection Program, Coast of California.	March, 1969

December, 1970 |
Geomorphic Framework Report, Dana Point to the Mexican Border, Coast of California Storm and Tidal Waves Study.	September, 1984
Sediment Sampling, Dana Point to the Mexican Border (Task 1D, Nov-83 to Jan-84) CCSTWS 84-5.	November, 1984
Littoral Zone Sediments, San Diego Region, October 1983-June 1984. CCSTWS 85-11.	December, 1985
Coastal Cliff Sediments, 1947 to present, San Diego Region, CCSTWS 87-2.	June, 1987
Coastal Cliff Sediment, 1887 to 1947, San Diego Region	December, 1988
Analysis of Beach and Nearshore Vibracore Samples, Oceanside, California OESBP 89-1.	January, 1989

Methods

1.07   Inasmuch as the description of the procedures used for the Fourier grain-shape and mineralogic analyses are lengthy, these discussions are presented under appropriate sectional headings later in this report. It should be noted here that the coastal subdivisions specified in the Scope of Work were defined after the sampling design had been formulated. Therefore the number of samples varies considerably between and among cells and subcells (an unbalanced experimental design). However, except for the La Jolla Cove subcell, there is a sufficient number of samples and adequate sample spacing to define the sand sources.

2. LITTORAL CELLS

2.01   Emery (1960) and Inman and Chamberlain (1960) identified a series of littoral cells along the southern California coast (Figure 1). These cells are based on the concept of longshore transport of dominantly fluvially-derived sediment, which is entrapped either by submarine canyon heads or by points of land which extend seaward from the general position of the coastline. Three major coastal divisions are present in the area from Dana Point southward to the United States-Mexico border. The Oceanside Littoral Cell extends from Dana Point to Point La Jolla. The second division is the lowland in the Pacific and Mission Beach area, which occurs on the former delta of the San Diego River. Alluvium from the San Diego River extends almost to Crystal Pier at Pacific Beach, where it changes to a natural barrier (spit) extending across most of Mission Bay. The jetties constructed at the mouth of Mission Bay have interrupted the transport of sand from Mission Beach to Ocean Beach (Kuhn and Shepard, 1984), therefore Ocean Beach may be treated as a pocket beach. In fact, the Mission Beach Littoral Cell as a whole may be considered a large pocket beach. The coastal reach from the entrance to San Diego Bay to the United States-Mexico border comprises the Silver Strand Littoral Cell.

2.02   The Scope of Work for this study specified that the Oceanside Littoral Cell be divided into five subcells (Figure 1). These are: the Capistrano Subcell (Dana Point to San Mateo Point), the San Onofre Subcell (San Mateo Point to the North Jetty at Oceanside Harbor), the Oceanside-Carlsbad Subcell (Oceanside Harbor to the onshore projection of Carlsbad Submarine Canyon), the Encinitas Subcell (from the onshore projection of Carlsbad Submarine Canyon to La Jolla Submarine Canyon), and the La Jolla Cove Subcell (La Jolla Submarine Canyon to Point La Jolla). These subcells are based on the observed physiography of the coast and adjacent continental shelf which affects the distribution of sediment and energy impinging along the coast. This should, in turn, affect the rate and net direction of longshore and cross shelf sand transport.

2.03   Although wave statistics and associated nearshore current measurements are most useful in documenting relatively short-term longshore transport directions, net transport direction and magnitude over significantly longer periods (tens to perhaps hundreds of years) may be approached using geomorphologic and sedimentologic data. Inasmuch as comparatively small sediment volumes may produce observable longshore transport features such as spits and fillets, considerable effort must be expended to quantitatively evaluate the magnitude of longshore vectoral components with respect to associated shore-normal vectoral components by means of slope array SXY gauges, beach profiles, and studies of sediment sources and transport paths. Furthermore, the role of recent, large storms in the dispersal of sediment between the littoral zone and innermost continental shelf requires considerable attention.

2.04   Assuming temperate drought conditions, which are temporally dominant in historic records for southern California (Inman, 1981), winter waves generally have a net energy flux component to the south due to their generation by northern Pacific storms passing close to southern California, whereas summer waves often show a net energy flux to the north due to their generation from more distant storms, either southwest of Acapulco or from Antarctica. As such, longshore sand transport is commonly bidirectional in the short term. From a longer-term perspective, net longshore transport appears to be south for the Oceanside Littoral Cell as a whole and the Mission Bay area, and north for the Silver Strand Littoral Cell.

4

3. FOURIER GRAIN-SHAPE ANALYSIS OF BEACH SAMPLES

Introduction

3.01   Since its introduction by Ehrlich and Weinberg in 1970, Fourier analysis of quartz grain shapes has been applied to a wide variety of natural tracer and petrofacies problems. The interested reader is referred to the following papers: Brown and others (1980), Ehrlich and others (1974), Ehrlich and Chin (1980), Ehrlich and others (1980), Hudson and Ehrlich (1980), Mazzullo and Ehrlich (1980, 1983), Mrakovitch and others (1976), Riester and others (1982), Van Nieuwenhuise and others (1978), and Young (1980). Fourier grain-shape studies completed in California include Ehrlich and others (1974), Porter and others (1979), Bloom (1979), Clark and Osborne (1982), Gaynor (1984), Osborne and others (1985), Bomer (1985), Ahlschwede (1988), Broadhead (1988), and Cho (1989).

3.02   Ehrlich and Weinberg (1970) describe a closed-form Fourier method to analyze the observed variation of two-dimensional, maximum-projection, grain-shape area. Grain shape may be estimated by an expansion of the periphery radius as a function of angle about the grain's center of gravity by a Fourier series. In Fourier analysis, a series of sine and cosine curves with periods equal to fundamental harmonics are fit to the observed data by a least squares technique. Fundamental harmonics are the prime fractions (1/2, 1/3, 1/4,....1/N), where N equals half the number of digitized points used to define the periphery of a grain. As the number of fundamental harmonics is increased, the computed curve converges with the observed data. The highest frequency that can be estimated is the Nyquist frequency which is equal to twice the distance between successive observations. If the Nyquist frequency is exceeded, error may be introduced by the incorporation of irresolvable high frequencies into lower frequencies (aliasing). The radius is given by:

$$R(\theta) = Ro + \sum_{n=1}^{\infty} Rn \cos (n\theta - \emptyset n)$$

where θ is the polar angle measured from an arbitrary reference line. The first term in the series Ro is equivalent to the average radius of the grain in the maximum projection orientation. For the remainder of the terms, n is the harmonic order, Rn is the harmonic amplitude, and $\emptyset n$ is the phase angle. The phase angle appears to provide little additional grain-shape information, and therefore is not considered further. It is important to note that the n'th harmonic contributes to the explanation of the observed shape variation as a figure with n "bumps." For example, the "zeroth" harmonic is a centered circle with an area equal to that of the maximum projection; the first harmonic is an off-centered circle; the second is a figure eight; the third is a trefoil; etc. The center of gravity of the maximum projection shape is used as the origin of the radius expansion to simplify interpretation of the Fourier series. Coordinates of points along the periphery of the maximum projection outline are required for the Fourier expansion. At least twice the number of such points must be known as the number of the highest desired harmonic. The initial origin of the periphery points may be arbitrary, because a later transformation places the origin at the center of gravity of the maximum grain-projection area. If a harmonic or periodic function exists within the data, the amplitude of the sine and cosine curves with periods close to the natural harmonic will be considerably larger than the amplitudes of other harmonics in the sequence.

5

3.03 Although conceptually similar to the closed-form methodology described by Ehrlich and Weinberg (1970), the methodology. The methodology employed in this report makes use of the newer and more widely used Fast Fourier Transform (FFT). This procedure involves the calculation of many values of the line spectrum using the FFT computer algorithm to produce a smoothed estimate of the continuous spectrum. The FFT algorithm, as its name implies, is extremely rapid and requires only $n \cdot \log_2 n$ arithmetic operations rather than the n^2 operations as do alternative methods. The reader is referred to Brigham (1974), Bloomfield (1976), and Bendat and Piersol (1971) for extensive treatments of the mathematically complex FFT.

Sample Collection

3.04 This study is based on the Fourier grain-shape analysis of 110 sand samples and the mineralogical analysis of 66 samples. Table 1 summarizes the types of analyses performed and the sand sources considered by littoral cell or subcell. The locations of the samples used are plotted on Plates 1 through 6. The sample locations expressed by range line and the date each sample was collected are listed in Appendix I.

Table 1. Summary of sample analyses by source and by littoral cell/subcell.

Cell/Subcell	Fourier Grain-shape Analysis						Mineralogical Analysis				
	River	Cliff	Shelf	Beach April (Wtr.)	Oct. (Sum.)	Total	River	Cliff	Beach April (Wtr.)	Oct. (Sum.)	Total
1-5. Oceanside											
1. Capistrano	1		3	3		7	1		3	3	7
2. San Onofre	4	8	9	6	4	31	4	11	6	6	27
3. Oceanside-Carlsbad	1		7	2	11	21	1		1	2	4
4. Encinitas	3	7	8	7	13	38	3	5	5	5	18
5. La Jolla Cove			3		1	4					
6. Mission Beach	1		1	2		4	1		2	2	5
7. Silver Strand	1	1	1	3		6	1		2	2	5
				Grand Total	111				Grand Total	66	

3.05 All of the river and virtually all of the cliff samples were collected by Kelly Ahlschwede and Ann Compton during April and June 1986, respectively. The river samples represent bedload sediment, and each was collected approximately two kilometers upstream of the river mouth to avoid the effects of tidal currents on grain size and mineral composition. The exact geographic and stratigraphic positions of nearly all of the sea cliff samples are given in Kuhn and others (1987). Sean Broadhead (1988) collected three

6

additional sea cliff samples to augment the initial set. Sample LJ-460 was collected from the basal Scripps Formation approximately 150 m north of Scripps Institution of Oceanography. Samples TP-467 and TP-480 were collected from recent cliff talus at the base of slope. Sample TP-467 was collected in May 1986 at the base of the Black's Beach landslide, which is below stratigraphic section TP2B of Kuhn and others (1987). This sample contains sediment largely if not wholly derived from the Scripps Formation. Sample TP-480 also was collected in May 1986 at the base of stratigraphic section TP 3A (Kuhn and others, 1987). This sample largely represents sand contribution from the Torrey Sandstone Formation. Sample SS-02 was collected by Anthony Price in February 1989 to estimate the cliff contribution in the Silver Strand Cell.

Beach samples were collected mostly by Kelly Ahlschwede and Ann Compton during April (end-of-winter) and October (end-of-summer) 1986. The beach samples were collected at MLLW at locations approximately one kilometer north and south of each major river mouth. These samples were collected by inserting a tin can approximately 15 centimeters normal to the shoreface to obtain small channel-samples. Sean Broadhead collected an additional set of seven beach samples mostly during November 1986. These are: TP-495 (May 1986), TP-492.5, TP-472, TP-467.8, TP-465.5, TP-464 and LJ-462. Beach samples CB-810 and CB-765 were collected by Anthony Price in February 1989 to provide upcoast transport information for the Encinitas subcell and downcoast information for the Oceanside-Carlsbad subcell, respectively.

3.06   Samples from 19 vibracores (Table 2) were used in this study to provide information concerning the contribution of inner shelf sand sources to the beach (onshore transport). These vibracores were collected by Ocean Inc. on board the RV Diamond Lady during January and February 1981. This work was completed under contract to the U.S. Army Coastal Engineering Research Center. Core descriptions, grain-size and petrographic modal analyses were performed by the Sedimentary Petrology Laboratory at the University of Southern California. The results of these analyses are discussed in Osborne and others (1983), Darigo (1984), and Darigo and Osborne (1986). Samples DB-1800, SC-1658, SO-1610, SO-1575, SO-1535, SO-1480 and PN-1322 were collected north of Oceanside Harbor in February 1989 at a water depth of -30 feet MLLW. As such, these samples may be considered either lowermost foreshore or innermost shelf.

Table 2.   The length of nineteen vibracores used in this study and the water depth from which each was recovered.

Core Designation (This study/CERC)	Recovered Length (cm)	Water Depth (ft)
PN-1123 (1721)	186	52
PN-1105 (1852)	208	55
PN-1090 (1675)	200	67
PN-1077 (2120)	168	37
OS-1073 (1656)	290	55
OS- 993 (1970)	93	45
OS- 985 (1884)	270	50
OS- 920 (1979.6)	221	52
OS- 915 (1891)	300	55
OB- 864 (1986)	92	41
CB- 860 (2053)	250	55
SD- 650 (1410)	129	67

TP- 519.5 (1369)	201	43
TP- 492 (1363)	293	45
TP- 464.5 (1259.6)	183	40
LJ- 454 (1267)	198	62
LJ- 443 (1275)	237	70
PB- 394 (1060)	151	89
SS- 205 (118)	190	42

Sample Preparation

3.07   Quartz grains from the 0.25-0.50 mm (1.0-2.0 phi) or medium sand fraction from each sample were used for the Fourier grain-shape analysis. Samples were first wet-sieved to obtain the desired size fraction to minimize attrition of the quartz grains during sieving. Sieving was followed by drying in convection ovens. After drying was completed, all strongly magnetic minerals were removed from the samples using a hand magnet. The samples were boiled in a solution of 10% hydrochloric acid with stannous chloride crystals for 20 minutes to remove iron-oxide coatings and carbonate cement (Carver, 1971). The hydrochloric acid residue was removed by rinsing the samples in de-ionized water. The quartz grains were etched clean by washing them in a hydrofluoric acid bath for one minute. Such etching does not significantly alter the shape of the grains (Schultz, 1980). All samples were then rinsed in de-ionized water and dried thoroughly.

3.08   Samples were examined under a petrographic microscope using a reflecting light source. Quartz grains were picked by using a very small brush. These grains were dry mounted on a glass slide, which enhances the contrast between the grain and its background (Ehrlich and Weinberg, 1970). Adequate contrast is essential in the operation of the Fourier grain-shape digitizing program.

Fourier Methodology

3.09   Digitizing of the individual quartz grains was accomplished using a Digital Graphics CAT-100 optical digitizer and the EDGE Fortran program written by Tim Fogarty (1985). In this process, a black and white camera projects the maximum two-dimensional image of the quartz grain from a standard binocular petrographic microscope to a video screen. The image of the grain appears dark in relation to the surrounding background since the microscope is lighted from below. A maximum contrast between grain edge and background allows the computer to scan the pixels of the video image and record all boundary points of the grain as Cartesian coordinates (X-Y coordinates). A pixel is determined as a boundary point if it is dark and one of its neighbors is light. While the Cartesian coordinates are computed, the centroid of the projected grain also is computed. The data is stored on floppy disk and transferred from the microcomputer to a Digital Equipment corporation VAX-11/750 computer.

3.10   The next step in the digitizing process is to prepare the data for the Fourier transform. The Cartesian coordinates are converted to polar coordinates (radius versus angle). The radius is the distance from a boundary point to the centroid; the angle used is the angle from the horizontal line bisecting the centroid to the boundary point. In order to examine the entire wavenumber amplitude spectrum (each wavenumber is analogous to one harmonic) of a grain during statistical analysis, the Fast Fourier Transform (Brigham,

8

1974) is used. One requirement of the Fast Fourier Transform is that the data be evenly-spaced. Since the boundary points of a grain are not evenly spaced, the data must be linearly interpolated. The boundary points are interpolated to 128 evenly-spaced points. The Fast Fourier Transform also requires that the data set be centered around zero. To center the data, the mean radius is subtracted from the radius versus angle data. This radius is later placed in the final amplitude spectrum set.

3.11   Upon completion of the Fast Fourier Transform, the amplitude of each wavenumber is calculated by the equation:

$$SQRT(Real**2 + Imaginary**2)$$

where SQRT = square root, Real = real number, Imaginary = imaginary number, and **2 = square of the number (Brigham, 1974). This computation allows the amplitude spectrum of an individual grain to be compared to the amplitude spectrum of other grains. This comparison is the first step in the analysis process and directs the path the statistical analyses will follow. Since the input data is real rather than imaginary, half of the wavenumbers are reflections, and are not used in the statistical analyses. This leaves 64 wavenumbers for analysis. Each wavenumber is represented by a vector and the occurrence of 64 wavenumbers results in the analysis of 64 dimensions in space.

3.12   Each sample contains approximately 215 digitized quartz grains. For ease in initial calculations, the characteristic, or average, grain was computed for each sample. To do this, all the vectors of a sample were summed and averaged. The average amplitude spectrum of each sample then is used for statistical analyses (Appendix 2).

Discriminant Function Analysis

3.13   Discriminant function analysis (DFA) is employed as the most appropriate multivariate statistical procedure to estimate the percentage of each beach sample derived from cliff, river and inner shelf sand sources within each littoral cell or subcell as well as longshore contributions from beaches upcoast and downcoast of the boundaries of each cell or subcell. DFA is one of the most powerful statistical procedures available to assign or partition samples into previously-defined populations. In the present study, interest is focused on assigning each of the 215 digitized grains in each beach sample to one of the sand sources identified for a given littoral cell or subcell.

3.14   Mathematically, DFA consists of computing a transform which gives the minimum ratio of the difference between or among a set of multivariate means to the multivariate dispersion (variance) of the set of previously-defined groups. For example, if one considers only two groups as consisting of two clusters of points in multivariate space, DFA computes the equation of the one orientation along which the two clusters have the greatest spatial separation while simultaneously each cluster has the least dispersion (variance). In this manner, the spatial separation of the two clusters is maximized, and, therefore, most distinct. Once the transform is computed, new samples easily may be classified into one of these two groups. Davis (1986, p. 478-502) provides a most readable summary of the mathematics associated with DFA.

9

3.15   In the present study, the International Mathematical Subroutine Library DFA subroutine was used to compute the required transform for the harmonic amplitude values of samples assigned to each sand source within a given littoral cell or subcell. Thus the multivariate spatial separation among the sand sources within each cell or subcell was maximized, while minimizing the dispersion for each source. Once the discriminatory equations were computed, the harmonic amplitude values for each of the 215 grains per beach sample within that cell or subcell were analyzed, and each grain was assigned to one of the defined sources. The number of grains in each beach sample assigned to a given source within that cell or subcell was computed and expressed as a percentage.

3.16   When DFA is used to initially assign the percentages of grains in a beach sample to a given source, the assignment assumes that each potential source is 100 percent unique with respect to grain shape. In reality, each potential source is a mixture of grain-shape components, therefore the initial assignment must be recast to reflect the unique grain-shape components characteristic of that source.

3.17   For example, beach sample TP-465.5-B-N may be considered as having been derived from cliff sample TP-500-C and river sample DM-590-R. DFA initially indicates that TP-465.5-B contains 42 percent cliff-derived grains and 58 percent river-derived grains. DFA may be used to compare the grain-shape composition of each potential sand source with that of each other source. In this case, it was determined that cliff sample TP-500-C contains 52 percent unique cliff-shaped grains and 48 percent river-shaped grains. River sample DM-590-R contains 12 percent cliff-shaped grains and 88 percent river-shaped grains. The initial percentage assignments of beach sample TP-465.5-B-N may be recast to more accurate source assignments by the simple multiplication of percentages.

3.18   The calculated percentage of TP-500-C grains equals the percentage of TP-465.5-B-N's TP-500-C-like grains times the percentage of TP-500-C's TP-500-C-like grains plus the percentage of TP-465.5-B-N's DM-590-R-like grains times the percentage of DM-590-R's TP-500-C-like grains. In short, (42% x 52%) + (58% X 12%) = 29 percent of beach sample TP-465.5-B-N may be considered as cliff-derived grains. The calculation for the percentage of river-derived grains is similar: namely, (58% X 88%) + (42% X 48%) = 71 percent. Thus the recast percentages for each source in this example indicate that beach sample TP-465.5-B-N contains approximately 29 percent of cliff-derived grains (TP-500-C) and 71 percent river-derived grains (DM-590-R). This procedure may be generalized to any number of potential sand sources in each littoral cell or subcell.

Results and Discussion

Oceanside Littoral Cell: Capistrano Subcell
(Dana Point to San Mateo Point)

3.19   The results of Fourier grain-shape analysis for the three end-of-winter beach samples examined in the Capistrano subcell are listed in Table 3 and illustrated in Figure 2. The sediment sources considered are San Juan Creek, northern shelf, southern shelf, San Mateo Creek and downcoast beach (San Onofre subcell). These results indicate a very high degree of compositional consistency with regard to grain shape within this subcell. The values from 26 to 31 percent indicating the volumetric contribution from San Mateo Creek show the greatest difference (5 percent); however, this difference is only marginally

10

1. Oceanside Cell: Capistrano Subcell (Dana Point to San Mateo Creek)

	SAN JUAN CREEK	NORTHERN SHELF	SOUTHERN SHELF	SAN MATEO CREEK	DOWNCOAST BEACH
DB-1895-B-A	12	8	13	26	41
DB-1815-B-A	12	7	11	31	39
SO-1605-B-A	13	8	12	28	39

River Sample: DB-1865-R, San Juan Creek
Northern Shelf Sample: DB-1800-S, Offshore of Dana Point Harbor
Southern Shelf Samples: SC-1658-S, SO-1610-S, Offshore of San Clemente
Downcoast River Sample: SO-1595-R, San Mateo Creek
Downcoast Beach Sample: SO-1580-B-A

Table 3.   Results of Fourier grain-shape analysis for end-of-winter samples from the San Onofre subcell.

1. OCEANSIDE CELL: CAPISTRANO SUBCELL
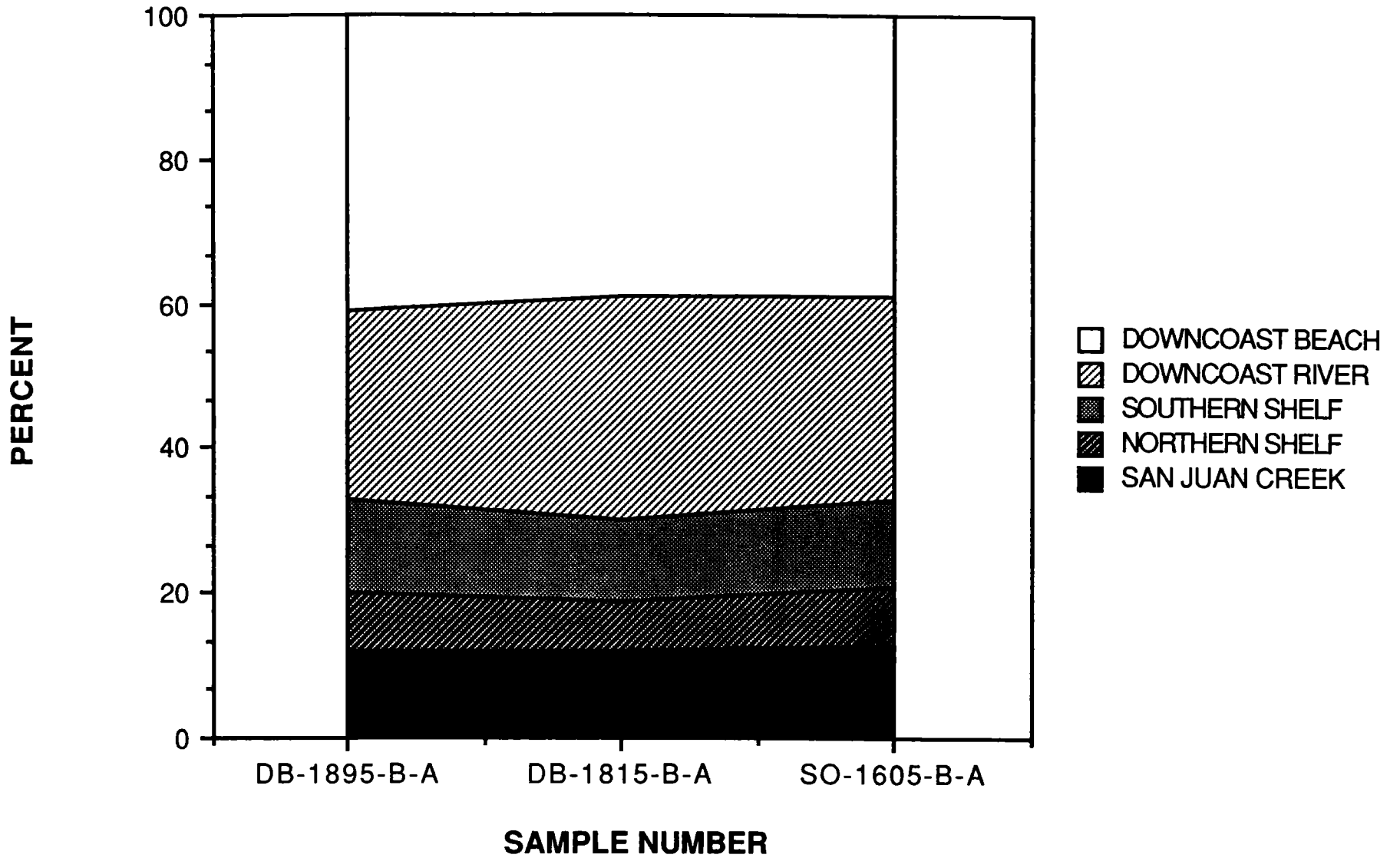
Figure 2. Grain-shape characteristics of end-of-winter beach samples from the Capistrano subcell.

significant. The one to two percent differences observed for the four other local sand sources are statistically insignificant.

3.20 The average sand contributions from the five local sources supplying the Capistrano subcell are as follows:

- San Juan Creek 12%;

- northern shelf 8%;

- southern shelf 12%;

- San Mateo Creek 28%; and

- downcoast beach (San Onofre subcell) 40%.

3.21 These results indicate three major sedimentologic relationships. First, the compositional homogeneity within this subcell suggests thorough mixing of the sand at each sample site derived from each of the five local sources. Such thorough mixing probably results from cross shore and bidirectional longshore transport within the Capistrano subcell during a relatively recent period of time. The exact time interval is not known.

3.22 The second major relationship is the compositional dominance of sand derived from the downcoast portions of the subcell. The observed dominance of sand from the downcoast portions of this subcell reflects the net effect of incremental, relatively long term sand accumulation. Any bedload discharge from San Juan Creek (Simon and others, 1988) has been greatly diluted by and thoroughly mixed with sand from downcoast sand sources, which suggests either (1) little sand has been derived from San Juan Creek during the residence time represented by the beach samples analyzed or (2) a tremendous volume of downcoast sand was transported northward during this time interval. The lack of a delta at the mouth of San Juan Creek and the fact that Dana Point Harbor requires little maintenance dredging suggest that little sand has been contributed from San Juan Creek in the recent past. Therefore, it is more likely that the sand derived from the downcoast portions of the subcell has been added incrementally. The dominance of sand from the downcoast portions of this subcell coupled with probable net longshore transport to the south (Tekmarine, Inc., 1987) argues for a relatively small bedload contribution from San Juan Creek.

3.23 The third major relationship is the occurrence of approximately twenty percent inner-shelf sediment in the beach samples. It is clear that some net onshore transport is occurring at both the northern and southern parts of this subcell. It is interesting to note that the average sand contribution from the southern shelf (12%) is greater than that of the northern shelf (8%), which supports the concept of a downcoast source for most of the sand in the Capistrano subcell.

13

<u>End-of-Winter (April 1986) Beach Samples</u>

3.24   The grain-shape composition for the six end-of-winter beach samples from the San Onofre subcell displays more grain-shape variation than observed in the Capistrano subcell (Table 4 and Figure 3).   The average sand contributions from the six local sources supplying the San Onofre subcell are as follows:

- upcoast beach (Capistrano subcell) 8%;

- San Mateo Creek 12%;

- northern shelf 5%;

- cliff 13%;

- Santa Margarita River 27%; and

- southern shelf 35%.

3.25   The range of values for the upcoast beaches (4%), northern shelf (5%) and cliff (2%) contributions are insignificant to marginal for the number of beach samples examined, therefore little genetic significance can be assigned to the observed longshore variations for these sand sources.   However, interesting longshore trends do occur for the contributions from San Mateo Creek, Santa Margarita River and the southern shelf.

3.26   The sand contribution from San Mateo Creek averages 16 percent for stations SO-1850 and SO-1530. This decrease to the south may represent either downcoast transport or dilution of San Mateo River sand by upcoast sand transport from the Santa Margarita River or southern shelf. Table 4 and Figure 3 indicate that approximately 62 percent of the beach sand in the San Onofre subcell is derived from the Santa Margarita River (27%) and southern shelf (35%). Ignoring the prominent peak at station PN-1300 for the moment, the contribution of Santa Margarita River sand decreases from approximately 32 percent south of PN-1300 to 11 percent north of PN-1300, which implies net upcoast transport. The peak of Santa Margarita River-like sand at PN-1300 is intriguing, and may represent bedload contribution from Las Flores Creek or, more likely, a pulse of sand discharged from the Santa Margarita River itself. Although speculative, the likelihood of the Santa Margarita River as opposed to Las Flores Creek as being the source for the sand in this peak is greater because of much higher average annual bedload discharge rates for the Santa Margarita River (Simon and others, 1988). Simon and others (1988) estimate the average annual sand and gravel yield for the Santa Margarita River as 25,500 tons as compared with 3,610 tons for Las Flores Creek. There is no record of substantive discharge from the Santa Margarita River during the winter of 1985-86, therefore the observed peak must be the result of an earlier discharge event. The last major discharge of the Santa Margarita River was in November-December 1984. During this period, 7.21 inches of rain fell at Lindberg Field, and this was recorded as the third wettest November and December in 134 years (Gerald Kuhn, personnel communication, 1989). Consequently, the observed peak must be at least 1.25 years old. Although the sand contribution from San Mateo Creek obviously was transported downcoast, the observed

14

2. Oceanside Cell (End-of-Winter): San Onofre Subcell (San Mateo Creek to North Jetty at Oceanside Harbor)

	UPCOAST BEACH	SAN MATEO CREEK	NORTHERN SHELF	CLIFF	SANTA MARGARITA RIVER	SOUTHERN SHELF
SO-1580-B-A	9	15	7	13	13	43
SO-1530-B-A	10	17	6	12	9	46
PN-1300-B-A	6	8	4	12	45	25
PN-1270-B-A	8	10	6	13	25	38
PN-1170-B-A	8	11	2	13	34	32
PN-1115-B-A	7	10	4	14	37	28

Upcoast Beach Sample: SO-1605-B-O
Northern River Samples: SO-1595-R, SO-1565-R, San Mateo Creek
Northern Shelf Samples: SO-1575-S, SO-1535-S, PN-1480-S, PN-1322-S, Offshore of San Mateo Creek
Cliff Samples: PN-1380-C, PN-1460-C, PN-1410-C, PN-1355-C, PN-1320-C, PN-1283-C
PN-1275-C, PN1220-C, San Onofre and Camp Pendleton Areas
Southern River Samples: PN-1150-R, PN-1285-R, Santa Margarita River
Southern Shelf Samples: PN-1123-S, PN-1105-S, PN-1090-S, PN-1077-S, Offshore of Oceanside

Table 4. Results of Fourier grain-shape analysis for end-of-winter samples from the San Onofre subcell.

15

2. OCEANSIDE CELL (END-OF-WINTER): SAN ONOFRE SUBCELL
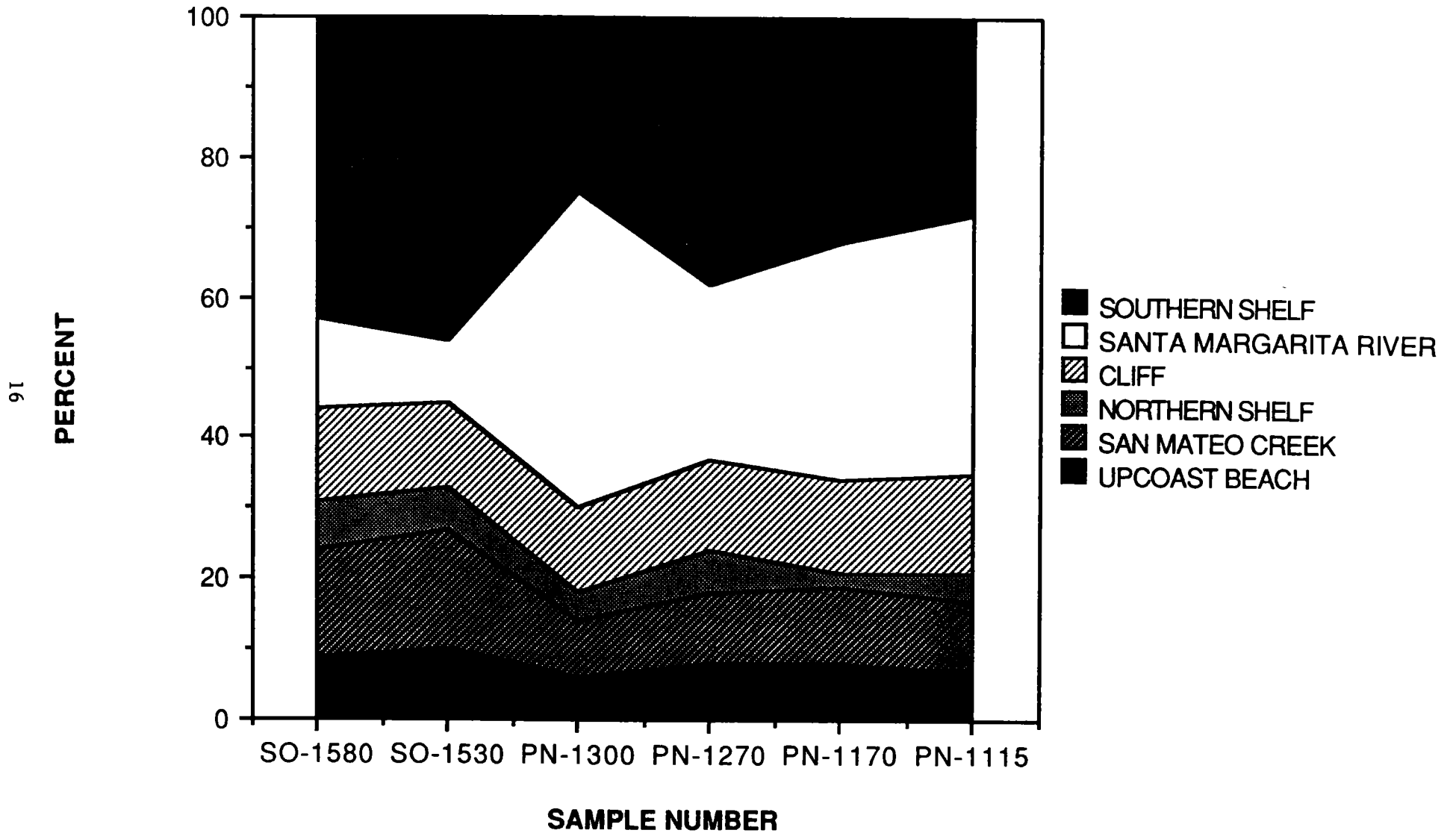
Figure 3. Grain-shape characteristics of end-of-winter beach samples
from the San Onofre subcell.

decrease in the amount of San Mateo River sand to the south may represent dilution by Santa Margarita River and southern shelf sand rather than distance from the San Mateo River. The percentage of San Mateo River sand in the San Onofre subcell may be rather constant, and the observed decrease south of SO-1530 may reflect dilution by Santa Margarita sand transported upcoast.

3.27　The contribution of southern shelf sand (35%) argues for considerable onshore as well as upcoast sand transport. Disregarding the effect of the peak of Santa Margarita River-like sand at PN-1300, the amount of southern shelf sand increases from approximately 33 percent south of PN-1300 to 44 percent north of this station. Inasmuch as the shape characteristics of the southern shelf sand is distinct from that of the northern shelf, this substantive upcoast increase must reflect a relatively long-term accumulation of incremental amounts of southern shelf sand. This, in turn, implies a rather continuous supply of shelf sand to the southern beaches and net upcoast transport.

3.28　Although a more temporally-controlled experiment is desirable, it appears that rather thorough sediment mixing has produced a relatively consistent grain shape composition for the San Onofre subcell with respect to the upcoast beach (Capistrano subcell), San Mateo Creek, northern shelf and cliff sources. Southern shelf sand apparently is being added rather continuously through onshore and upcoast transport. The principal source of variation observed in this sample set appears to be sand input from the Santa Margarita River, which apparently is delivering sand to the upcoast beaches in an episodic manner, presumably related to high-discharge events.

End-of-Summer (October 1986) Beach Samples

3.29　The grain-shape composition for the four end-of-summer beach samples from the San Onofre subcell is shown in Table 5 and Figure 4. The average sand contributions from the six local sources considered are as follows:

- upcoast beach (Capistrano subcell) 8%;

- San Mateo Creek 11%;

- northern shelf 3%;

- cliff 14%;

- Santa Margarita River 33%; and

- southern shelf 32%.

3.30　The compositional variation for upcoast beach (Capistrano subcell) (2%), San Mateo River (5%), northern shelf (2%) and cliff (2%) is insufficient with respect to the number of beach samples analyzed to assign any genetic significance to the observed longshore trends. As for the end-of-winter sample set, the greatest range of observed values is associated with the Santa Margarita River (24%) and the southern shelf (13%) sources.

17

2. Oceanside Cell (End-of-Summer): San Onofre Subcell (San Mateo Creek to North Jetty at Oceanside Harbor)

	UPCOAST BEACH	SAN MATEO CREEK	NORTHERN SHELF	CLIFF	SANTA MARGARITA RIVER	SOUTHERN SHELF
PN-1300-B-O	8	12	3	14	27	36
PN-1270-B-O	8	13	4	14	25	36
PN-1170-B-O	6	8	2	12	49	23
PN-1115-B-O	8	11	3	14	30	34

Upcoast Beach Sample: SO-1605-B-O
Northern River Samples: SO-1595-R, SO-1565-R, San Mateo Creek
Northern Shelf Samples: SO-1575-S, SO-1535-S, PN-1480-S, PN-1322-S, Offshore of San Mateo Creek
Cliff Samples: PN-1380-C, PN-1460-C, PN-1410-C, PN-1355-C, PN-1320-C, PN-1283-C
    PN-1275-C, PN1220-C, San Onofre and Camp Pendleton Areas
Southern River Samples: PN-1150-R, PN-1285-R, Santa Margarita River
Southern Shelf Samples: PN-1123-S, PN-1105-S, PN-1090-S, PN-1077-S, Offshore of Oceanside

Table 5. Results of Fourier grain-shape analysis for end-of-summer samples from the San Onofre subcell.

2. OCEANSIDE CELL (END-OF-SUMMER): SAN ONOFRE SUBCELL
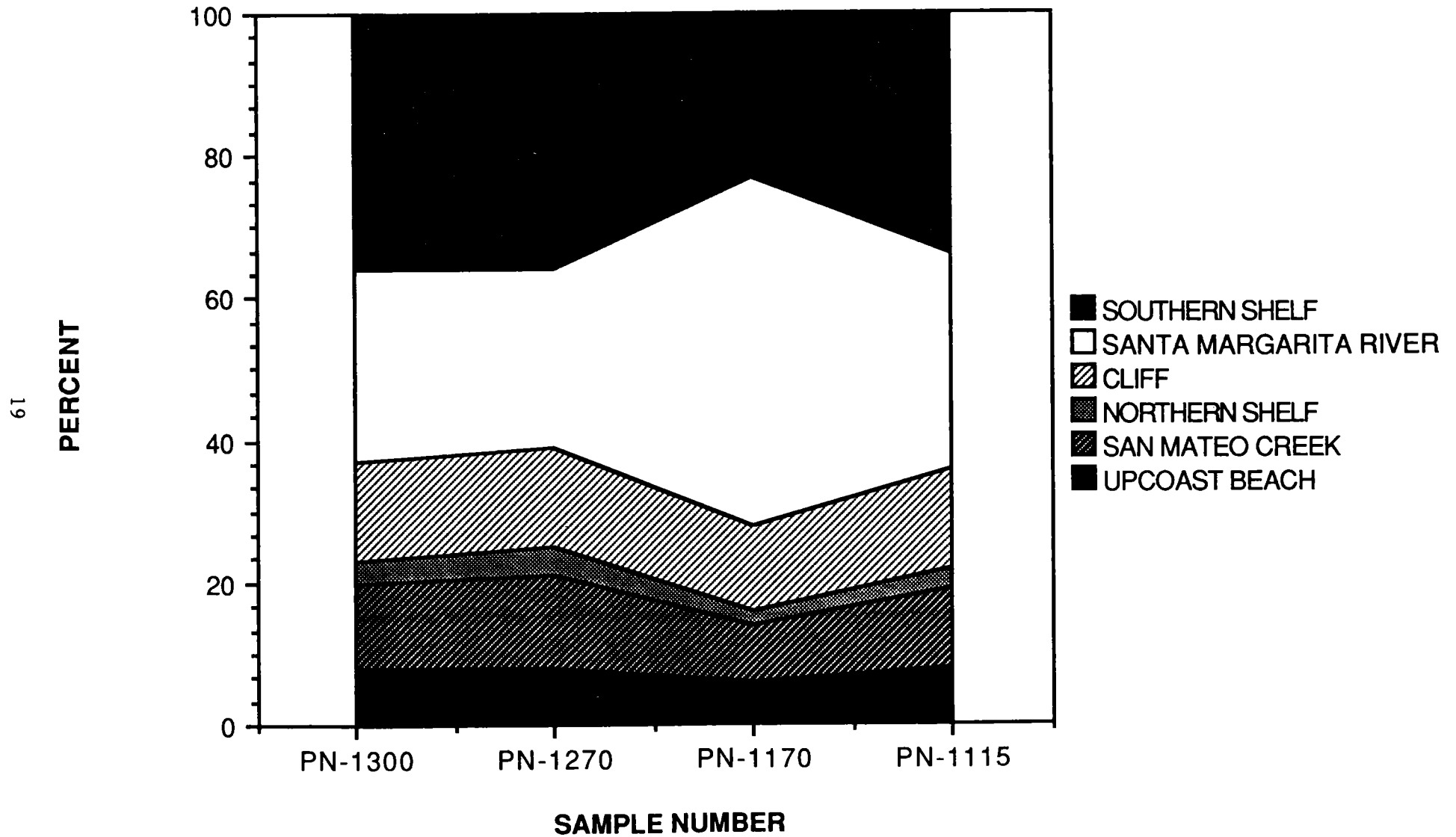
Figure 4. Grain-shape characteristics of end-of-summer beach samples from the San Onofre subcell.

3.31   There is an average increase of approximately 6 percent in Santa Margarita grain shapes in the San Onofre subcell from April to October 1986. This clearly demonstrates net upcoast transport during this six-month interval. It appears that the end-of-winter peak at station PN-1300 migrated upcoast and was homogenized into a more uniform percentage of Santa Margarita sand, and the end-of-summer peak at station 1170 represents a distinct discharge event. Inasmuch as there is no evidence for a high discharge event from April to October 1986, the exact age of this event is not known. It is important to note, however, that Fourier grain-shape analysis has the resolution to identify and trace such pulses of beach sand following a known high-discharge event.

3.32   There is an average reduction of 3 percent southern shelf sand in the San Onofre subcell from April to October 1986. For the end-of-summer sample set, the southern shelf contribution ranges from 34 to 36 percent, except at station PN-1170, where it apparently is diluted to 23 percent by the addition of Santa Margarita sand.

3.33   Overall, the grain-shape composition of the San Onofre subcell remained much the same from April to October 1986. The only significant change is the upcoast transport of Santa Margarita River sand, which altered the grain-shape composition of associated beach samples.

Transition between Capistrano and San Onofre Subcells

3.34   The southernmost beach sample of the Capistrano subcell (SO-1605-B-A) contains 39 percent of the grain shape associated with the northernmost beach sample from the San Onofre subcell (SO-1580-B-A). Likewise, sample SO-1580-B-A contains 9 percent of the grain shape associated with the upcoast beach sample SO-1605-B-A. Therefore it is clear that leakage of littoral sand does occur between the Capistrano and San Onofre subcells.

Oceanside Littoral Cell: Oceanside-Carlsbad Subcell
(South Jetty at Oceanside Harbor to the Onshore Projection of Carlsbad Submarine Canyon)

3.35   The results of Fourier grain-shape analysis for the three beach samples from the Oceanside-Carlsbad subcell are shown in Table 6 and Figure 5. The average sand contributions from the five local sources supplying this subcell are:

- upcoast beach (San Onofre subcell) 11%;

- northern shelf 28%;

- San Luis Rey River 6%;

- southern shelf 9%; and

- downcoast beach (Encinitas subcell) 46%.

20

3. Oceanside Cell: Oceanside-Carlsbad Subcell (Oceanside Harbor to Onshore Projection of Carlsbad Submarine Canyon)

	UPCOAST BEACH	NORTHERN SHELF	SAN LUIS REY RIVER	SOUTHERN SHELF	DOWNCOAST BEACH
OS-1030-B-O	12	25	7	8	48
OS-1030-B-A	10	32	6	11	41
CB-810-B-F	11	27	5	8	49

Upcoast Beach Sample: PN-1115-B-O
Northern Shelf Samples: OS-1073-S, OS-915-S, Offshore of Oceanside
River Sample: OS-1050-R, San Luis Rey River
Southern Shelf Samples: OS-985-S, OS-993-S, OS-920-S, OS-915,-S, CB-864-S,
                         CB-860-S, Offshore of Carlsbad
Downcoast Beach Sample: CB-765-B-F

Table 6.   Results of Fourier grain-shape analysis for samples from the Oceanside-Carlsbad
           subcell.

3. OCEANSIDE CELL: OCEANSIDE-CARLSBAD SUBCELL
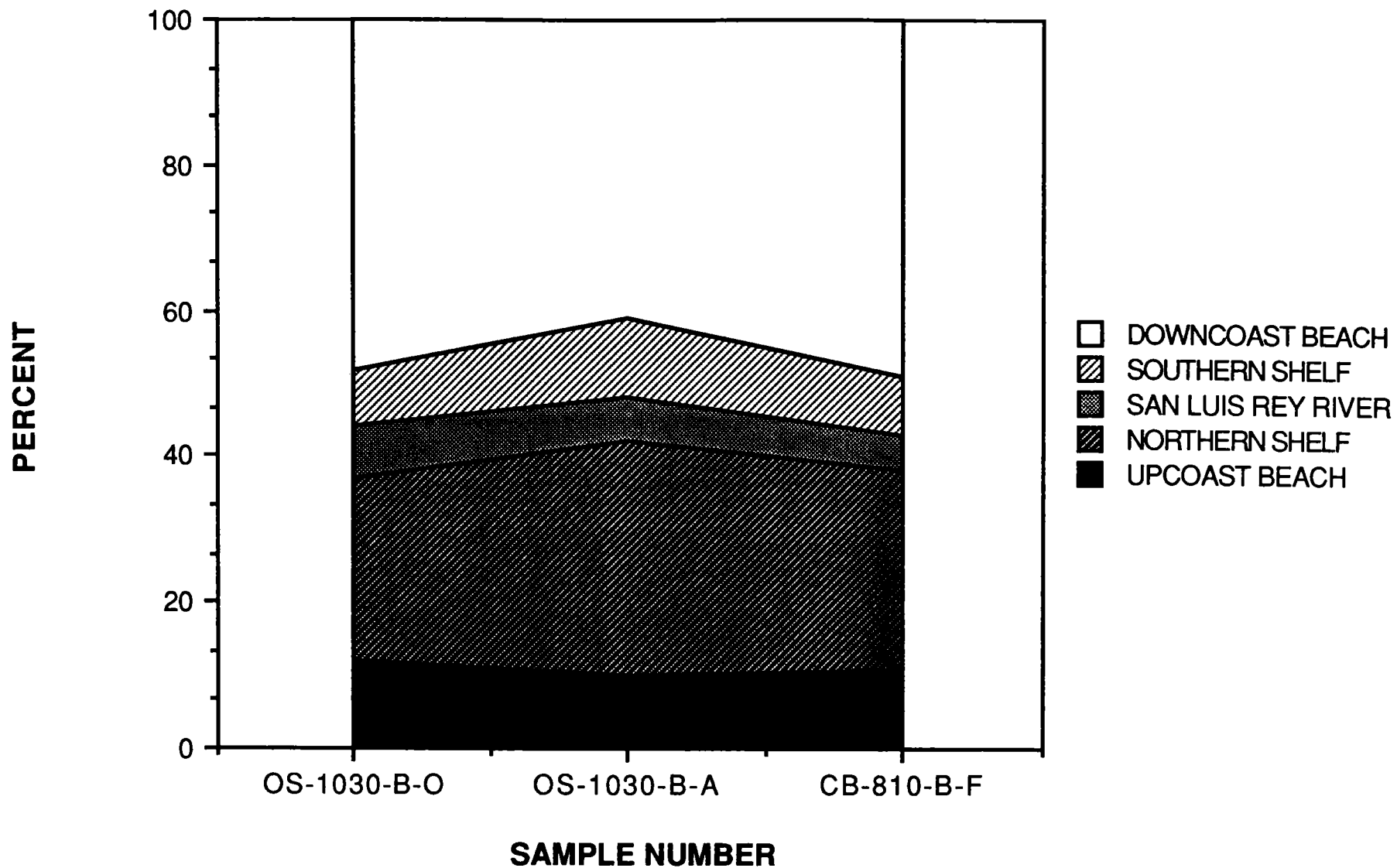
Figure 5. Grain-shape characteristics of beach samples from the Oceanside-Carlsbad subcell.

3.36   The range of variation for the upcoast beach contribution (San Onofre subcell) (2%), San Luis Rey River (2%) and southern shelf (3%) are statistically insignificant; however, the variation for the northern shelf (7%) and downcoast beach (Encinitas subcell) (8%) contributions appear to be significant in both a seasonal and a longer-term sense. Interestingly enough, the variation observed between the set of 1985 beach samples (OS-1030-B-A and OS-1030-B-O) and the February 1989 beach sample (CB-810-B-F) appears to be on the same order of magnitude as the seasonal variation between the end-of-winter and end-of-summer beach samples for 1986. Although the sample size for this subcell is small, it appears that the beach sand samples display a high degree of compositional homogeneity.

3.37   The most interesting aspects of the grain-shape composition of the beach samples in this sample set are the apparent compositional homogeneity, and the dominance of sand shapes derived from the northern shelf (28%) and the downcoast beach (46%). One might expect a substantive contribution from the San Luis Rey River (Simon and others, 1988); however, bedload discharge from the San Luis Rey River may have been greatly reduced by the Pacific Street crossing. In any case, it is clear that any such contribution has been greatly diluted by sand from other local sources. Inasmuch as the last major rainfall occurred in November-December 1984, any bedload contribution from the San Luis Rey River was greatly diluted during the following 1.25 or more years. The dominance of sand shapes characteristic of the northern shelf and downcoast beaches indicates the importance of onshore and upcoast longshore transport, respectively. The compositional homogeneity reflects rather thorough mixing during an unknown time interval.

Transition between the San Onofre and Oceanside-Carlsbad Subcells

3.38   Except for beach nourishment projects, the northern breakwater and south jetty at Oceanside Harbor are fairly effective barriers to longshore sand transport, and Oceanside Harbor itself is a sediment sink. Consequently, there is little reason to expect substantive volumes of sand to be exchanged between the San Onofre and Oceanside-Carlsbad subcells.

Oceanside Littoral Cell: Encinitas Subcell

(Onshore Projection of Carlsbad Submarine Canyon to La Jolla Submarine Canyon)

End-of-Winter (April 1986) Beach Samples

3.39   Table 7 and Figure 6 show the results of Fourier grain-shape analysis for the six end-of-winter samples from the Encinitas subcell. The average sand contribution from each source is as follows:

- upcoast beach (Oceanside-Carlsbad subcell) 41%;

- San Dieguito River 5%;

- northern shelf 22%;

- cliff 12%;

- downcoast beach (La Jolla Cove subcell) 8%; and

23

4. Oceanside Cell (End-of-Winter): Encinitas Subcell (Onshore Projection of Carlsbad Submarine Canyon to La Jolla Submarine Canyon)

	UPCOAST BEACH	SAN DIEQUITO RIVER	NORTHERN SHELF	CLIFF	SOUTHERN SHELF	DOWNCOAST BEACH
CB-765-B-F	45	6	23	13	10	3
SD-645-B-A	42	5	21	14	11	7
SD-625-B-A	39	5	22	12	11	11
DM-595-B-A	39	5	24	11	12	9
TP-545-B-A	43	5	20	13	9	10
TP-520-B-A	40	5	25	12	11	7

Upcoast Beach Sample: CB-810-B-F
River Samples: DM-590-R, SD-635-R, TP-530-R, San Diequito River
Northern Shelf Samples: TP-519.5-S, SD-650-S, Offshore of Encinitas
Cliff Samples: TP-500-C, TP-466-C, TP-465-C, TP-463.6-C, TP-463-C, Torrey Pines Area
Southern Shelf Samples: LJ-454-S, TP-492-S, TP-464.5-S, Offshore of La Jolla
Downcoast Beach Sample: LJ-427-B-O

Table 7. Results of Fourier grain-shape analysis for end-of-winter samples from the Encinitas subcell.

4. OCEANSIDE CLEE (END-OF-WINTER): ENCINITAS SUBCELL

Legend:
- DOWNCOAST BEACH
- SOUTHERN SHELF
- CLIFF
- NORTHERN SHELF
- SAN DIEQUITO RIVER
- UPCOAST BEACH

Axis labels: PERCENT (y-axis, 0 to 100), SAMPLE NUMBER (x-axis: CB-765, SD-645, SD-625, DM-595, TP-545, TP-520)
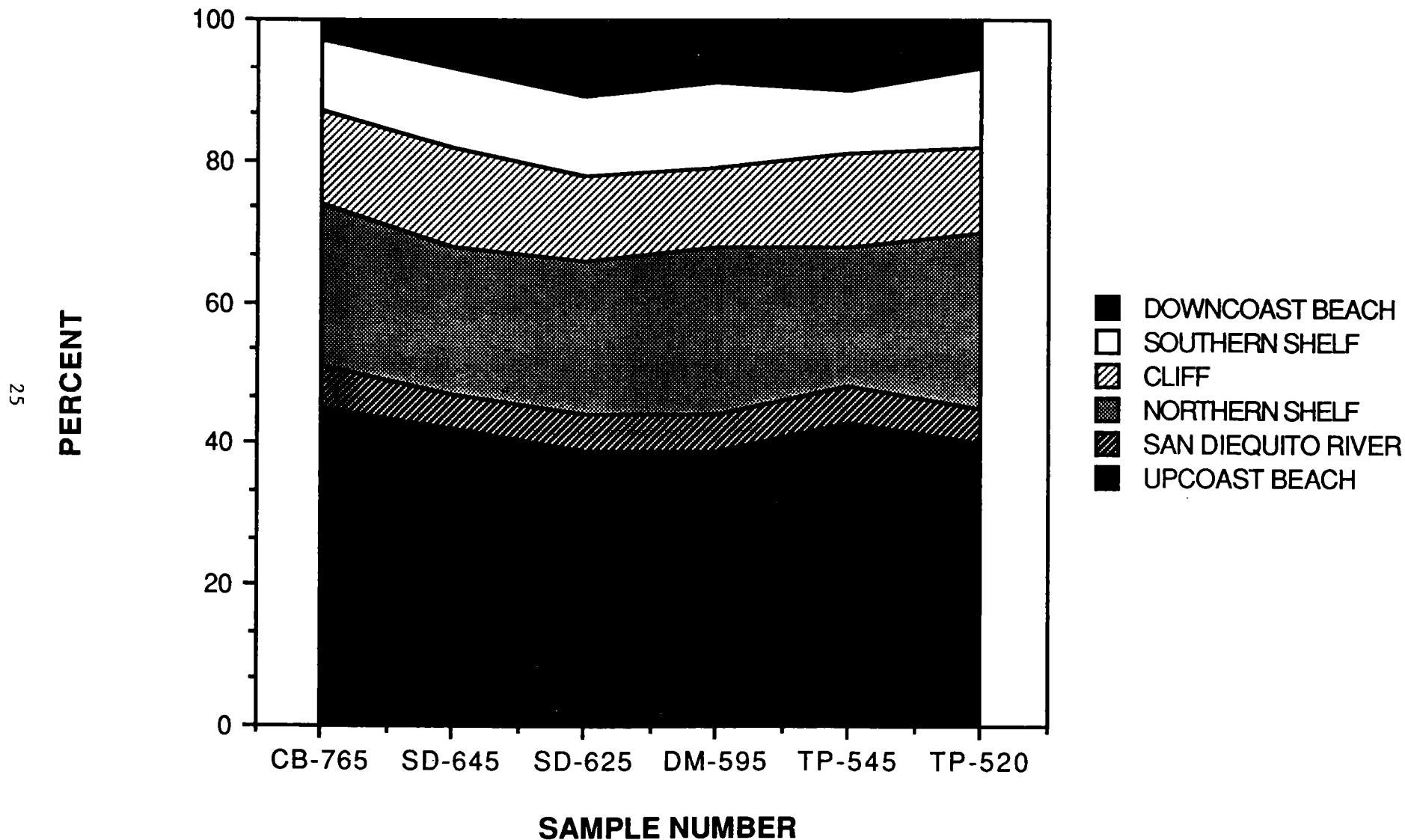
Figure 6. Grain-shape characteristics of end-of-winter beach samples from the Encinitas subcell.

• southern shelf 11%.

3.40   The range of variation for the contributions from the San Dieguito River (1%), cliff (3%) and southern shelf (3%) are statistically insignificant; however, the observed range of variation for the upcoast beach (Oceanside-Carlsbad subcell) (6%), northern shelf (5%) and particularly the downcoast beach (La Jolla Cove subcell) (8%) requires explanation. It is useful to present the results obtained for the end-of-summer samples before discussing the sources of compositional variation for the Encinitas subcell.

End-of Summer (October 1986) Beach Samples

3.41   The grain-shape results for the six end-of-summer beach samples from the Encinitas subcell are listed in Table 8 and illustrated in Figure 7. The average sand contribution from each local source is as follows:

> • upcoast beach (Oceanside Carlsbad subcell) 41%;
>
> • San Dieguito River 5%;
>
> • northern shelf 26%;
>
> • cliff 12%;
>
> • downcoast beach (La Jolla Cove subcell) 4%; and
>
> • southern shelf 12%.

3.42   The range of variation observed for the grain-shape contributions from the upcoast beach (Oceanside-Carlsbad subcell) (4%), San Dieguito River (1%), cliff (3%), downcoast beach (La Jolla Cove subcell) (4%) and southern shelf are insignificant. The variation associated with the northern shelf (6%) may be marginally significant.

3.43   The end-of-winter and end-of-summer values for the average sand contributions are equal for the upcoast beach (41%), San Dieguito River (5%) and cliff (12%), and vary by only 1 percent for the southern shelf (11 and 12 percent), respectively). Thus, at least 70 percent of the shape composition for the Encinitas subcell appears to be seasonally constant for the observed sample set.

3.44   The end-of-summer beach samples contain an average of 4 percent more northern shelf sand and 4 percent less downcoast beach sand (Tables 7 and 8; Figures 6 and 7). Inasmuch as these 4 percent differences are close to the limits of methodological resolution, the differences between the means of the end-of-winter and end-of-summer sample sets for the northern shelf and for the downcoast beach sources were examined using Student t-tests. In both cases, the observed differences are not significant at the 5 percent significance level. Therefore the beach samples from the Encinitas subcell must be considered seasonally homogeneous with respect to the 1986 sample sets.

26

4. Oceanside Cell (End-of-Summer): Encinitas Subcell (Onshore Projection of Carlsbad Submarine Canyon to La Jolla Submarine Canyon)

	UPCOAST BEACH	SAN DIEQUITO RIVER	NORTHERN SHELF	CLIFF	SOUTHERN SHELF	DOWNCOAST BEACH
SD-645-B-O	43	6	21	13	10	7
SD-625-B-O	41	6	27	10	13	3
DM-595-B-O	41	5	26	12	12	4
DM-575-B-O	42	5	25	12	11	5
TP-545-B-O	39	5	28	11	14	3
TP-520-B-O	41	5	27	12	12	3

Upcoast Beach Sample: CB-810-B-F
River Samples: DM-590-R, SD-635-R, TP-530-R, San Diequito River
Northern Shelf Samples: TP-519.5-S, SD-650-S, Offshore of Encinitas
Cliff Samples: TP-500-C, TP-466-C, TP-465-C, TP-463.6-C, TP-463-C, Torrey Pines Area
Southern Shelf Samples: LJ-454-S, TP-492-S, TP-464.5-S, Offshore of La Jolla
Downcoast Beach Sample: LJ-427-B-O

Table 8. Results of Fourier grain-shape analysis for end-of-summer samples from the Encinitas subcell.

4. OCEANSIDE CELL (END-OF-SUMMER): ENCINITAS SUBCELL
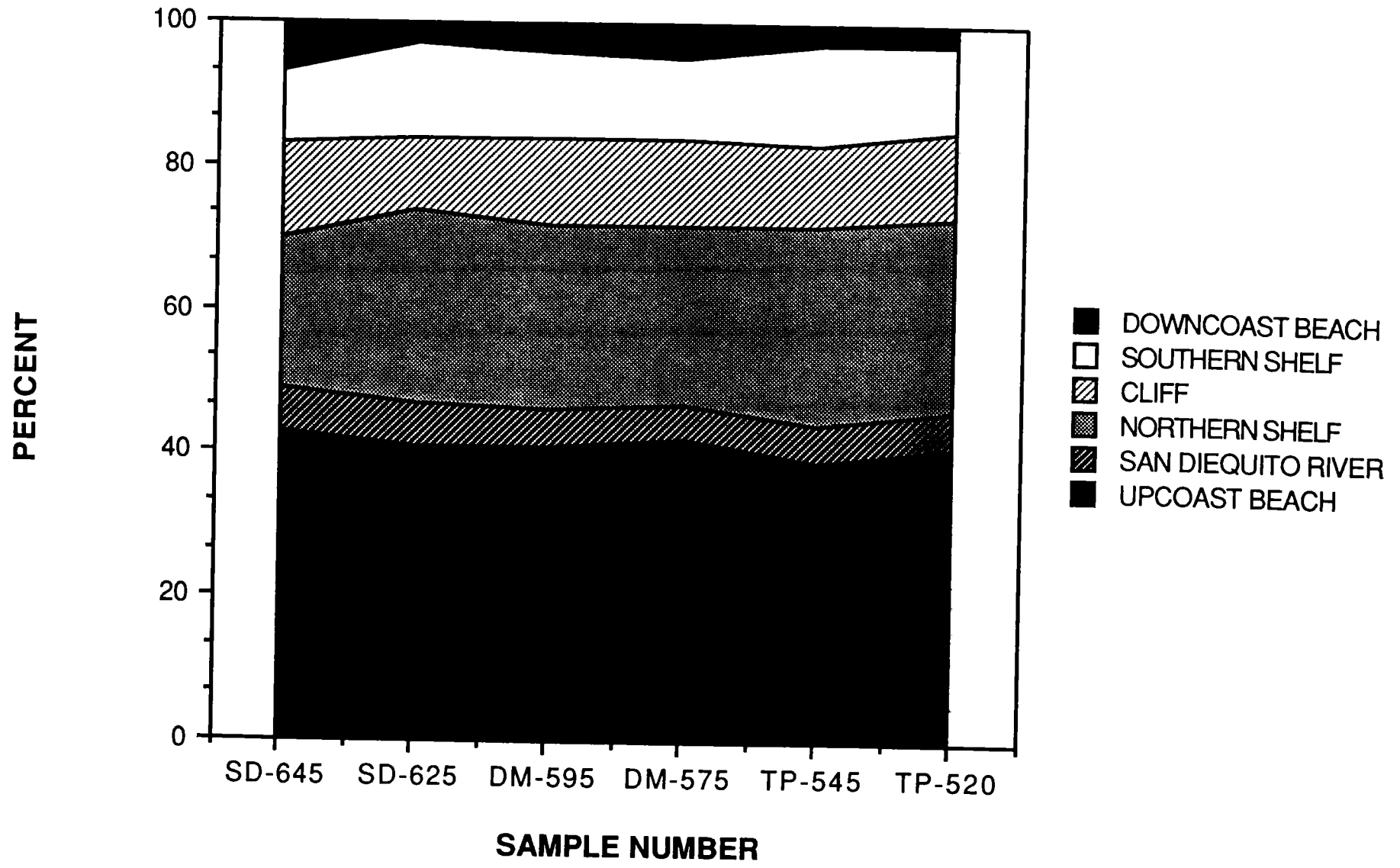
Figure 7. Grain-shape characteristics of end-of-summer beach samples from the Encinitas subcell.

3.45 The results of Fourier grain-shape analysis show the dominance of the upcoast beach and northern shelf in supplying sand to the beach of the Encinitas subcell. This indicates onshore transport of inner shelf sand in the northern part of the subcell and net downcoast transport of upcoast beach and northern shelf sand. The small volumetric contribution of the San Dieguito River agrees well with the small annual discharge rates computed by Simon and others (1988). The relatively small contributions from downcoast beach and the southern shelf indicate the secondary importance of upcoast transport in the Encinitas subcell. In terms of sediment budget considerations, it is important to note that the beach samples in this subcell contain an average of 33 percent inner shelf sand and 12 percent cliff sand. Again, the compositional homogeneity of the grain shapes in the beach sample set suggests thorough mixing during an unknown residence time.

Transition between Oceanside-Carlsbad and Encinitas Subcells

3.46 The southernmost beach sample of the Oceanside-Carlsbad subcell (CB-810-B-F) has derived 49 percent of its grain-shape composition from the northernmost sample of the Encinitas subcell (CB-765-B-F). Similarly, the northernmost sample of the Encinitas subcell (CB-765-B-F) has derived 45 percent of its shape composition from the southernmost beach sample of the Oceanside-Carlsbad subcell (CB-810-B-F). It is clear from these high exchange values that no physical or oceanographic condition created an effective barrier between these two subcells for the 1986 sample set.

Oceanside Littoral Cell: La Jolla Cove Subcell

3.47 The sample control for the La Jolla subcell is wholly inadequate to produce useful scientific information. The one beach sample available from this subcell (LJ-427-B-O) was collected from a small pocket beach south of Rocky Point (Table 9 and Figure 8). The nearest upcoast beach sample (LJ-460-B-O) was obtained from the beach at Scripps Institution of oceanography, which is located considerably north of Rocky Point. Likewise, shelf samples (LJ-454-S and LJ-443-S) were collected well upcoast of beach sample LJ-427-B-O, and at water depths of -62 and -70 feet MLLW, respectively.

3.48 The occurrence of Scripps and La Jolla Submarine Canyons and at least five well-defined pocket beaches upcoast of Rocky Point as well as the steep offshore slopes associated with the Point La Jolla area render it highly unlikely that any upcoast sand is transported to the beach south of Rocky Point. It also is highly unlikely that any shelf sand is transported onshore or alongshore to the area south of Rocky Point. The grain-shape composition of sample LJ-427-B-O must reflect that of the sea cliffs backing this pocket beach. Unfortunately, no cliff sample is available from the Rocky Point area to test this hypothesis.

Mission Beach Littoral Cell

3.49 The coastal lowland associated with Pacific and Mission beaches occupies the former delta of the San Diego River (Kuhn and Shepard, 1984). The deltaic sediment extends almost to Crystal Pier. The only volumetrically important natural sand sources for the Mission Beach Cell are the San Diego River and the inner shelf. Simon and Li (1988) estimate an average annual yield of only 2,300 tons of coarse-grained sediment for the San Diego River. Three jetties constructed across the mouth of Mission Bay terminated the

5. Oceanside Cell: La Jolla Cove Subcell (La Jolla Submarine Canyon to La Jolla Point)

	UPCOAST BEACH	NORTHERN SHELF	SOUTHERN SHELF
LJ-427-B-O	36	29	36

Upcoast Beach Sample: LJ-460-B-O
Northern Shelf Sample: LJ-454-S, Offshore of La Jolla
Southern Shelf Sample: LJ-443-S, Offshore of Point La Jolla

Table 9. Results of Fourier grain-shape analysis for end-of-summer sample from La Jolla Cove subcell.

5. OCEANSIDE CELL: LA JOLLA COVE SUBCELL
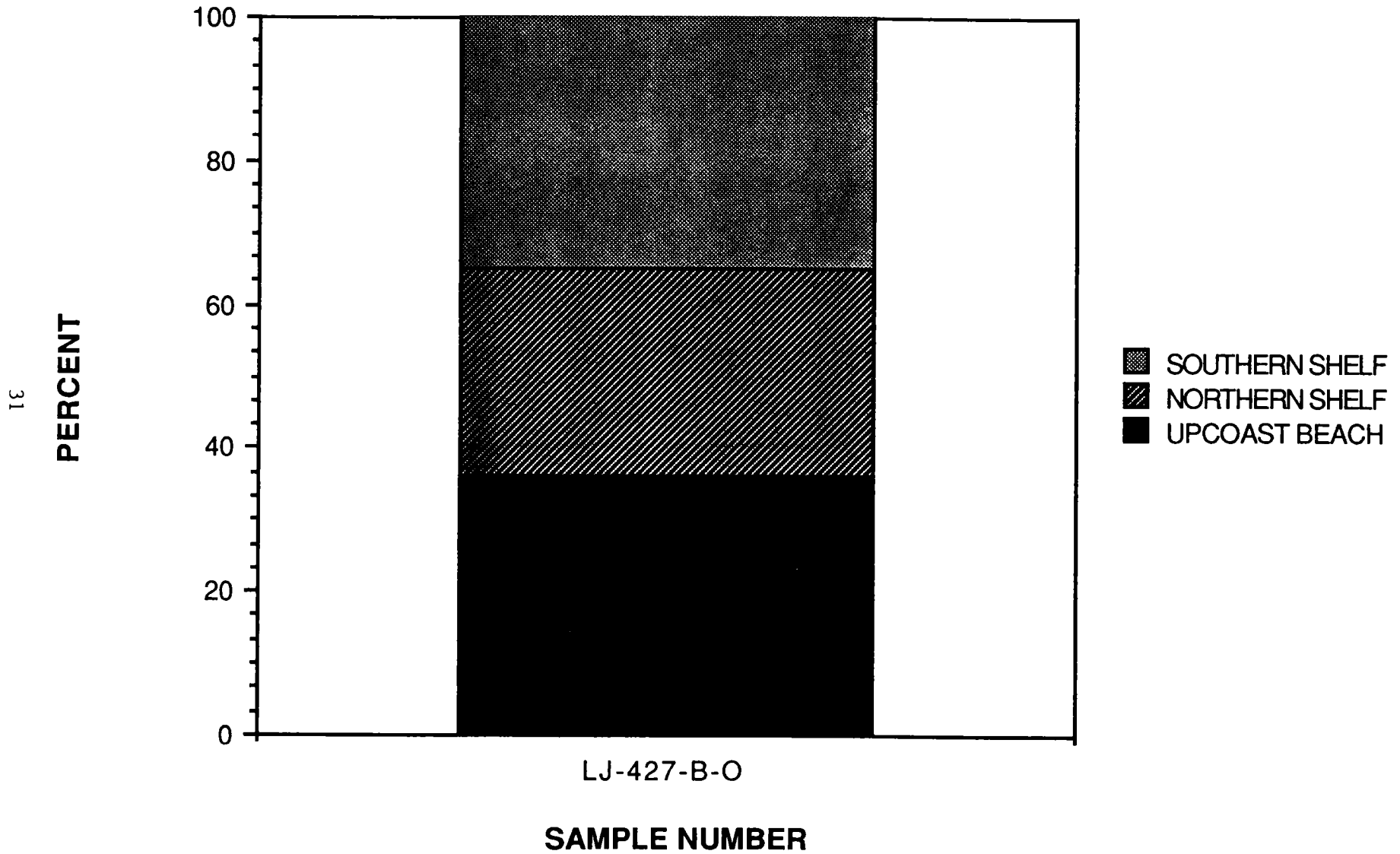
Figure 8.   Grain-shape characteristics of end-of-summer beach sample from the La Jolla Cove subcell.

supply of sand from Mission Beach to Ocean Beach, therefore Ocean Beach may be treated as a pocket beach.

3.50   The average grain-shape composition for the two beach samples from the Mission Beach Cell is as follows (Table 10 and Figure 9):

- San Diego River 24%; and

- inner shelf 76%.

The 1 percent variation observed for the shape composition from each source is statistically insignificant. The shelf sample (PB-394-S) was obtained at a water depth of -89 feet MLLW, and there is no suggestion that onshore sand transport occurred from such a depth. Rather, the shelf grain-shape contribution must reflect onshore transport of similarly-shaped sand from much shallower water depths. The high percentage of inner shelf sand in the beach samples must reflect rather small volumetric increments that have accumulated during an unknown residence time in the absence of substantive dilution by river-derived sand.

<center>Silver Strand Littoral Cell</center>

3.51   The Silver Strand Littoral Cell extends from several miles south of the United States-Mexico border to Zuniga Jetty at the entrance to San Diego Bay. According to Tekmarine, Inc. (1987), there is a sediment transport imbalance within the Silver Strand Cell. As a result, accretion is expected to continue in the Zuniga Jetty area, and beach erosion will be of particular concern in the following three areas: (1) from Hotel Del Coronado to about 4 miles south; at Imperial Beach, due mostly to the slow degradation of the Tijuana River delta; and (3) at Playas de Tijuana (the southern end of the cell), again due to erosion of the Tijuana River delta.

3.52   The average grain-shape composition for the two beach samples in the Silver Strand Cell is as follows (Table 11 and Figure 10):

- northern shelf 11%;

- Tijuana River 40%;

- downcoast beach (south of Tijuana River) 38%; and

- cliff (northernmost extension of Playas de Tijuana) 11%.

3.53   The range of values for the northern shelf (4%) and cliff (2%) are not significant; however, the range of values for the Tijuana River (13%) and downcoast beach (6%) sources requires explanation. One important source of variance is the 34-month time interval which elapsed between sampling of the southern and northern beach samples. The southern beach sample (SS-020-B-A) was collected in April 1986, whereas the northern beach sample (SS-160-B-F) was not collected until February 1989.

<center>3 2</center>

6. Mission Beach Cell:

	SAN DIEGO RIVER	SHELF
MB-330-B-A	24	76
OB-225-B-A	25	75

River Sample: OB-267-R, San Diego River

Shelf Sample: PB-394-S, Offshore of San Diego River

Table 10. Results of Fourier grain-shape analysis for end-of-winter samples from Mission Beach Littoral Cell.

6. MISSION BEACH CELL
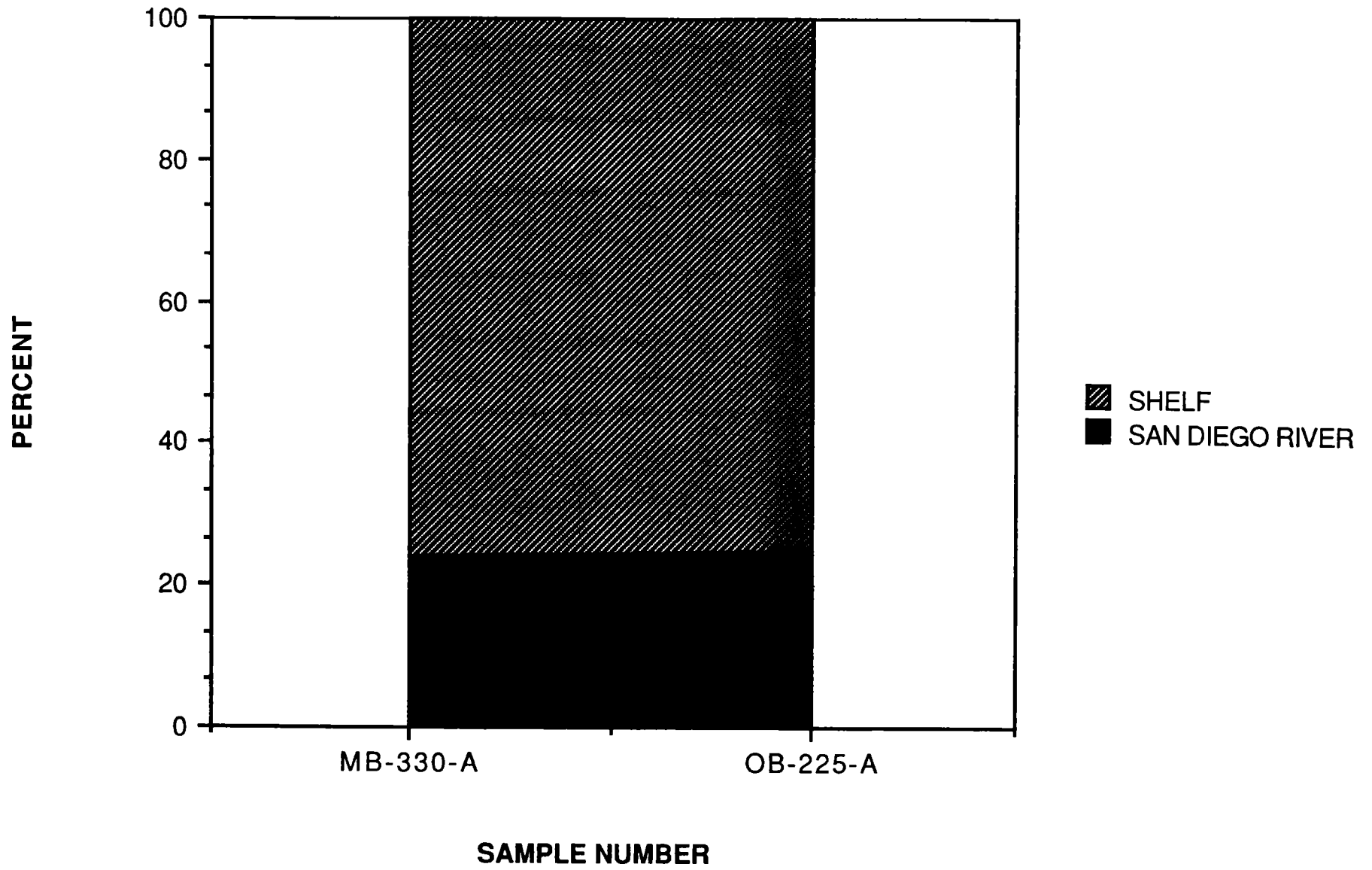
Figure 9.   Grain-shape characteristics of end-of-winter beach samples from
the Mission Beach Littoral Cell.

7. Silver Strand Cell:

	NORTHERN SHELF	TIJUANA RIVER	DOWNCOAST BEACH	CLIFF
SS-160-B-F	9	46	35	10
SS-020-B-A	13	33	41	12

Northern Shelf Sample: SS-205-S, Offshore of Point Loma
River Sample: SS-008-R, Tijuana River
Downcoast Beach Sample: SS-004-B-A
Cliff Sample: SS-002-C, Border Field State Park, South of Downcoast Beach
               Sample

Table 11. Results of Fourier grain-shape analysis for samples from the Silver Strand Littoral Cell.

7. SILVER STRAND
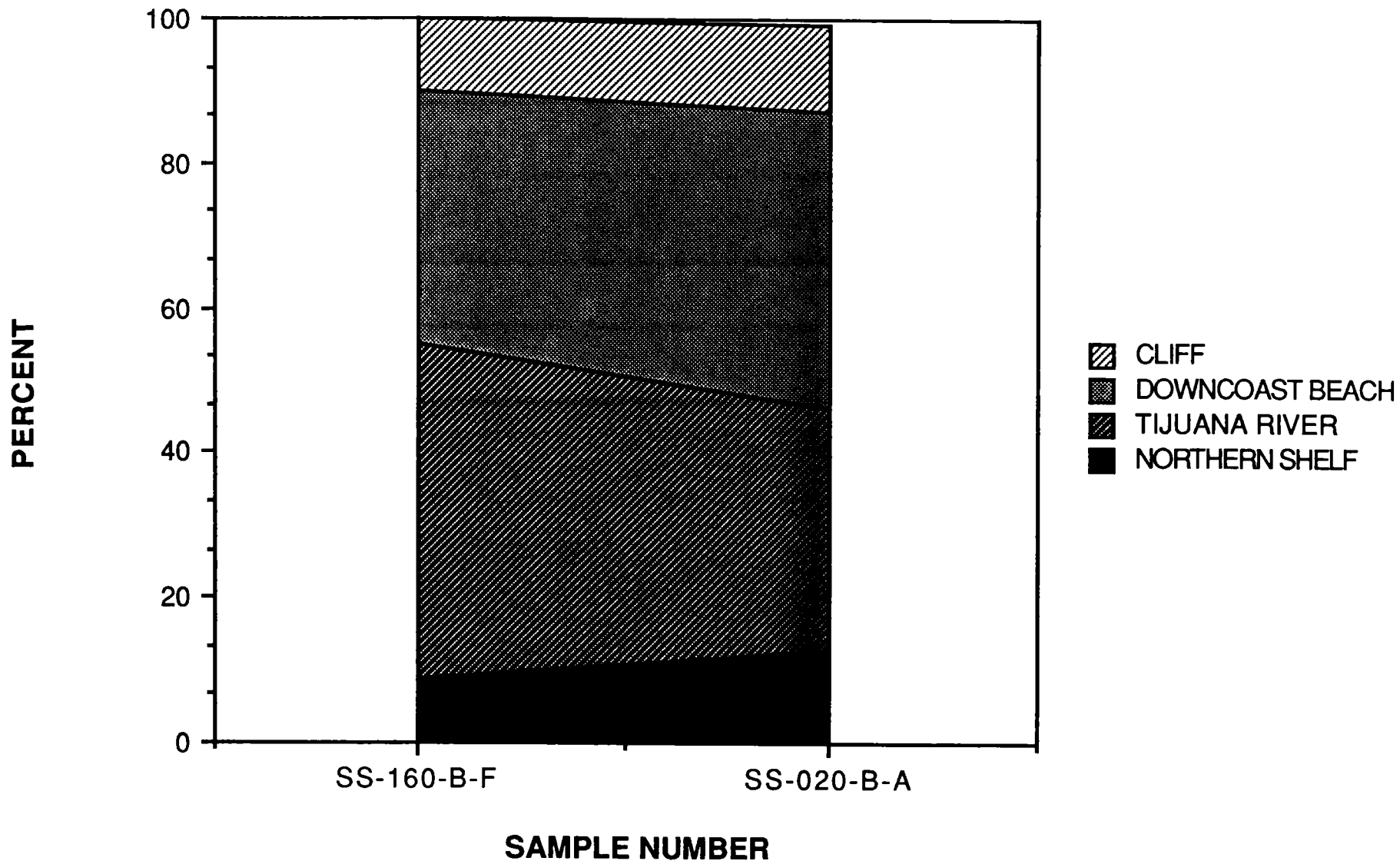
Figure 10.   Grain-shape characteristics of beach samples from the Silver
             Strand Littoral Cell.

3.54 Inasmuch as the two beach samples were collected upcoast of the Tijuana River, the overwhelming dominance of sand derived from the downcoast portions of this cell which contain the principal sand sources (Tijuana River, downcoast beach and cliff) clearly demonstrates net upcoast transport. The northern shelf sample (SS-205-S) was obtained offshore of Point Loma at a water depth of -42 feet MLLW. There is no published evidence to suggest net onshore transport of inner shelf sand from water depths as great as 42 feet. The fact that the two beach samples contain from 9 to 13 percent of their grain-shape composition from this source must reflect onshore and perhaps upcoast longshore transport from shallower inner-shelf sources with similar grain-shapes located farther south.

4. MINERALOGY OF LITTORAL CELLS AND SUBCELLS

Sediment Sources

4.01   Inasmuch as the mineralogical constituents of sedimentary strata are directly or indirectly derived from crystalline rocks exposed at the earth's surface, it is necessary to consider (1) the ultimate crystalline source rocks and (2) the local fluvial and cliff sediment sources.

4.02   The 5 to 10 percent of the earth's surface that is mountainous supplies at least 80 percent of the siliciclastic sediment to modern depositional basins. Furthermore, the rates of denudation are directly proportional to relief, and, in general, it appears that streams draining areas of high relief have the highest proportion of bedload (Blatt and others, 1972, p. 24-26). It is therefore appropriate to consider the crystalline terranes exposed at higher elevations as the dominant ultimate source rocks for the Oceanside sample set.

4.03   The relative weatherability of rocks is dependent on their mineralogy, mode of formation, post-depositional history and prevailing climate. Hydrated minerals of low-temperature igneous rocks are more stable at the pressure and temperature conditions of the earth's surface than are non-hydrated minerals formed at higher temperatures. Therefore, rocks containing minerals of the latter group such as basalt, gabbro and diorite tend to weather at a higher rate than would granite, particularly in a humid climate. Inasmuch as beach sand in southern California is mostly quartz and feldspar, only coarsely-crystalline rocks containing these minerals are considered as major ultimate sources.

4.04   Igneous and metamorphic rocks of acid-plutonic composition (quartz and feldspar) in the southern California batholith decompose into clay minerals and sand-size sediment grains. The feldspars are much more subject to mechanical and chemical breakdown than is quartz. The high ratio of feldspar to quartz in all river, cliff and beach sand samples in this study indicates a proximal source for beach sediment, and strongly suggests that the dominant ultimate source is plutonic rock of the southern California batholith.

4.05   Plutonic rocks of the southern California batholith are generally quartz diorite and gabbro. The quartz diorite contains large crystals of plagioclase and potassium feldspar. Hornblende and biotite are present in minor amounts. The gabbroic units are compositionally variable, but consist mostly of calcic feldspar and pyroxene, with minor amounts of quartz and biotite. Larsen (1948) named the principal units in the southern California batholith the Woodson Mountain Granodiorite, the Bonsall Tonalite, and the San Marcos Gabbro (Table 12). Tables 12 summarizes the modal mineralogic composition for the April 1985 and April 1986 Oceanside sample set and the principal source rocks (Osborne et al, 1985). Error analysis indicates that estimates of the true values for the major minerals in the 1985 and 1986 samples sets are within ± 4 percent of the obtained value with a 95 percent confidence. The compositional data for the Woodson Mountain Granodiorite, Bonsall Tonalite and San Marcos Gabbro are from Larsen (1948). It is clear from Table 12 that crystalline rocks in the southern California batholith are capable of producing the major mineral assemblages present in the sample set. Accessory minerals such as zircon, sphene and rutile commonly are associated with acid plutonic rocks; piedmontite and clinozoisite-epidote are associated with mafic igneous rocks; and actinolite-

Table 12. Modal mineralogic composition of the Oceanside sample set and the principal source rocks (from Osborne, 1986). Neither the major or heavy mineral sets sum to 100 percent due to the omission of other lithologic constituents associated with each set.

Principal Detrital Minerals Identified in Sample Set	April 1985 Oceanside Sample Set (%)	April 1986 Oceanside Sample Set (%)	November 1987 Oceanside Sample Set (%)	January-February 1981 Vibracore Sample Set (%)	Woodson Mountain Granodiorite (%)	Bonsall Tonalite (%)	San Marcos Gabbro (%)
MAJOR MINERALS							
Quartz	43	36	49	39	33 (30-40)	20-25	4 (0-10)
Potassium Feldspar	10	9	21	28	20 (10-30)	4-15	Tr
Plagioclase Feldspar	38	29	5	7	41 (30-55)	55-60	59 (47-66)
HEAVY MINERALS							
Biotite	53	27	22	8	5 (1-8)	5-15	3 (0-6)
Opaque Minerals	1	1	2	5	Tr	Tr	3
Pyroxene	Tr	Tr	Tr	Tr	Tr	Tr	8 (0-28)
Augite				Tr	Tr	Tr	7 (0-17)
Hornblende	31	52	65	61	1 (0-2)	10	
Garnet	Tr	Tr	1	Tr		Tr	13 (1-42)
Sphene	1	1	1	3			
Piedmontite	Tr	Tr		Tr			
Clinozoisite-Epidote	4	5	9	11			
Actinolite-Tremolite	1	Tr	Tr	Tr			
Glaucophane	Tr	Tr	Tr	Tr			
Glaucophane Schist	3	2	1	Tr			

tremolite are high-rank metamorphic minerals and may be associated with glaucophane schists.

4.06 The occurrence of glaucophane, glaucophane schist and actinolite-tremolite reflects ultimate derivation from the Mesozoic metamorphic age (110 million years before present) Catalina Schist terrane, which consists of a glaucophane-rich, blueschist. Stuart (1979, p. 36) reports a diverse set of clast types derived from the Catalina Schist terrane, which occur in the San Onofre Breccia. These include clasts of (1) the blueschist facies, which is rich in glaucophane and contains quartz, albite and chlorite; (2) the glaucophanic greenschist facies, which is rich in epidote and contains albite; (3) the greenschist facies, which is rich in actinolite and contains epidote, albite and chlorite; (4) the quartz schist facies, which consists of foliated quartz with greenschist and abundant glaucophane; (5) the saussurite gabbro facies, which contains actinolite, zoisite, clinozoisite and albite; (6) the amphibolite facies which contains amphibole, zoisite and garnet; and (7) the serpentinite facies, which contains calcite, tremolite, chlorite and actinolite. Catalina Schist terranes presently are exposed on Santa Catalina Island and Palos Verdes Hills, and occur in the subsurface of the Los Angeles basin. Such terranes are not known to occur within the uplands associated with the southern California batholith. The San Onofre Breccia (Miocene) is the most extensive deposit containing Catalina Schist detritus (Stuart, 1979). Scattered exposures of this unit occur from Santa Cruz Island southeastward to the Laguna Beach-Oceanside area, and then again south of Tijuana. The San Onofre Breccia is exposed as a ridge extending from San Onofre Mountain near Dana Point almost to Oceanside, and this exposure as well as younger sedimentary strata exposed along the coastal cliffs may have served as the local source for the glaucophane, glaucophane schist and perhaps the actinolite-tremolite grains present in the sample sets.

4.07 Other sedimentary rocks may or may not be potential sand sources. Clay-shale and siliceous shale, such as occurs in the Monterey Formation, are not likely to produce coarse-grained beach materials regardless of mineralogy and rates of weathering. Sandstones, on the other hand, represent the recycling of mostly quartz and feldspar eroded from plutonic igneous rocks and are excellent potential sand sources. This would include the sandstone members of the Cretaceous Williams Formation; the Delmar Formation and Torrey Sandstone of Eocene age that are widespread in the study area; and the Capistrano and San Mateo Formations of Miocene through Pleistocene age. Terrace and eolian deposits of limited thickness that contain suitable beach materials occur along a narrow strip parallel to the shoreline.

Methodology

4.08 Mineralogic analyses were performed on the fine- and medium-grained sand fraction (0.125 to 0.420 mm in diameter) for both the light (specific gravity 2.9) and heavy (specific gravity > 2.9) minerals. The light mineral fractions were mounted on glass slides, ground flat, polished and stained with sodium cobaltinitrite and malachite green to aid in feldspar identification. Conventional petrographic thin sections were used to analyze the heavy mineral fractions. Four hundred grains were identified and recorded for each mineralogic analysis. Accordingly, the resultant mineralogical data were divided into two sets. The first set reflected the total mineral composition of each sample, containing quartz, potassium feldspar, plagioclase feldspar, and the total heavy mineral suite. The second set contained only the heavy mineral fraction of each sample, and included the following minerals: biotite, opaque minerals, pyroxene (other than augite), augite, hornblende, beryl,

corundum, sphene, clinozoisite-epidote, and glaucophane schist (a rock fragment). Each of these data sets was recalculated to sum to 100 percent. The following minerals were deleted prior to recasting for the purpose of illustration because of their infrequent occurrence and small concentrations in the obtained samples: actinolite/tremolite, andalusite, apatite, garnet, glaucophane, muscovite, olivine, piedmontite, rutile, sillimanite, sphene topaz, tourmaline, wollastonite, zircon, zoisite, and the category "doubtful determination". All mineral occurrences however were included in sedimentologic evaluation.

Results and Discussion

Mineralogic Trends within River Samples

4.09   Eleven rivers were sampled approximately one kilometer inland from the ocean river mouth; each river has the potential to discharge sediment into the littoral zone of the study area (Figures 11a and 11b). Sample sites for these rivers are represented by open square symbols in Figures 11a and 11b. Several minerals including glaucophane, garnet, epidote, sphene, and hypersthene show considerable variation between contributing fluvial sources within coastal San Diego County (Figures 12 and 13; and Tables 13 and 14). Observed heavy mineral assemblages reflect compositional changes in the strata of the coastal upland terraces that are drained by rivers. The rivers that discharge into the Silver Strand and Mission Beach Littoral Cells dissect plutonic igneous rocks containing smaller isolated metamorphic bodies. Metamorphic clasts occur within the sea cliffs in northern Oceanside Littoral Cell. Mineralogic divisions can be recognized between river samples that discharge into the Oceanside, Mission Beach and Silver Strand Littoral Cells (Figures 11a and 11b).

4.10   The San Onofre Breccia, a variably-textured Miocene deposit containing metamorphic (blueschist facies) clasts, crops out as a continuous ridge from San Mateo Creek to San Luis Rey River. This formation provides a source for sediment adjacent to the San Onofre subcell. Metamorphic clasts from the San Onofre Breccia are resedimented into younger formations and terrace deposits along the coast, including the Bay Point and Linda Vista Formations. The San Onofre Breccia, of limited areal extent, provides the only source of glaucophane in the Peninsular Ranges. Glaucophane also occurs in the coastal cliffs within this segment, and gullies provide the path for transport into the littoral zone where no river drainages are present.

Mineralogic Trends Within Cliff Samples

4.11   Seacliffs that contribute an appreciable amount of sediment to the adjacent littoral zone occur extensively from San Onofre to Oceanside and in the Torrey Pines area (Kuhn and others, 1987 and 1988). All the cliff samples were collected within these coastal regions. Cliff sample sites are denoted by solid square symbols in Figures 11a and 11b.

4.12   A metamorphic mineral assemblage containing glaucophane occurs along the northern San Onofre cliffs and an igneous plutonic suite of minerals occurs in the southern cliffs of the Encinitas area. Both light and heavy minerals are useful to define this boundary along the coast (Figures 14 and 15). Coastal cliffs that contribute sediment to the adjacent beaches back the Encinitas and San Onofre subcells. Stratigraphic changes

4 1
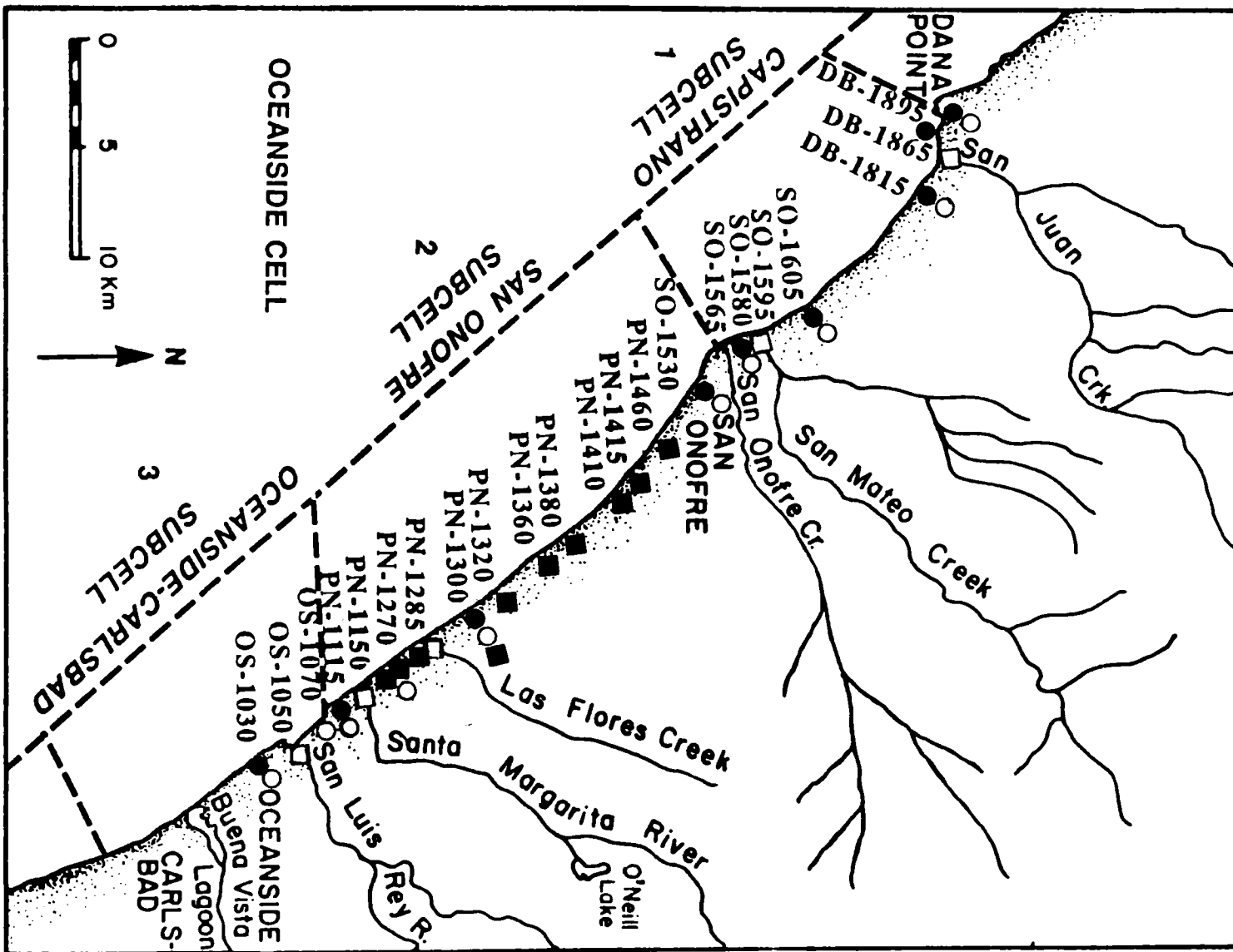
Figure 11A. Location map of samples sites: Dana Point to Carlsbad.
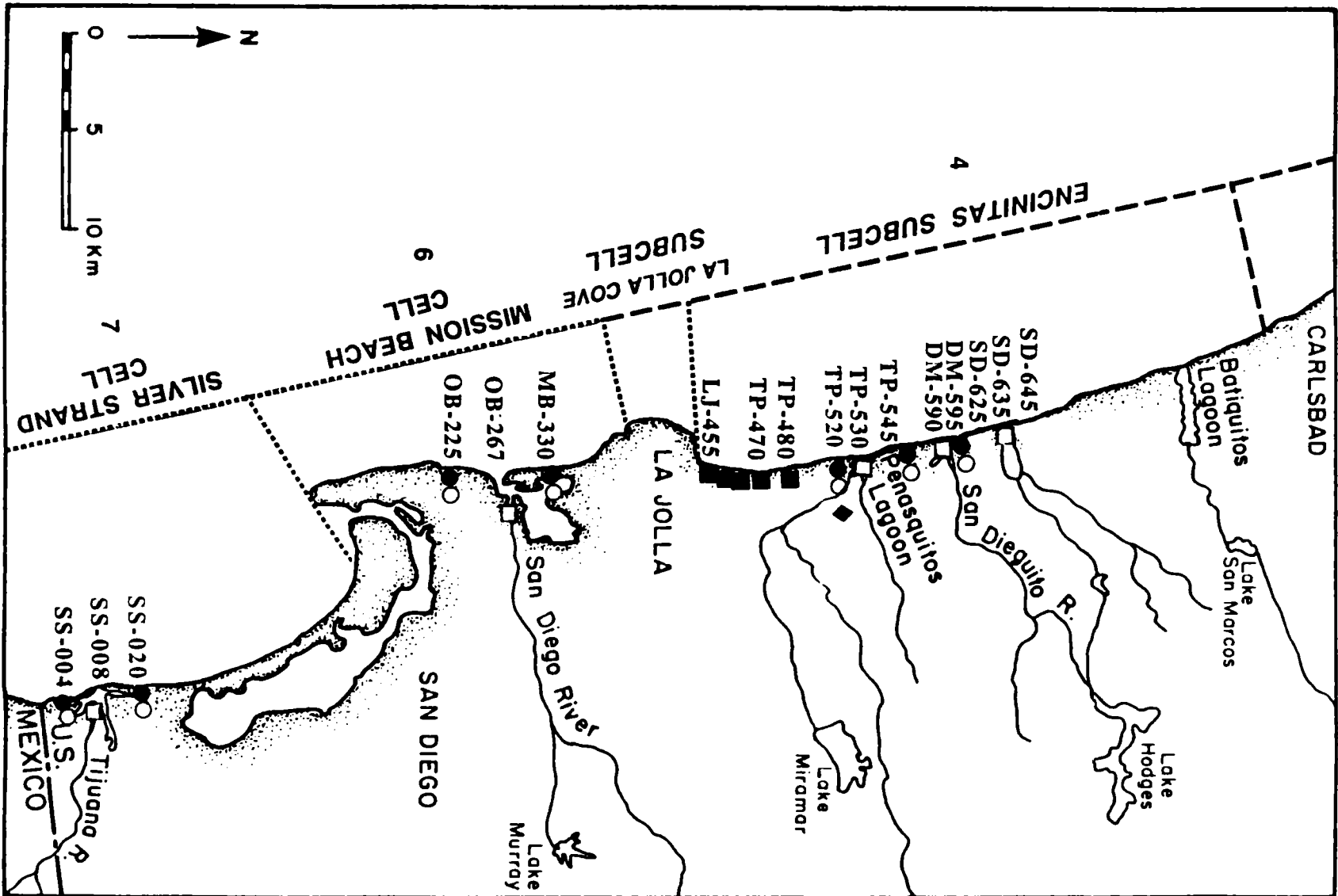
Figure 11B. Location map of sample sites: Carlsbad to U.S.-Mexico Border.

43

1986 BEACHES: MINERAL AVERAGES BY SUBCELL

MINERAL	SUBCELL	7 SILVER STRAND	6 MISSION BEACH	5 LJ COVE	4 ENCINITAS	3 CARLSBAD-OCEANSIDE	2 SAN ONOFRE	1 CAPISTRANO		AVERAGE
QUARTZ	WINTER	69.0	75.2	----	62.5	68.7	63.2	56.7		63.6
	SUMMER	65.9	74.2	----	65.6	66.7	58.3	65.7		63.9
PLAGIOCLASE FELDSPAR	WINTER	15.0	9.2	----	15.6	10.6	13.7	12.9		13.9
	SUMMER	9.8	2.7	----	6.4	8.3	9.1	10.5		8.3
POTASSIUM FELDSPAR	WINTER	7.0	4.8	----	7.4	8.9	11.3	12.5		9.3
	SUMMER	12.7	11.8	----	9.4	9.1	10.4	11.6		10.7
TOTAL HEAVY MINERAL	WINTER	9.1	10.9	----	14.6	12.0	12.1	19.2		13.3
	SUMMER	11.8	11.4	----	18.6	16.1	21.7	12.4		17.0
BIOTITE	WINTER	9.0	1.6	----	2.9	26.7	6.5	2.4		6.1
	SUMMER	4.2	4.0	----	1.1	4.7	3.2	1.8		2.8
COMPOSITE	WINTER	2.2	1.7	----	5.5	2.3	12.1	8.9		7.2
	SUMMER	1.7	3.0	----	5.1	4.5	12.5	14.1		8.0

Table 13A. Compositional averages for quartz, plagioclase feldspar, potassium feldspar and total heavy minerals in 1986 beach samples by season for each littoral cell or subcell.

44

1986 BEACHES: MINERAL AVERAGES BY SUBCELL

MINERAL	SUBCELL	7 SILVER STRAND	6 MISSION BEACH	5 LJ COVE	4 ENCINITAS	3 CARLSBAD-OCEANSIDE	2 SAN ONOFRE	1 CAPISTRANO		AVERAGE
EPIDOTE	WINTER	3.3	2.0	----	13.4	2.7	22.1	15.8		13.8
	SUMMER	1.7	0.7	----	11.4	6.9	24.9	18.2		14.1
GARNET	WINTER	0.4	0.0	----	0.9	0.0	2.2	6.1		2.0
	SUMMER	0.2	0.7	----	0.9	0.8	4.2	2.7		2.0
GLAUCOPHANE	WINTER	0.4	0.0	----	1.7	1.0	4.2	0.7		2.0
	SUMMER	0.1	0.0	----	2.2	0.0	2.5	0.0		1.5
HORNBLENDE	WINTER	78.2	84.0	----	61.1	64.0	33.4	31.6		52.0
	SUMMER	87.2	83.7	----	74.4	74.0	24.4	47.4		57.7
HYPERSTHENE	WINTER	3.1	1.7	----	1.9	1.3	1.8	0.8		1.9
	SUMMER	1.5	2.0	----	1.3	1.2	0.9	1.7		1.3
OPAQUE	WINTER	1.6	8.7	----	8.1	1.0	14.6	26.4		11.7
	SUMMER	1.2	4.3	----	2.8	6.4	19.9	7.7		8.9
SPHENE	WINTER	1.3	0.3	----	2.3	0.3	2.3	5.9		2.5
	SUMMER	1.2	0.7	----	2.0	1.4	3.5	4.3		2.3

Table 13B. Compositional averages for selected heavy minerals in 1986 beach samples by season for each littoral cell or subcell.

45

RIVERS AND CLIFFS: HEAVY MINERAL SUBCELL AVERAGES

MINERAL	SUBCELL	7	6	5	4	3	2	1		AVERAGE
EPIDOTE	RIVER	1.7	0.7	----	16.0	7.3	10.9	8.3		10.0
	CLIFF	----	----	----	11.4	----	22.3	----		16.9
GARNET	RIVER	0.0	0.0	----	1.3	0.3	0.3	8.0		2.4
	CLIFF	----	----	----	1.1	----	1.5	----		1.3
GLAUCOPHANE	RIVER	0.0	0.0	----	6.6	0.3	1.8	0.0		1.3
	CLIFF	----	----	----	0.1	----	5.7	----		2.9
HORNBLENDE	RIVER	89.0	74.3	----	51.6	54.3	56.8	34.3		57.7
	CLIFF	----	----	----	22.9	----	22.1	----		22.5
HYPERSTHENE	RIVER	2.0	1.0	----	0.9	0.3	2.2	2.0		1.5
	CLIFF	----	----	----	0.0	----	0.6	----		0.3
OPAQUE	RIVER	0.3	1.7	----	5.2	0.7	2.3	27.7		5.0
	CLIFF	----	----	----	12.2	----	3.9	----		8.1
SPHENE	RIVER	1.7	0.7	----.	5.8	2.7	2.2	5.7		3.4
	CLIFF	----	----	----	6.9	----	2.5	----		4.7

Figure 14A. Compositional averages for quartz, plagioclase feldspar, potassium feldspar and total heavy minerals in 1986 river and cliff samples by season for each littoral cell or subcell.

RIVERS AND CLIFFS: MINERAL AVERAGES BY SUBCELL

MINERAL	SUBCELL	7 SILVER STRAND	6 MISSION BEACH	5 LJ COVE	4 ENCINITAS	3 CARLSBAD-OCEANSIDE	2 SAN ONOFRE	1 CAPISTRANO		AVERAGE
QUARTZ	RIVER	62.2	60.1	----	63.1	67.5	59.8	50.8		60.8
	CLIFF	----	----	----	56.5	----	61.3	----		58.9
PLAGIOCLASE FELDSPAR	RIVER	12.1	9.8	----	17.4	23.8	14.8	14.2		15.2
	CLIFF	----	----	----	20.8	----	15.1	----		18.0
POTASSIUM FELDSPAR	RIVER	5.9	7.0	----	10.8	3.9	10.6	10.9		9.3
	CLIFF	----	----	----	15.1	----	10.3	----		12.7
TOTAL HEAVY MINERAL	RIVER	20.0	23.3	----	9.1	5.0	14.9	24.2		14.2
	CLIFF	----	----	----	7.6	----	14.3	----		10.4
BIOTITE	RIVER	3.0	17.7	----	8.9	25.7	4.6	0.7		8.4
	CLIFF	----	----	----	36.9	----	29.5	----		33.4
COMPOSITE	RIVER	1.3	3.7	----	7.9	7.3	19.3	12.0		11.4
	CLIFF	----	----	----	9.4	----	11.2	----		10.3

Table 14B. Compositional averages for selected heavy minerals in 1986 river and cliff samples by season for each littoral cell or subcell.
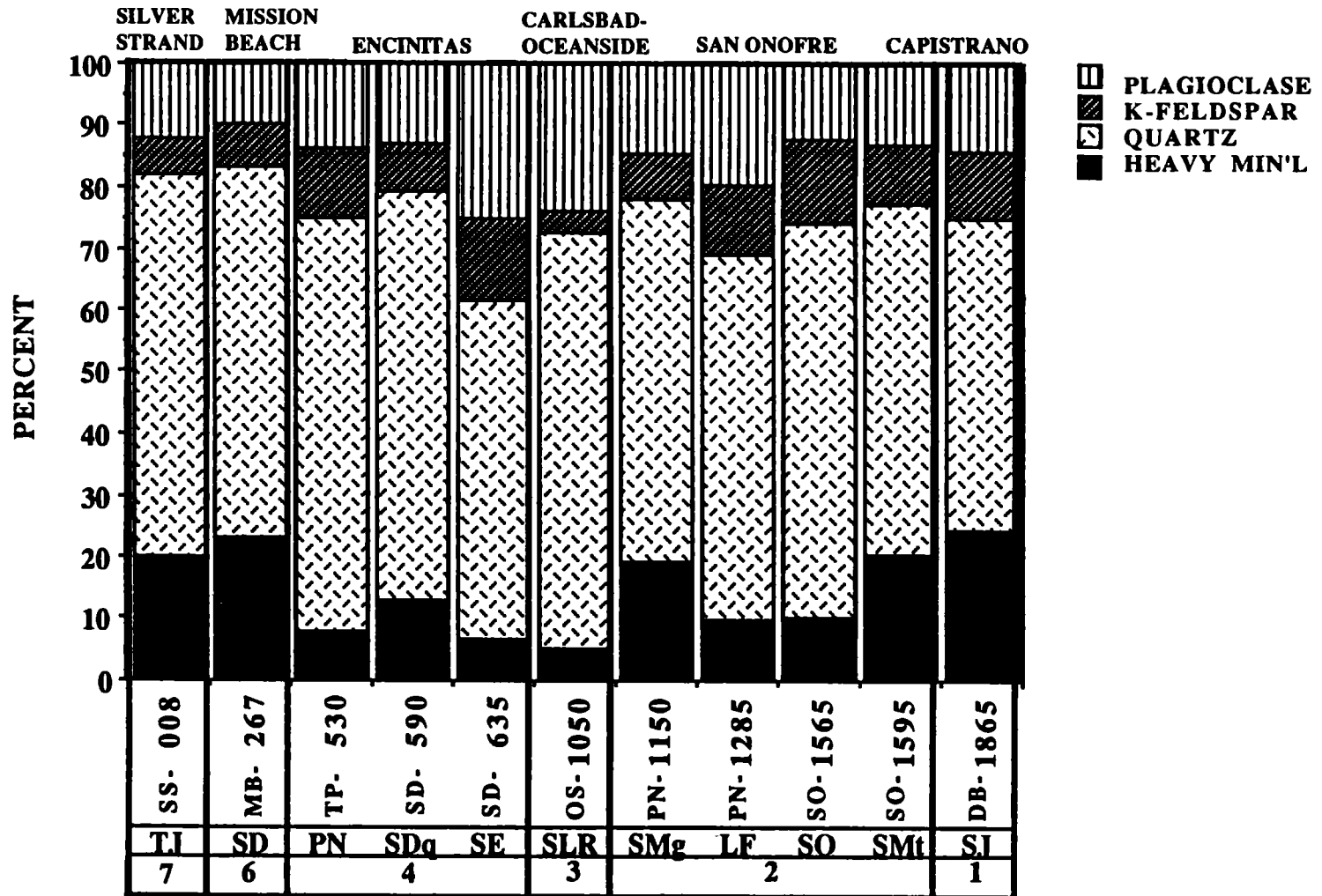
Figure 12. Total mineral histogram for river samples in San Diego County, 1986.
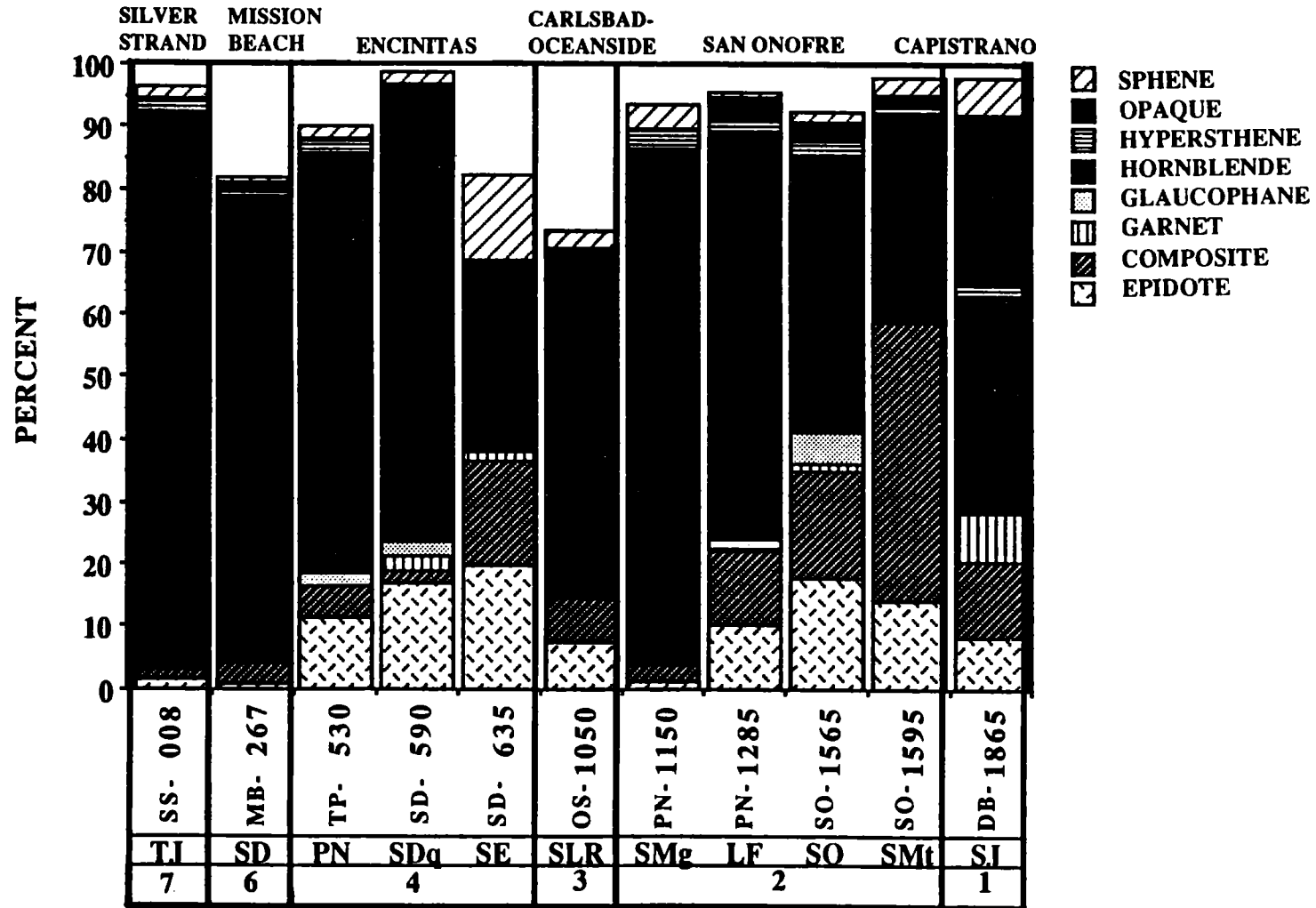
Figure 13. Major heavy mineral histogram for river samples in San Diego County, 1986.

49
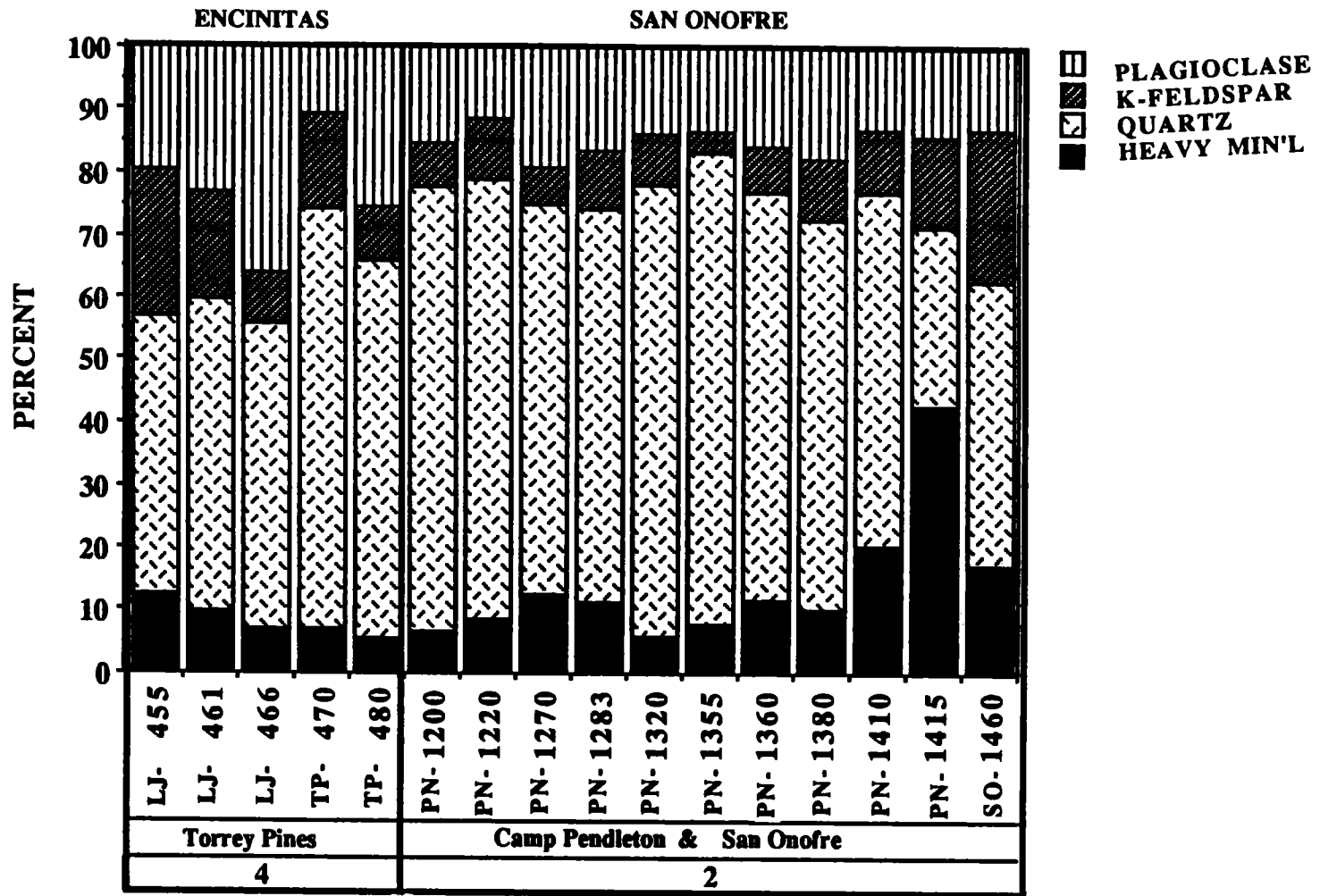
Figure 14. Total mineral histogram for coastal cliff samples, 1986.
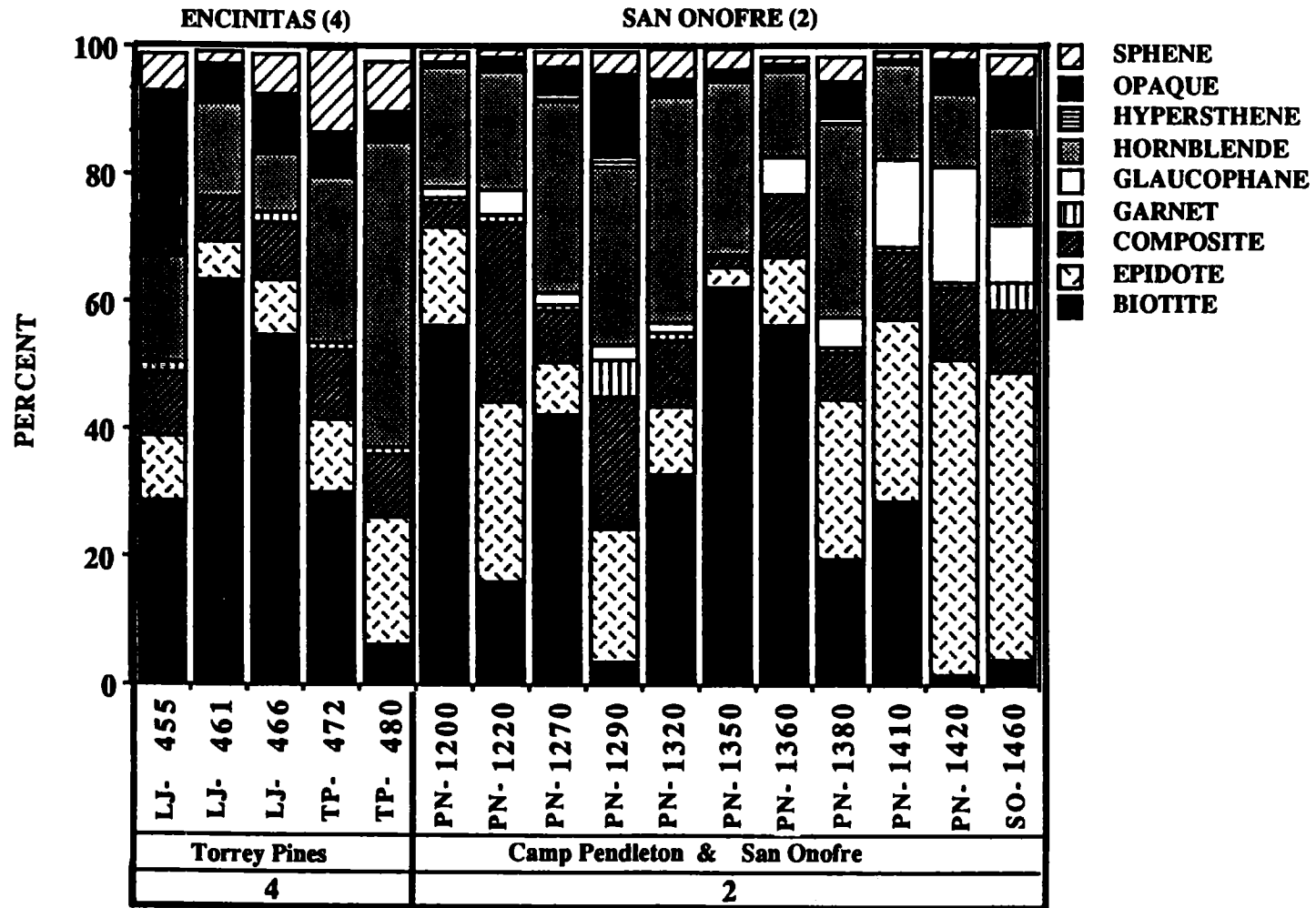
Figure 15. Major heavy mineral histogram for coastal cliff samples, 1986.

distinguish the Miocene and Quaternary alluvial deposits of the San Onofre-Camp Pendleton cliffs from the Eocene formations in the Torrey Pines cliffs. Kuhn and others (1988) discuss coastal cliff and terrace petrofacies in detail, including minor accessory minerals.

Mineralogic Trends within Beach Samples

4.13   Samples from the beach include local source contributions from both rivers and cliffs. Sediment samples were collected in both April and October of 1986, on the beach approximately one kilometer north and south from each of the eleven sampled river mouths. The beach sample sets are represented by solid circles for the end-of-winter sediment, and open circles mark the sample locations for the end-of-summer beach sand (Figure 11A and 11B). This sampling design was constructed to evaluate fluvial and cliff contributions to the littoral zone sediment. Total mineral composition for the end-of-winter and end-of-summer sample sets are presented in area plots (Figures 16 and 17). Heavy mineral assemblages within the April and October 1986 sample sets are illustrated by area plots (Figures 18 and 19). The importance of shelf contribution to the beach cannot be evaluated mineralogically, because no offshore samples were analyzed. Beach sand represents a rather homogeneous, well-sorted mixture of minerals from each of its various local sources.

4.14   Quartz accounts for more than half of the mineralogic composition of beach sand in each of the sample sets. Total heavy minerals, potassium and plagioclase feldspar generally occur in subequal proportions from approximately ten to fifteen percent each. The total heavy minerals generally are the second-most abundant component. Feldspar percentages display seasonal variation. For a given littoral subcell or cell, more plagioclase than potassium feldspar occurs on the beach at the end-of-winter than at the end-of-summer. Moreover, a greater abundance of potassium than plagioclase feldspar occurs on all of the 1986 beaches at the end-of-summer throughout all of the subcells (Table 14A).

4.15   Hornblende typically forms the major constituent of heavy minerals for all of the beach sand samples, ranging from 30% to 80% (Figure 14B). More hornblende is present within an end-of-summer sample set than an end-of-winter sample set for all of the subcells, except for the San Onofre subcell and the Mission Beach Littoral Cell. Epidote, composite particles, and opaque grains constitute the other predominant constituents for all of the 1986 beach sample sets. Sphene and hypersthene occur in small proportions in the subcells sampled during 1986 (Figure 14B). Garnet and glaucophane are the most diagnostic minerals because these occur exclusively in the San Onofre, Oceanside-Carlsbad, and Encinitas subcells. Glaucophane identifies source lithology because it occurs in the San Onofre Breccia, Bay Point, and Linda Vista Formations, which have limited exposures. Therefore, trends of sediment deposition and littoral transport patterns can be recognized by the occurrence and concentration of glaucophane.
Systematic increases in the amount of biotite within a coastal segment can be used to infer the net direction of sediment transport since biotite's hydraulic behavior differs from lag deposits typical of most heavy minerals. Other accessory minerals, including actinolite, augite, apatite, zircon and zoisite provide useful information for subcell differentiation.

1986 WINTER BEACH: TOTAL MINERLOGY
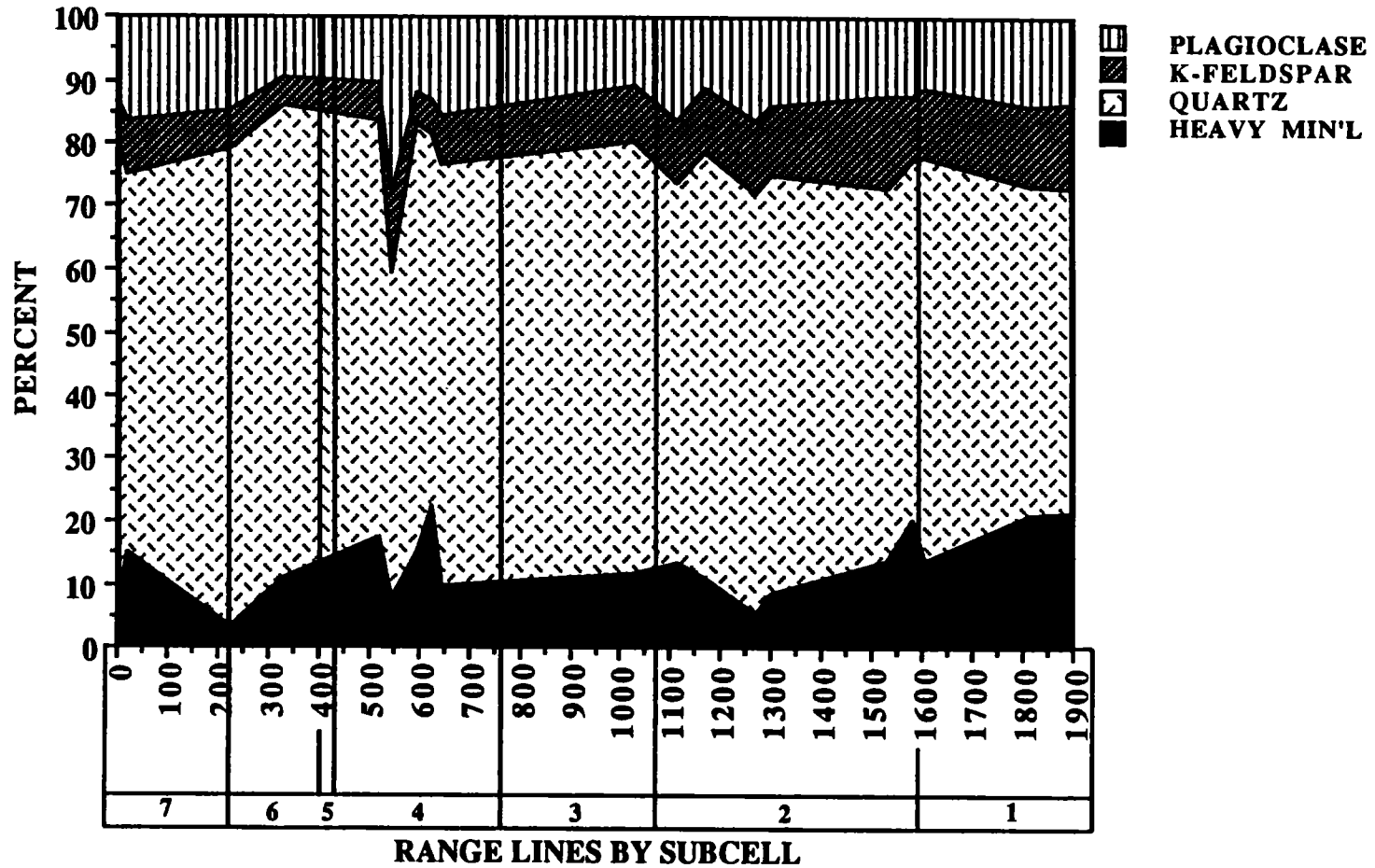
Figure 16. Total mineral area plot of end-of-winter beach samples, 1986.

1986 SUMMER BEACH: TOTAL MINERALOGY
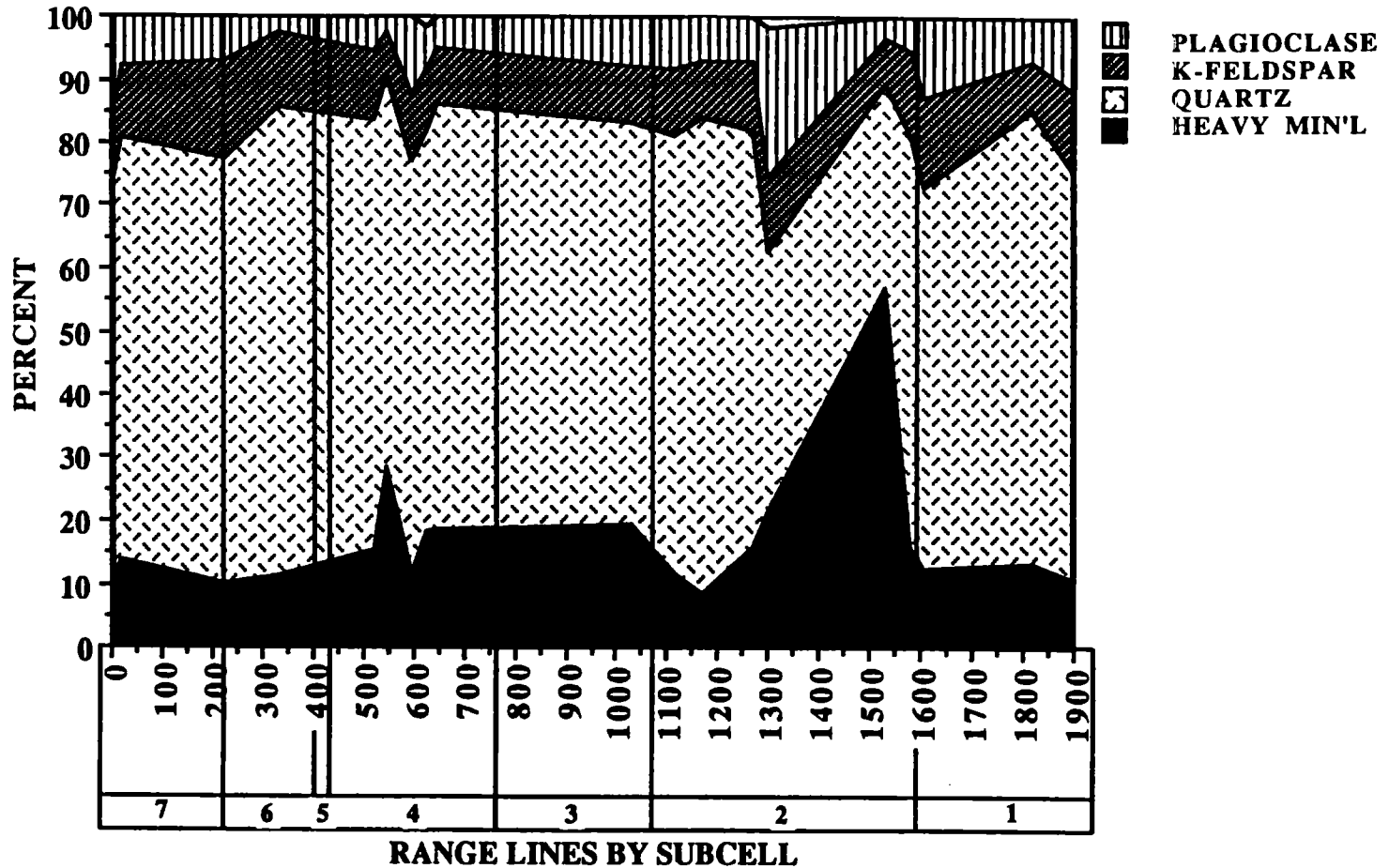
Figure 17. Total mineral area plot of end-of-summer beach samples, 1986.

1986 WINTER BEACH: HEAVY MINERALS
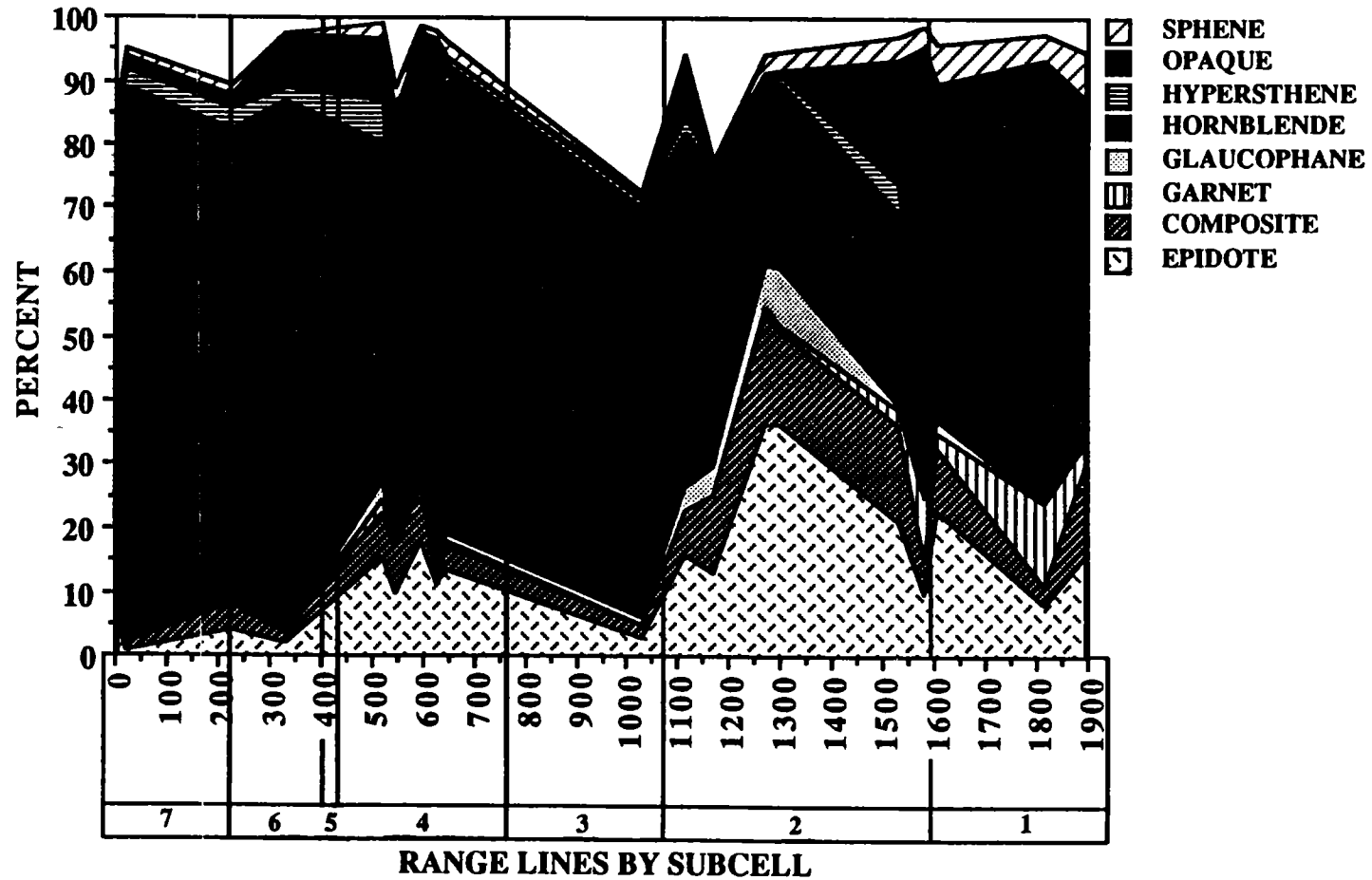
Figure 18.   Major heavy mineral area plot of end-of-winter beach
             samples, 1986.

1986 SUMMER BEACH: HEAVY MINERALS
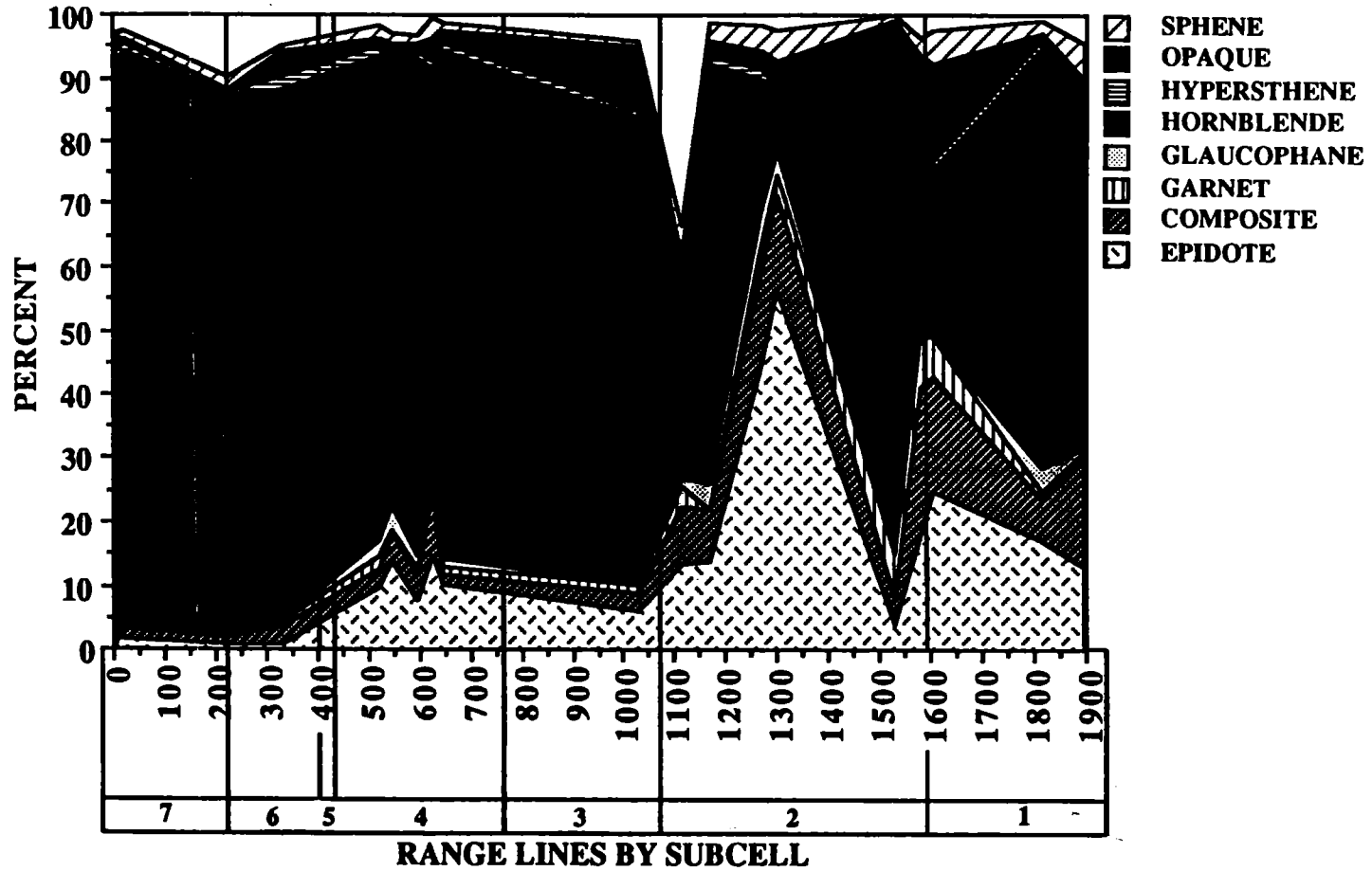
Figure 19. Major heavy mineral area plot of end-of-summer beach
samples, 1986.

Oceanside Littoral Cell: Capistrano Subcell

Mineralogy of River Sample

4.16   Significant mineralogic differences within San Juan Creek (DB-1865) distinguish the river composition of the Capistrano subcell from that of the other subcells. San Juan Creek contains the smallest amount of hornblende (34.3%) as compared to rivers from other subcells (Table 13B). Subequal amounts of opaque grains (27.7%) and a range of high percentages for heavy minerals occur in San Juan Creek (Figure 13B). Much more garnet (8.0%) occurs in San Juan Creek than rivers draining into other subcells. No glaucophane is detected within the Capistrano subcell river drainage. Epidote (8.3%) and composite particles (12%) make up large proportions of the river's heavy mineral content. Almost 6% of the total heavy mineral of San Juan Creek is sphene, and there is 2% hypersthene. No coastal cliffs contribute sediment to the Capistrano subcell beaches. Line plots of single mineral species are presented in Figures 20 through 38 to illustrate mineral concentrations of river and cliff sediment. Mineral averages for a specific mineral is given for each subcell. Similarly, line plots of single mineral species are presented in Figures 39 through 57 to illustrate mineral concentrations in the 1986 winter and summer beach sediment, and the average mineral percentage within each subcell is presented. These figures will be referred to throughout the following sections.

Mineralogy of Beach Samples

4.17   Quartz comprises more than half of the mineral composition of the beach sand in the Capistrano subcell, from DB-1900 to SO-1600. There is less quartz (56.7%) in the 1986 end-of-winter beach samples than those collected at the end-of-summer (65.7%) (Figure 39). Conversely, a greater heavy mineral and feldspar content exists for the end-of-winter beach sample set as compared to the end-of-summer set. Although there is a decrease in the total heavy minerals from the 19.2% for Capistrano subcell end-of-winter sample set (DB-1900 to SO-1600) to 12.1% for the 1986 end-of-winter beach sample set in San Onofre subcell (SO-1600 to OS-1080); a southward incease in heavy minerals on the beach occurs during the summer (Figure 42). This apparent concentration of heavy minerals appears to reflect the seasonal nature of bidirectional sediment transport. Feldspar also shows a seasonal variation. There is more plagioclase feldspar on the beach at the end-of-winter, and there is more potassium feldspar on the beach at the end-of-summer from DB-1900 to SO-1600 (Figures 40 and 41).

4.18   The Capistrano subcell extends from Dana Point to San Mateo Creek. The mineralogic composition of this subcell suggests a relatively high-energy depositional environment. There are only small percentages of biotite present in the beach samples from DB-1900 to SO-1600 during both summer (1.8%) and winter (2.4%) (Figure 43). Biotite is deposited in environments characterized by relatively low mechanical energy; therefore, the beaches in the Capistrano subcell may be interpreted as high-energy depositional environments,

4.19   There is less hornblende on the beaches of the Capistrano subcell (DB-1900 to SO-1600) than other subcells (Figure 48). The 1986 end-of-winter beach samples within this area contain 31.6% hornblende, in contrast to the 52% average hornblende content for the entire beach sample set (Table 14b). Opaque grains show a substantial seasonal

57
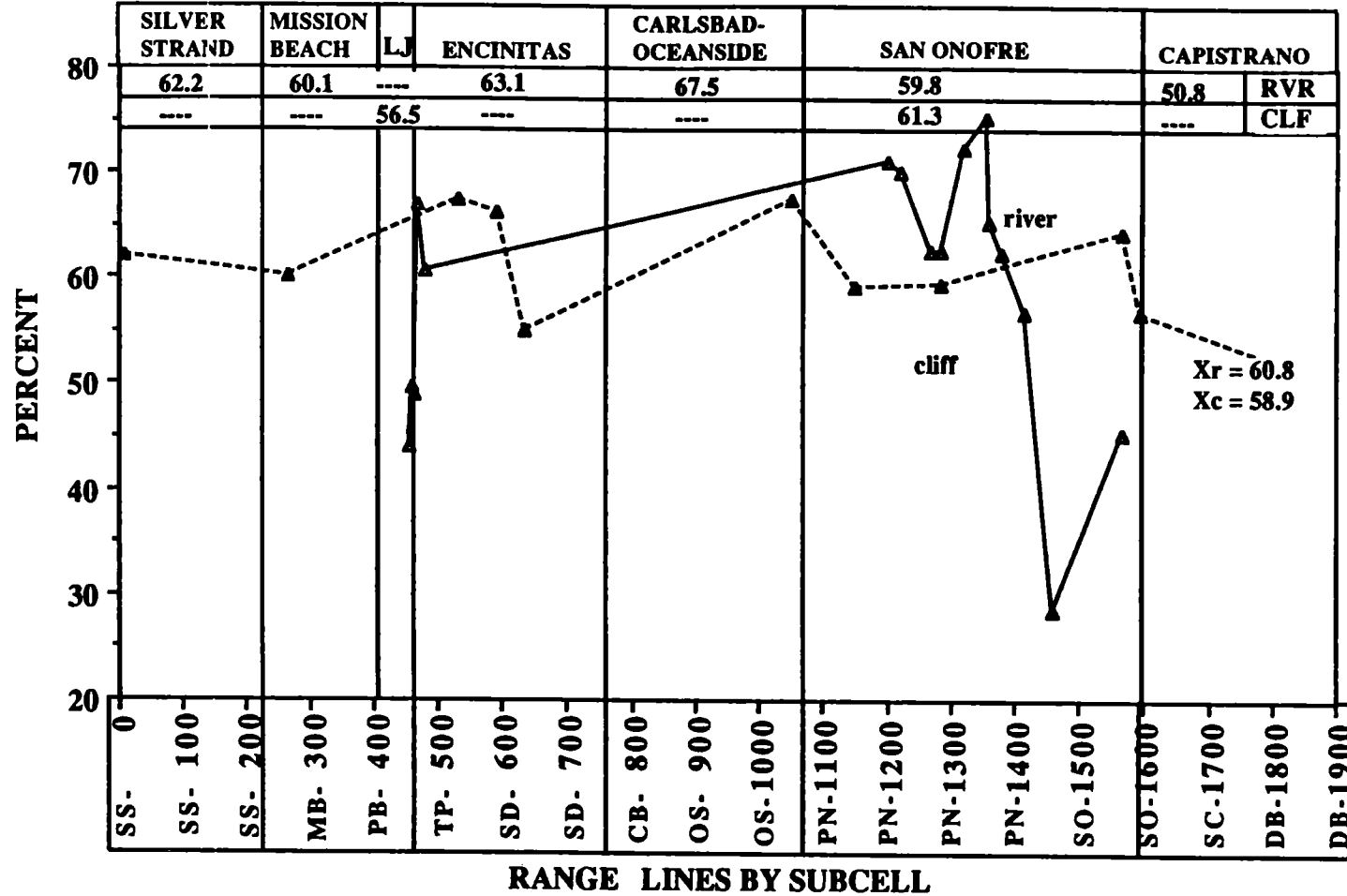
Figure 20. Line graph showing quartz percentages for all 1986 river and cliff samples.
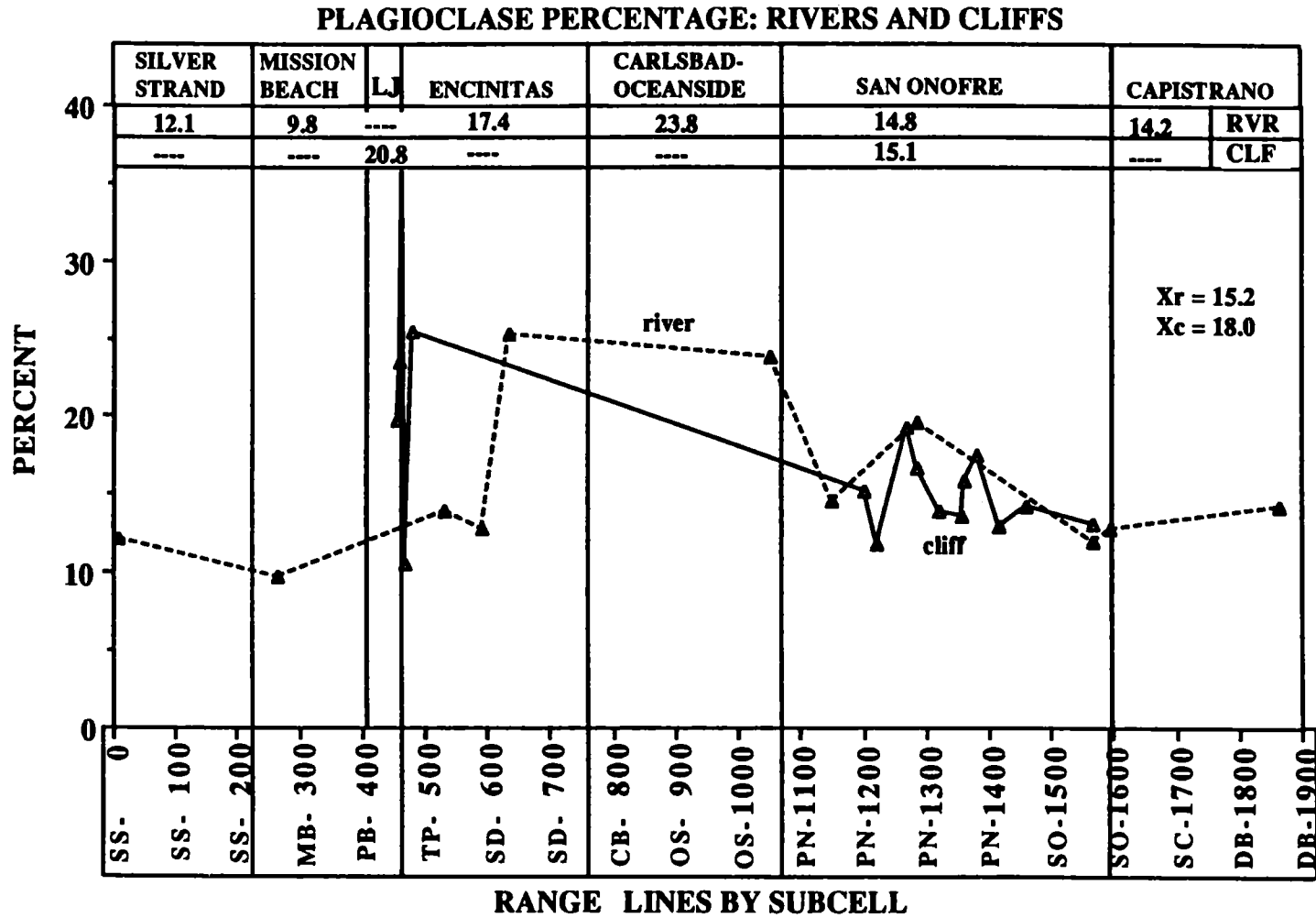
Figure 21. Line graph of plagioclase percentages for all 1986 river and cliff samples.

K-FELDSPAR PERCENT: RIVERS AND CLIFFS

SILVER STRAND	MISSION BEACH	LJ	ENCINITAS	CARLSBAD-OCEANSIDE	SAN ONOFRE	CAPISTRANO	
2.0	1.0	----	0.9	0.3	2.2	2.0	RVR
----	----	0.0	----	----	0.6	----	CLF

PERCENT

river

cliff

$Xr = 1.5$
$Xc = 0.3$

30
20
10
0

SS- 0
SS- 100
SS- 200
MB- 300
PB- 400
TP- 500
SD- 600
SD- 700
CB- 800
OS- 900
OS-1000
PN-1100
PN-1200
PN-1300
PN-1400
SO-1500
SO-1600
SC-1700
DB-1800
DB-1900

RANGE LINES BY SUBCELL
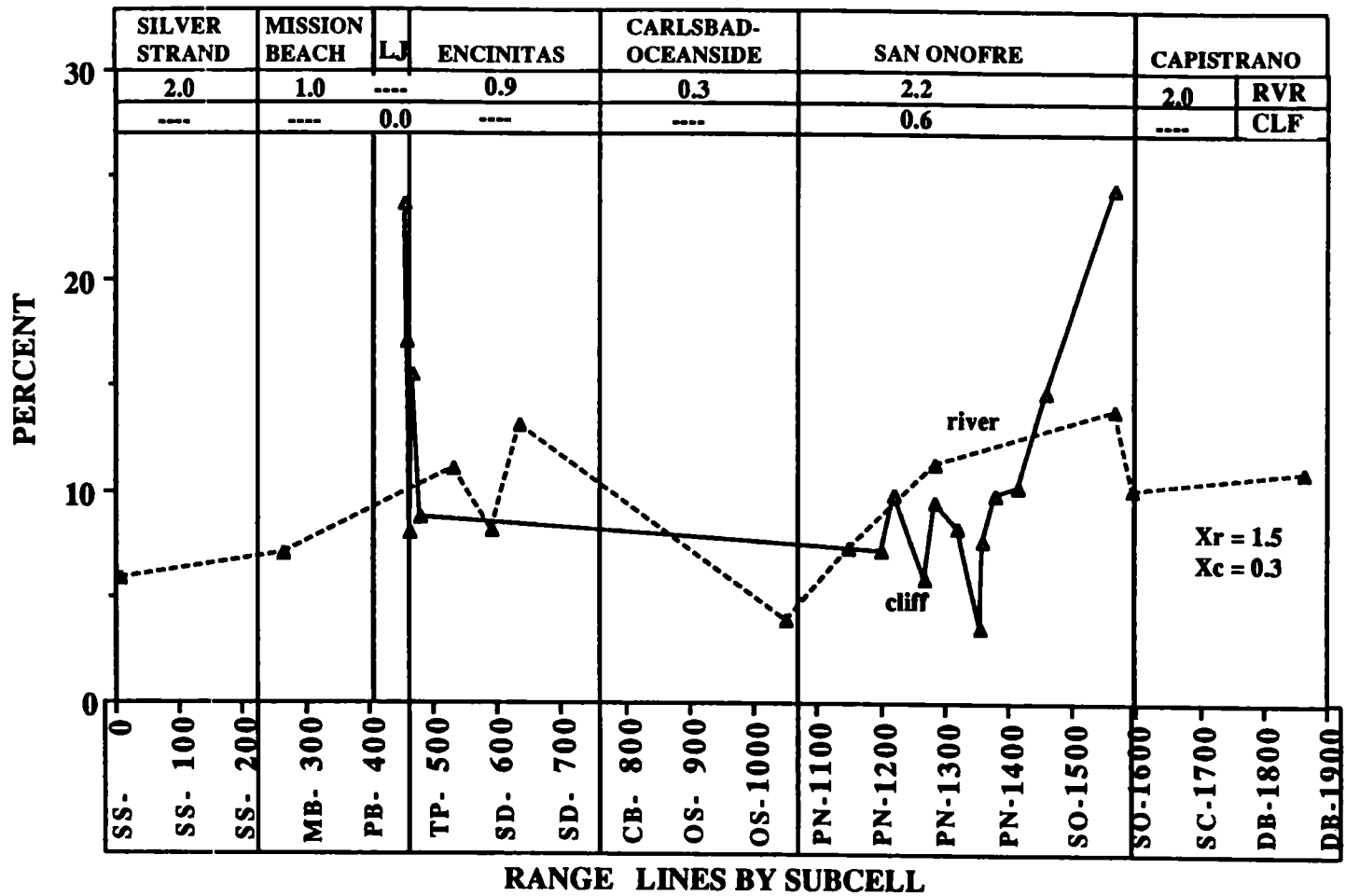
Figure 22. Line graph showing potassium feldspar percentages for all 1986 river and cliff samples.
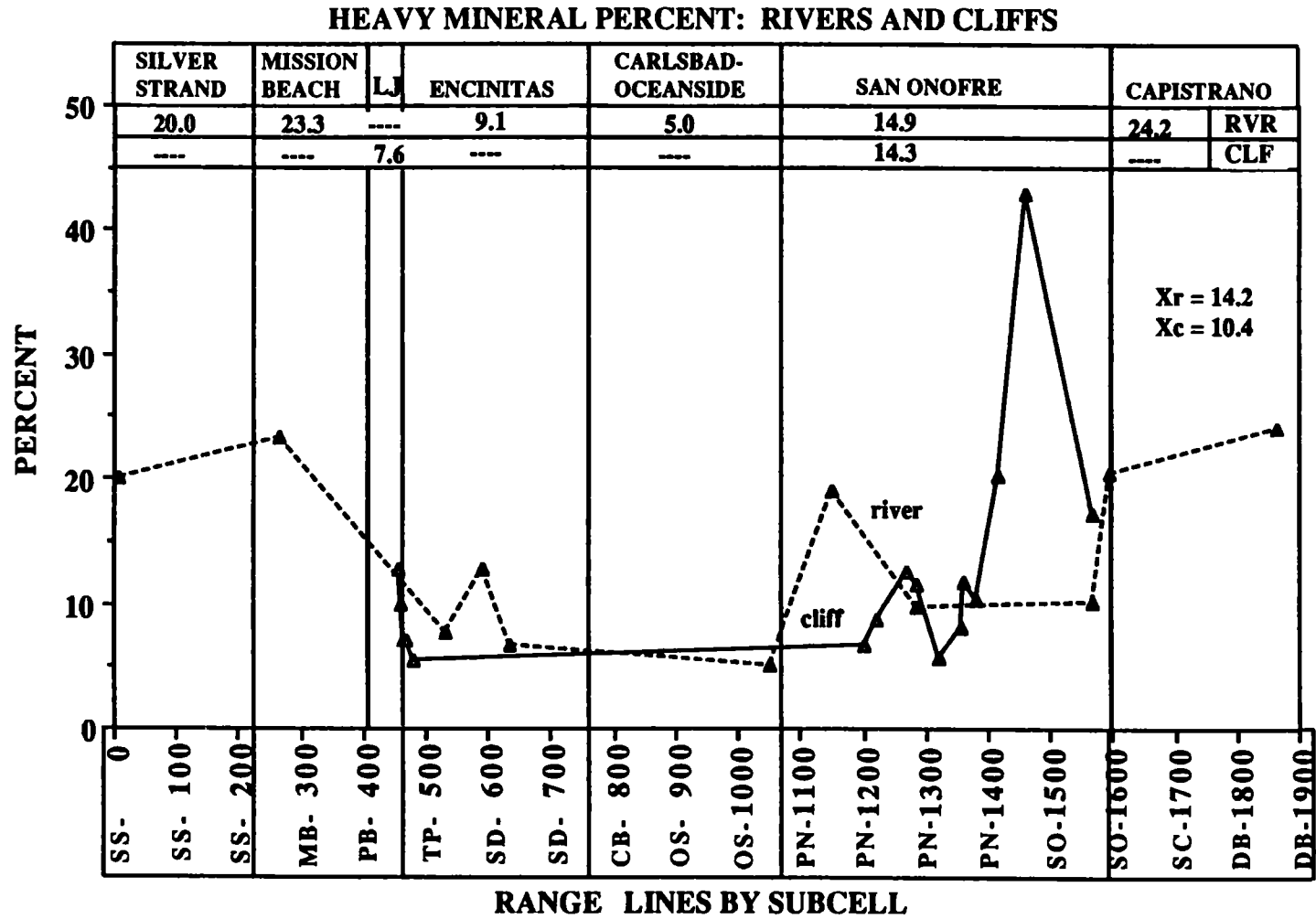
Figure 23. Line graph of heavy mineral percentages for all 1986 river and cliff samples.

19

BIOTITE PERCENTAGES: RIVERS AND CLIFFS

SILVER STRAND	MISSION BEACH	LJ	ENCINITAS	CARLSBAD-OCEANSIDE	SAN ONOFRE	CAPISTRANO	
3.0	17.7	----	8.9	25.7	4.6	0.7	RVR
----	----	36.9	----	----	29.5	----	CLF

Xr = 8.4
Xc = 33.2

cliff

river

PERCENT

RANGE LINES BY SUBCELL

62
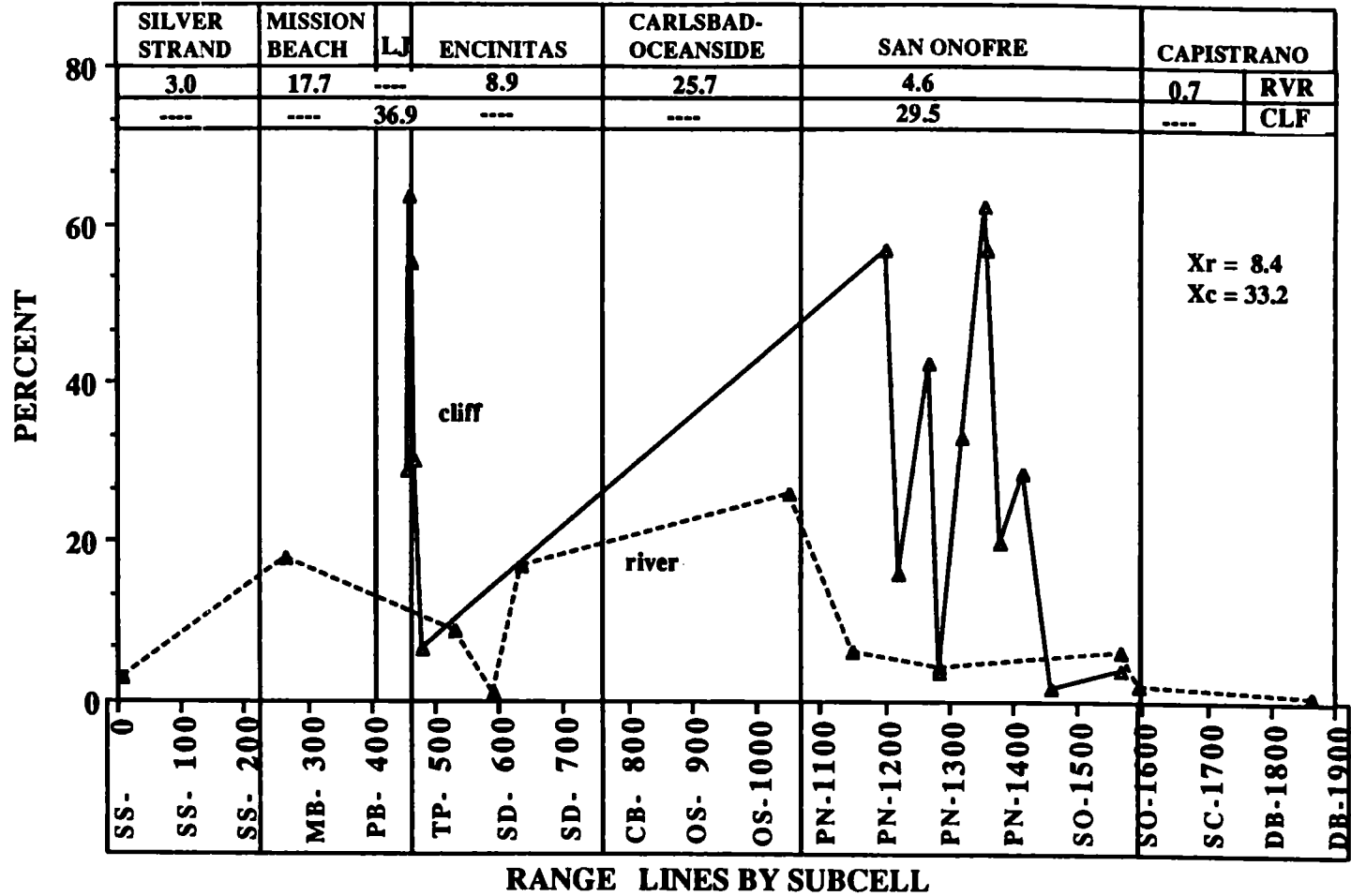
Figure 24. Line graph showing biotite percentages for all 1986 upland area samples.

COMPOSITE PERCENTAGES: RIVERS AND CLIFFS

SILVER STRAND	MISSION BEACH	LJ	ENCINITAS	CARLSBAD-OCEANSIDE	SAN ONOFRE	CAPISTRANO	
1.3	3.7	----	7.9	7.3	19.3	12.0	RVR
----	----	9.4	----	----	11.2	----	CLF
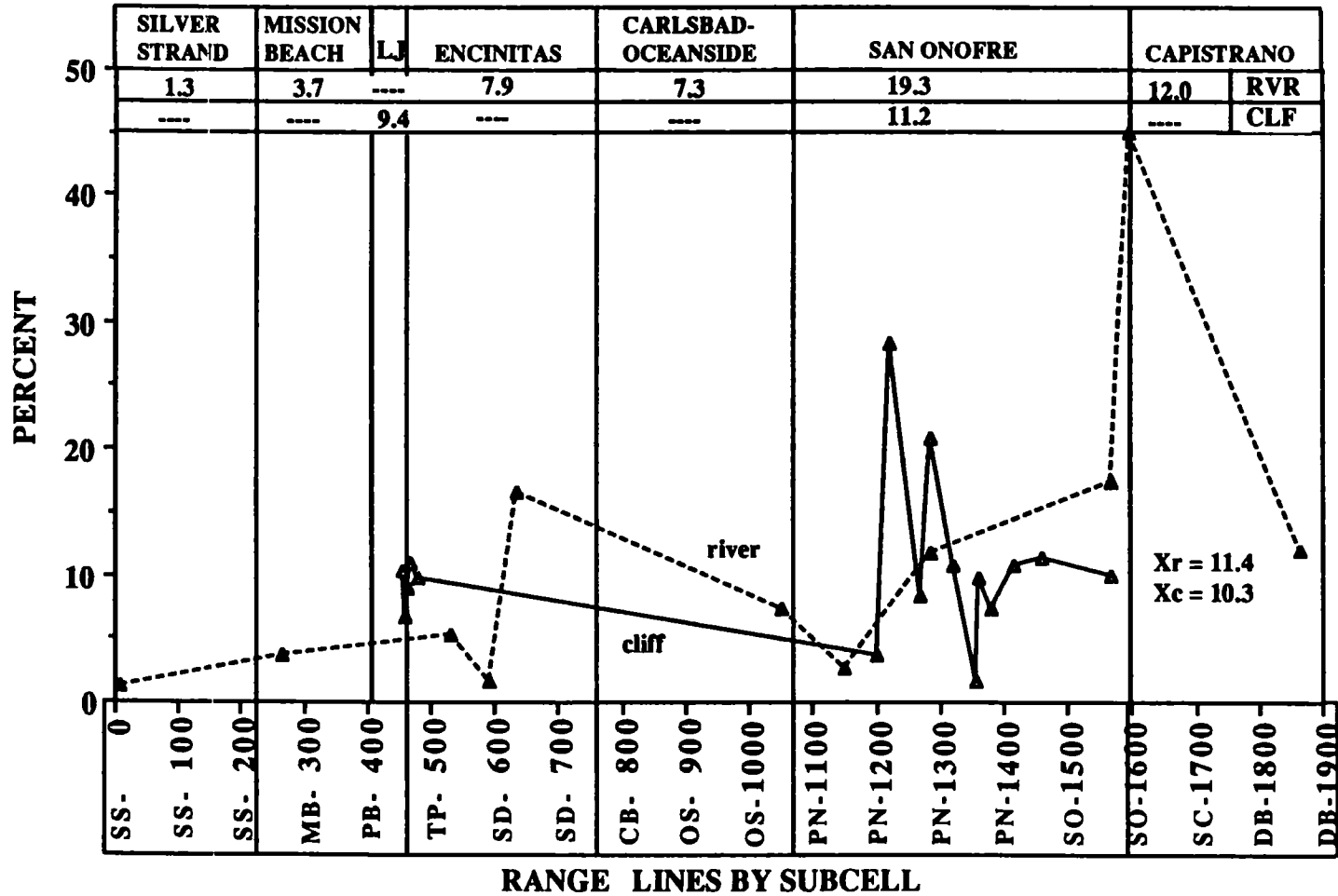
Figure 25. Line graph of composite particle percentages for all 1986 upland area samples.

EPIDOTE PERCENTAGES: RIVERS AND CLIFFS

SILVER STRAND	MISSION BEACH	LJ	ENCINITAS	CARLSBAD-OCEANSIDE	SAN ONOFRE	CAPISTRANO	
1.7	0.7	----	16.0	7.3	10.9	8.3	RVR
----	----	11.4	----	----	22.3	----	CLF

Xr = 10.0
Xc = 16.9

cliff

river

PERCENT

RANGE LINES BY SUBCELL

(x-axis: SS-0, SS-100, SS-200, MB-300, PB-400, TP-500, SD-600, SD-700, CB-800, OS-900, OS-1000, PN-1100, PN-1200, PN-1300, PN-1400, SO-1500, SO-1600, SC-1700, DB-1800, DB-1900)

64
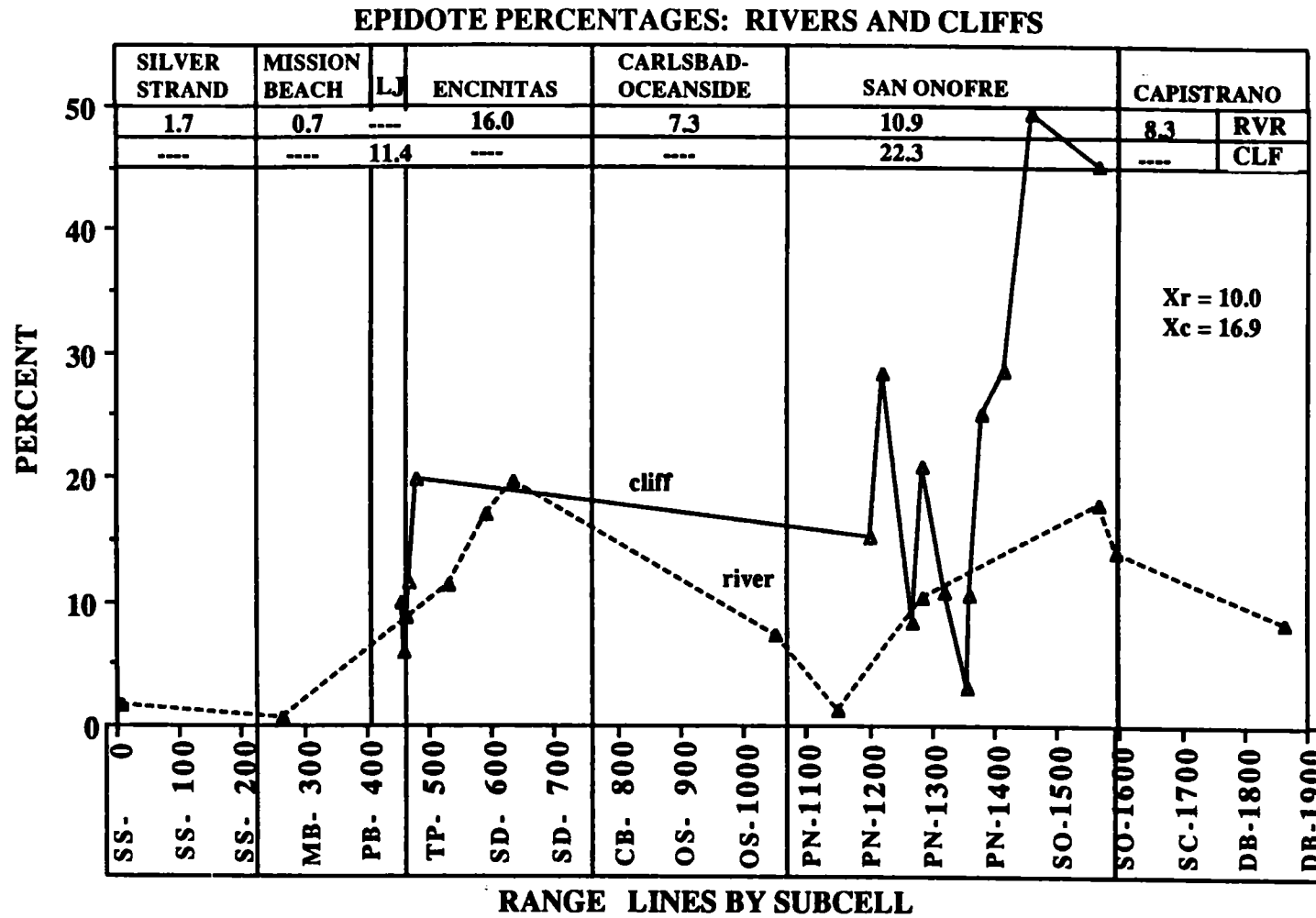
Figure 26. Line graph showing epidote percentages for all 1986 upland area samples.

GARNET PERCENTAGES: RIVERS AND CLIFFS

SILVER STRAND	MISSION BEACH	LJ	ENCINITAS	CARLSBAD-OCEANSIDE	SAN ONOFRE	CAPISTRANO	
0.0	0.0	---	1.3	0.3	0.3	8.0	RVR
----	----	---	1.1	----	1.5	----	CLF

Xr = 2.4
Xc = 1.3
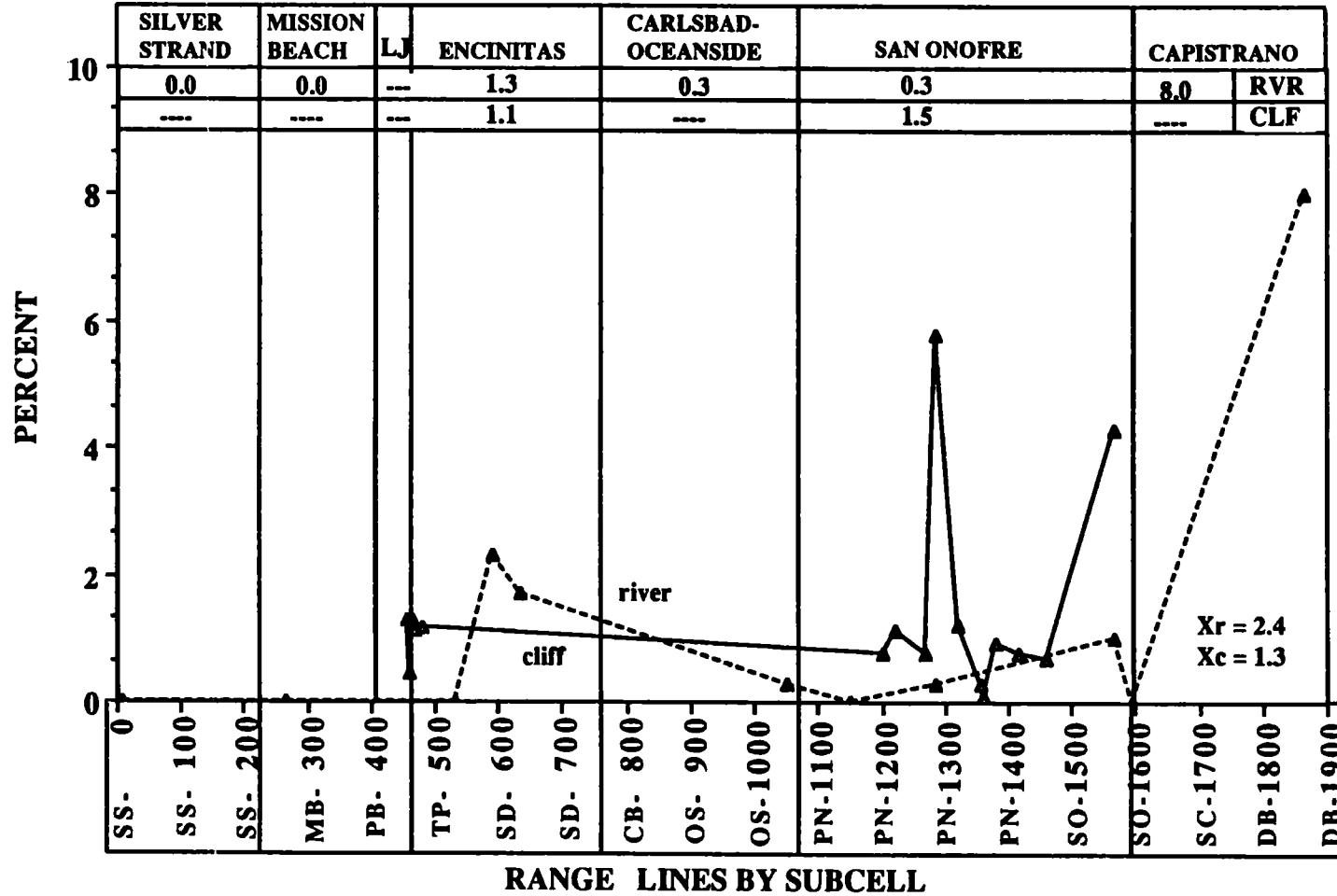
Figure 27. Line graph showing garnet percentages for all 1986 upland area samples.

GLAUCOPHANE PERCENT: RIVERS AND CLIFFS

SILVER STRAND	MISSION BEACH	LJ	ENCINITAS	CARLSBAD-OCEANSIDE	SAN ONOFRE	CAPISTRANO	
0.0	0.0	---	6.6	0.3	1.8	0.0	RVR
----	----	---	0.1	----	5.7	----	CLF

Xr = 1.3
Xc = 2.9

PERCENT

RANGE LINES BY SUBCELL

SS-0, SS-100, SS-200, MB-300, PB-400, TP-500, SD-600, SD-700, CB-800, OS-900, OS-1000, PN-1100, PN-1200, PN-1300, PN-1400, SO-1500, SO-1600, SC-1700, DB-1800, DB-1900
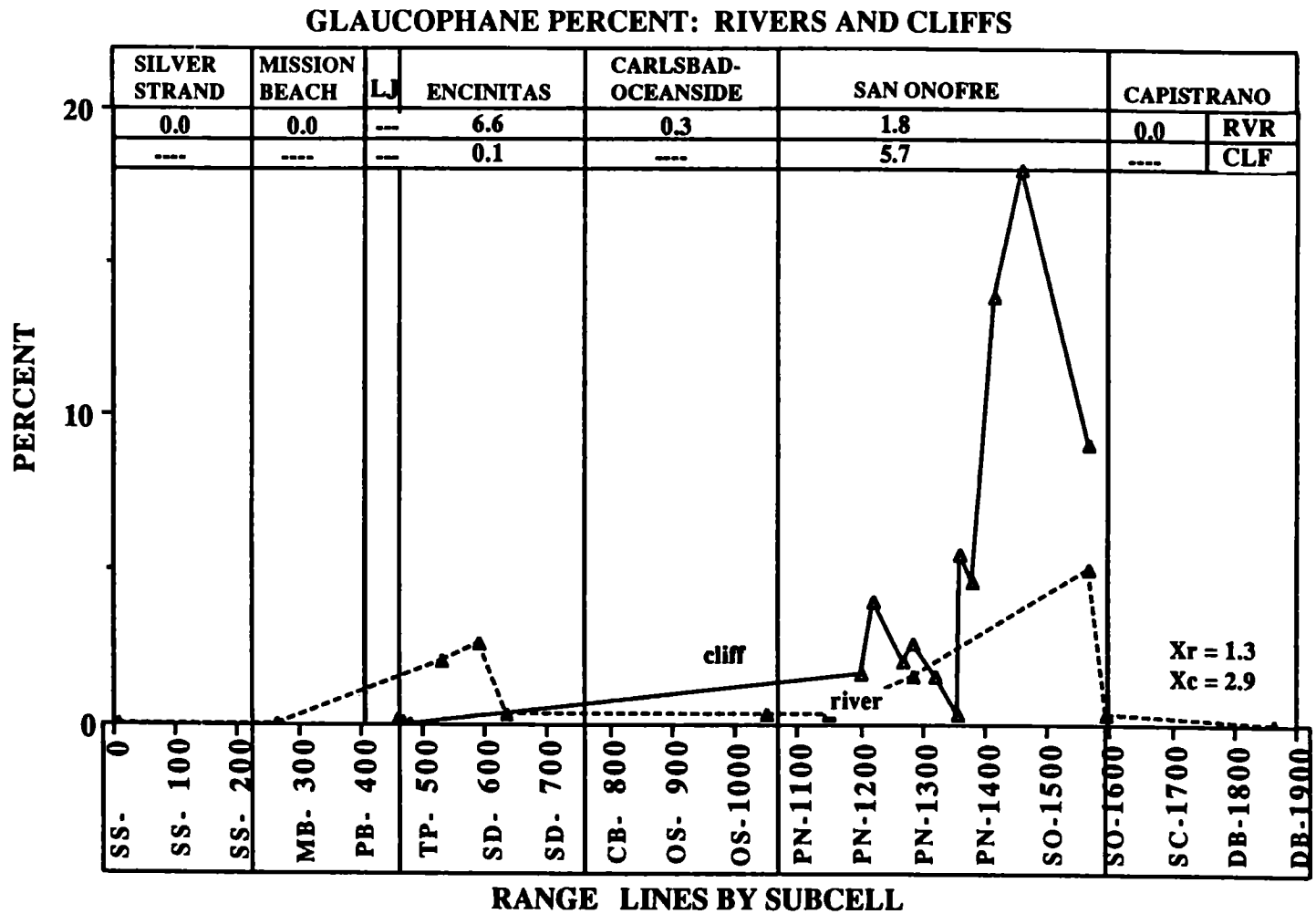
Figure 28. Line graph showing hornblende percentages for all 1986 upland area samples.

HORNBLENDE PERCENTAGES: RIVER AND CLIFFS

SILVER STRAND	MISSION BEACH	LJ	ENCINITAS	CARLSBAD-OCEANSIDE	SAN ONOFRE	CAPISTRANO	
89.0	74.3	----	51.6	54.3	56.8	34.3	RVR
----	----	22.9	----	----	22.1	----	CLF

Xr = 57.7
Xc = 22.5
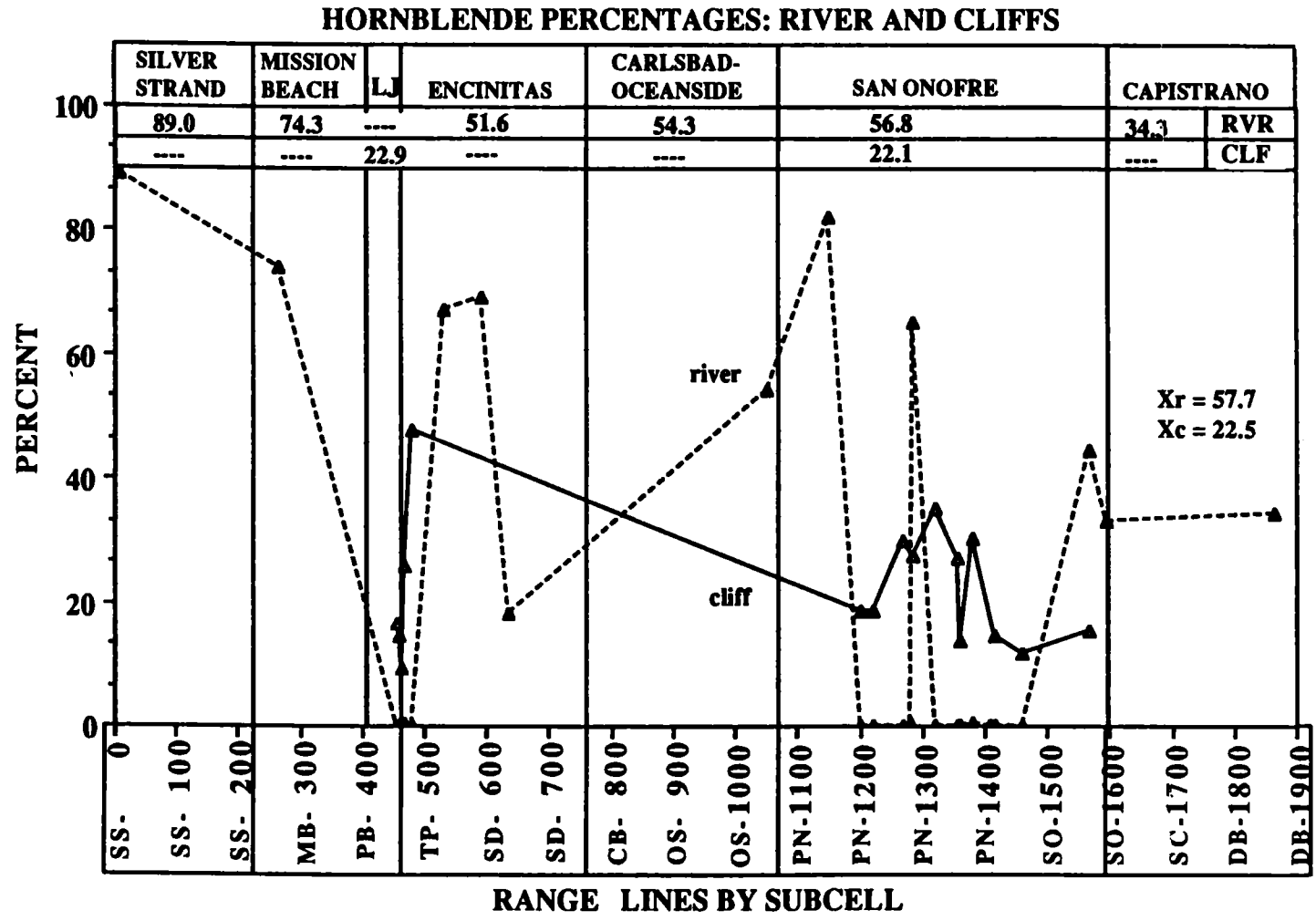
Figure 29. Line graph showing hornblende percentages for all 1986 upland area samples.

HYPERSTHENE PERCENT: RIVERS AND CLIFFS

SILVER STRAND	MISSION BEACH	LJ	ENCINITAS	CARLSBAD-OCEANSIDE	SAN ONOFRE	CAPISTRANO	
2.0	1.0	----	0.9	0.3	2.2	2.0	RVR
----	----	0.0	----	----	0.6	----	CLF

PERCENT

river

cliff

Xr = 1.5
Xc = 0.3

SS- 0
SS- 100
SS- 200
MB- 300
PB- 400
TP- 500
SD- 600
SD- 700
CB- 800
OS- 900
OS-1000
PN-1100
PN-1200
PN-1300
PN-1400
SO-1500
SO-1600
SC-1700
DB-1800
DB-1900

RANGE LINES BY SUBCELL
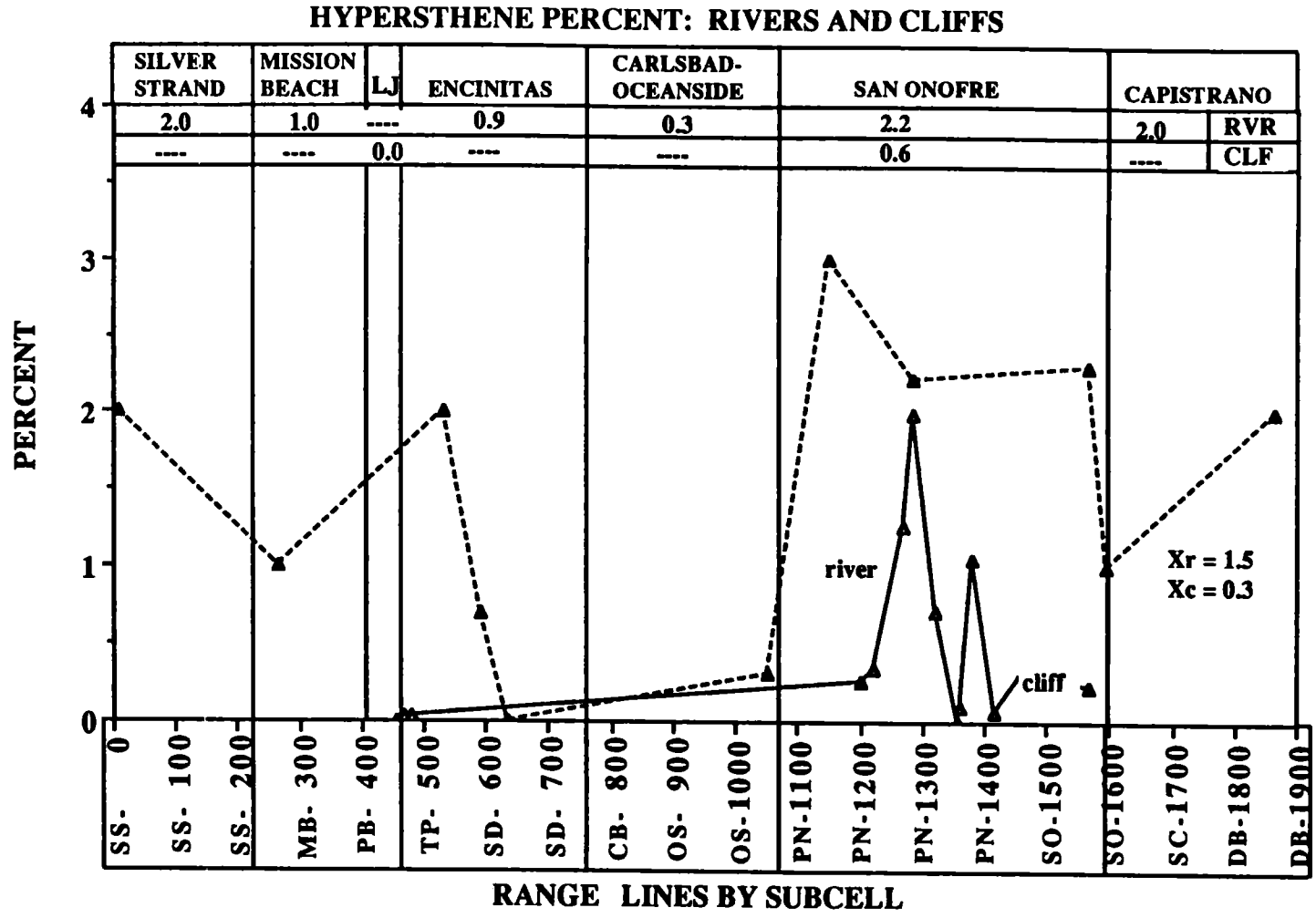
Figure 30. Line graph showing hypersthene percentages for all 1986 upland area samples.

OPAQUE GRAINS: RIVERS AND CLIFFS

SILVER STRAND	MISSION BEACH	LJ	ENCINITAS	CARLSBAD-OCEANSIDE	SAN ONOFRE	CAPISTRANO	
0.3	1.7	----	5.2	0.7	2.3	27.7	RVR
----	----	12.2	----	----	3.9	----	CLF

PERCENT

30

20

10

0

river

cliff

Xr = 2.9
Xc = 5.0

SS- 0
SS- 100
SS- 200
MB- 300
PB- 400
TP- 500
SD- 600
SD- 700
CB- 800
OS- 900
OS-1000
PN-1100
PN-1200
PN-1300
PN-1400
SO-1500
SO-1600
SC-1700
DB-1800
DB-1900

RANGE LINES BY SUBCELL

69
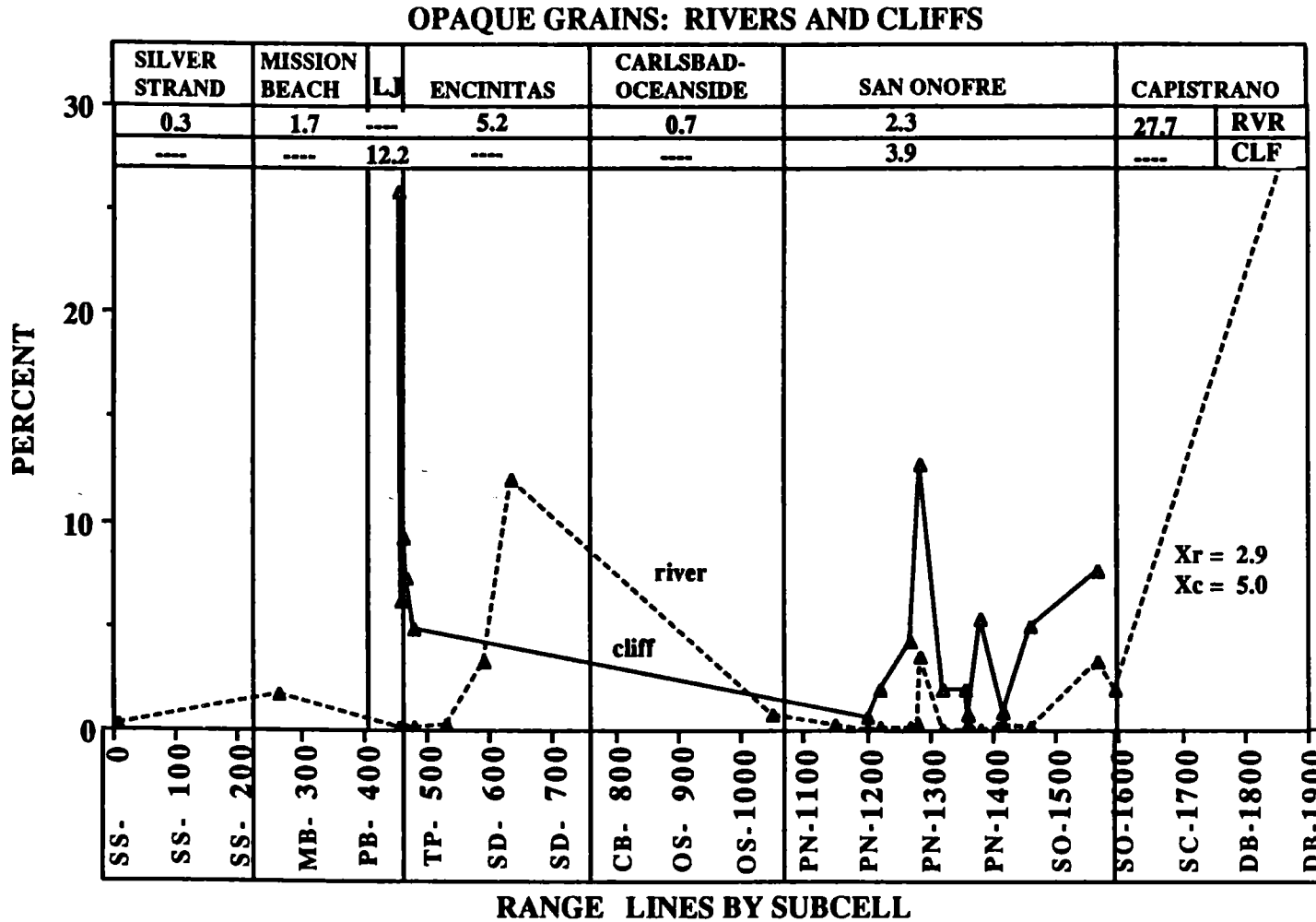
Figure 31. Line graph showing opaque percentages for all 1986 upland area samples.

SPHENE PERCENTAGES: RIVERS AND CLIFFS

SILVER STRAND	MISSION BEACH	LJ	ENCINITAS	CARLSBAD-OCEANSIDE	SAN ONOFRE	CAPISTRANO	
1.7	0.7	----	5.8	2.7	2.2	5.7	RVR
----	----	6.9	----	----	2.5	----	CLF
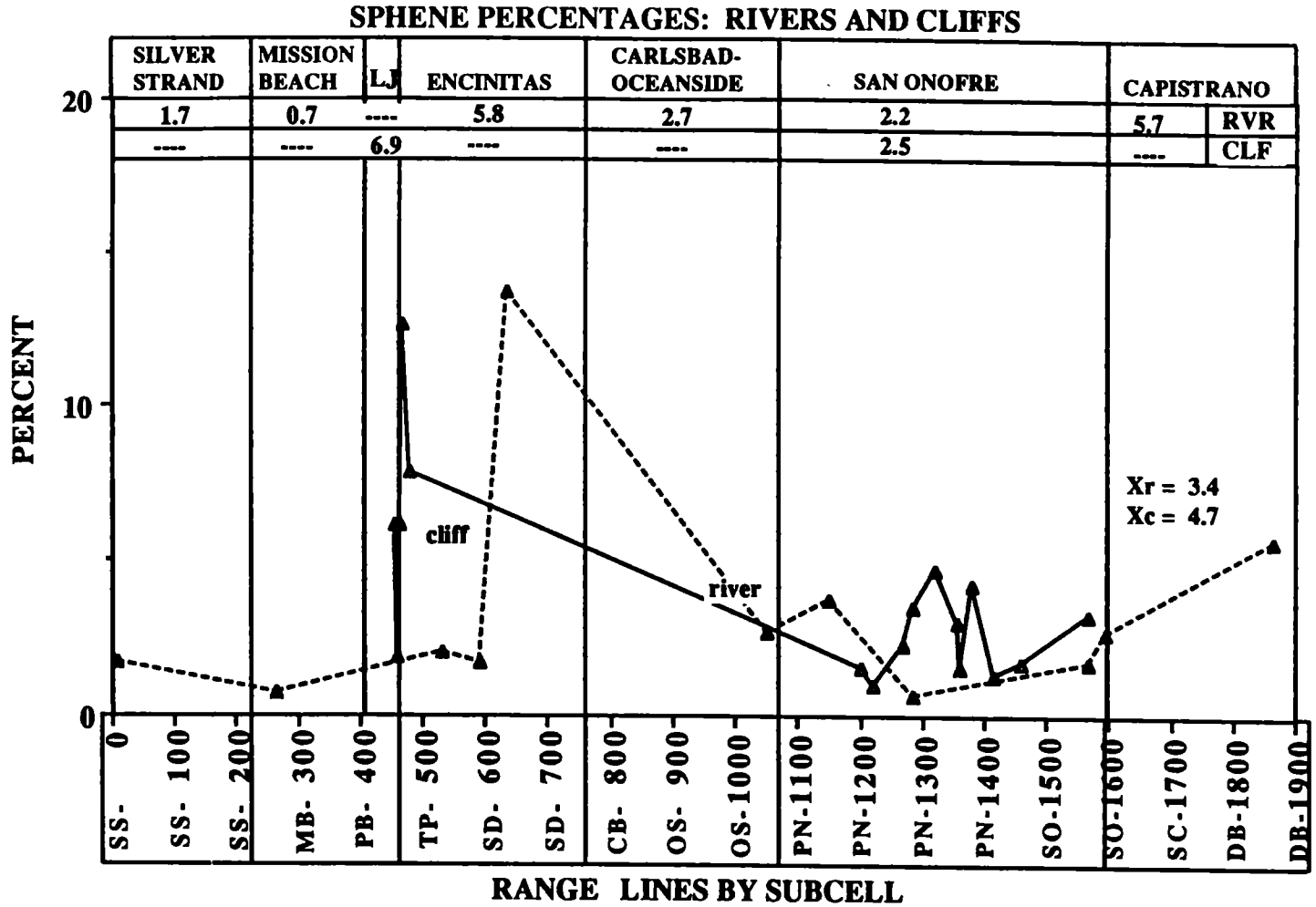
Figure 32. Line graph showing sphene percentages for all 1986 upland area samples.

ACTINOLITE PERCENTAGES: RIVERS AND CLIFFS

SILVER STRAND	MISSION BEACH	LJ	ENCINITAS	CARLSBAD-OCEANSIDE	SAN ONOFRE	CAPISTRANO	
0.0	0.0	----	0.0	0.2	0.4	0.3	RVR
----	----	0.0	----	----	0.3	----	CLF

PERCENT

0.5
0.4
0.3
0.2
0.1
0.0

river

cliff

Xr = 0.3
Xc = 0.4

SS-0 SS-100 SS-200 MB-300 PB-400 TP-500 SD-600 SD-700 CB-800 OS-900 OS-1000 OS-1100 PN-1200 PN-1300 PN-1400 PN-1500 SO-1600 SO-1700 SC-1800 DB-1900 DB-2000

RANGE LINES BY SUBCELL
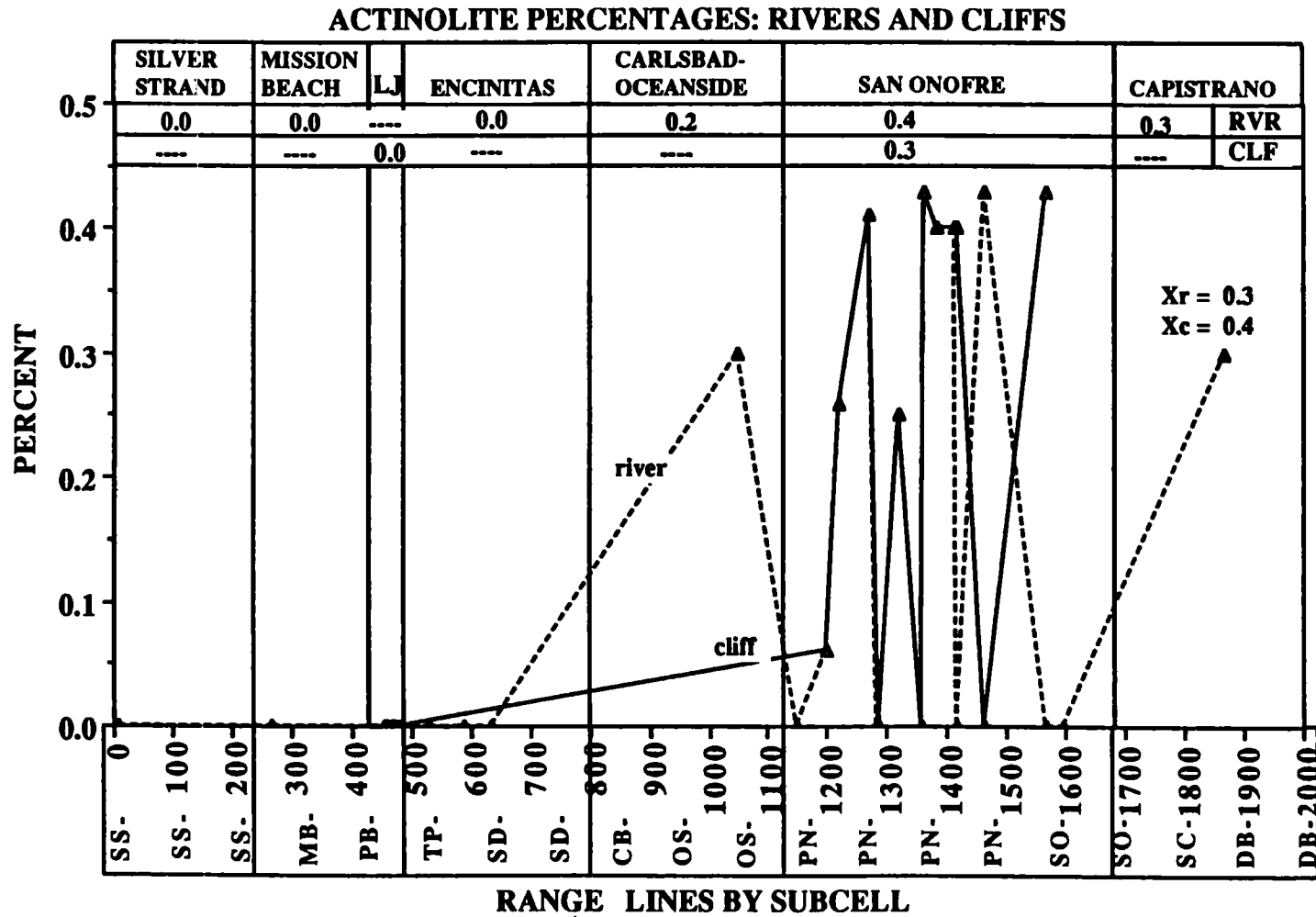
Figure 33. Line graph showing actinolite percentages for all 1986 river and cliff samples.

APATITE PERCENTAGES: RIVERS AND CLIFFS

SILVER STRAND	MISSION BEACH	LJ	ENCINITAS	CARLSBAD-OCEANSIDE	SAN ONOFRE	CAPISTRANO	
0.0	0.0	----	0.0	0.3	0.0	0.0	RVR
----	----	----	0.3	----	0.1	----	CLF

Xr = 0.0
Xc = 0.2

Figure 34. Line graph showing apatite percentages for all 1986 river and cliff samples.

AUGITE PERCENTAGES: RIVERS AND CLIFFS

SILVER STRAND	MISSION BEACH	LJ	ENCINITAS	CARLSBAD-OCEANSIDE	SAN ONOFRE	CAPISTRANO	
0.7	0.3	---	0.3	0.0	0.3	0.7	RVR
----	----	---	0.1	----	0.1	---	CLF

Xr = 0.4
Xc = 0.1

river

cliff

PERCENT

1.2
1.0
0.8
0.6
0.4
0.2
0.0

SS-0 SS-100 SS-200 MB-300 PB-400 TP-500 SD-600 SD-700 CB-800 OS-900 OS-1000 PN-1100 PN-1200 PN-1300 PN-1400 SO-1500 SO-1600 SC-1700 DB-1800 DB-1900

RANGE LINES BY SUBCELL
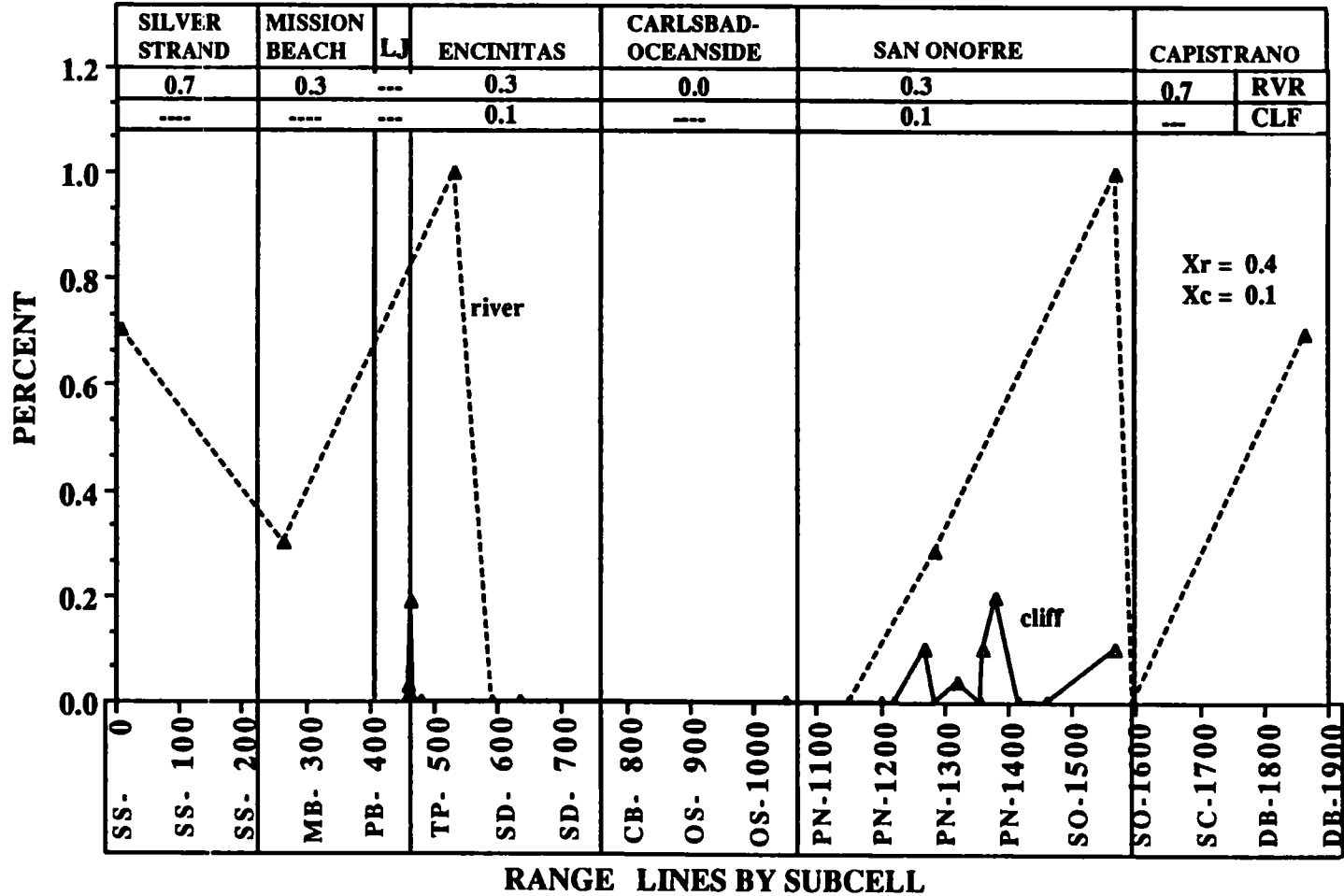
Figure 35. Line graph showing augite percentages for all 1986 river and cliff samples.

OLIVINE PERCENTAGES: RIVERS AND CLIFFS

SILVER STRAND	MISSION BEACH	LJ	ENCINITAS	CARLSBAD-OCEANSIDE	SAN ONOFRE	CAPISTRANO	
0.0	0.0	----	0.0	0.0	0.0	0.0	RVR
----	----	----	0.0	----	0.1	----	CLF

Xr = 0.0
Xc = 0.1

PERCENT

cliff

river

SS- 0 SS- 100 SS- 200 MB- 300 PB- 400 TP- 500 SD- 600 SD- 700 CB- 800 OS- 900 OS-1000 PN-1100 PN-1200 PN-1300 PN-1400 SO-1500 SO-1600 SC-1700 DB-1800 DB-1900

RANGE LINES BY SUBCELL
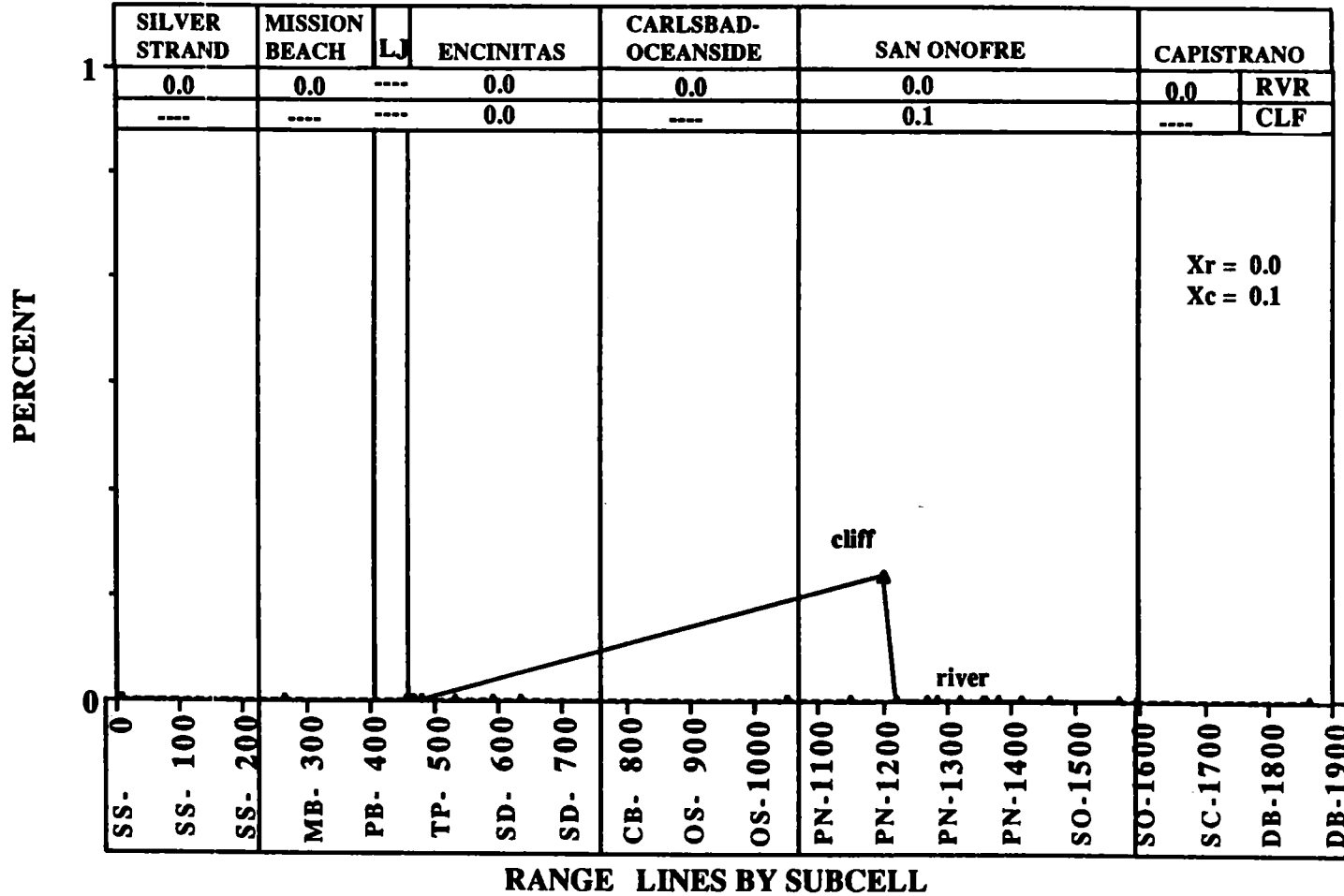
Figure 36. Line graph showing olivine percentages for all 1986 upland area samples.

ZIRCON PERCENTAGES: RIVERS AND CLIFFS

SILVER STRAND	MISSION BEACH	LJ	ENCINITAS	CARLSBAD-OCEANSIDE	SAN ONOFRE	CAPISTRANO	
0.0	0.0	----	0.0	0.3	0.0	0.2	RVR
----	----	----	0.2	----	0.1	----	CLF

PERCENT

0.4

0.3

0.2

0.1

0.0

cliff

river

$Xr = 0.1$
$Xc = 0.2$

SS- 0 SS- 100 SS- 200 MB- 300 PB- 400 TP- 500 SD- 600 SD- 700 CB- 800 OS- 900 OS-1000 PN-1100 PN-1200 PN-1300 PN-1400 SO-1500 SO-1600 SC-1700 DB-1800 DB-1900

RANGE LINES BY SUBCELL
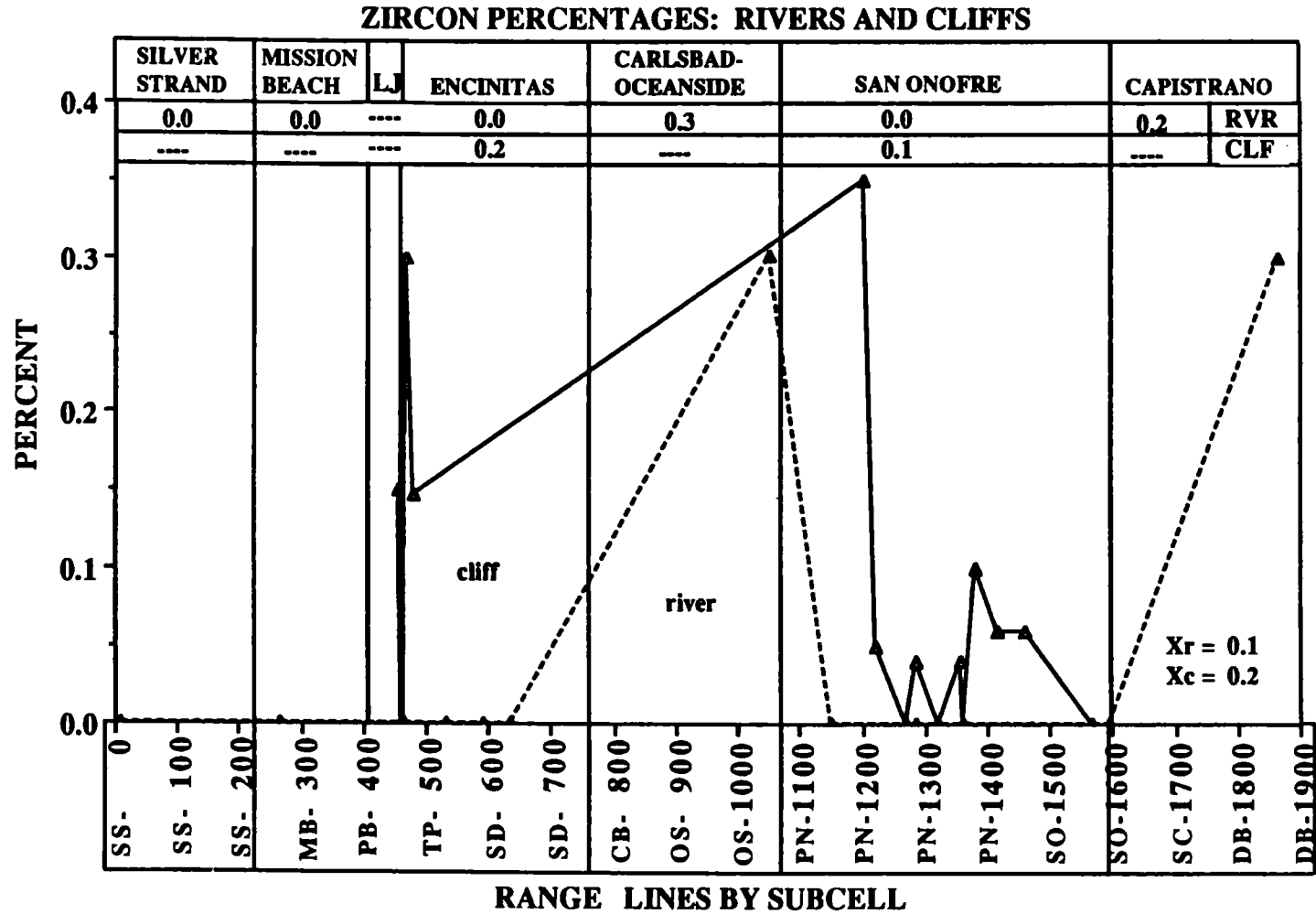
Figure 37. Line graph showing zircon percentages for all 1986 upland area samples.

ZOISITE PERCENTAGES: RIVERS AND CLIFFS

SILVER STRAND	MISSION BEACH	LJ	ENCINITAS	CARLSBAD-OCEANSIDE	SAN ONOFRE	CAPISTRANO	
0.0	0.0	----	0.1	0.0	0.0	0.0	RVR
----	----	----	0.3	----	0.2	----	CLF

0.4

0.3

PERCENT

0.2

0.1

0.0

river

cliff

Xr = 0.0
Xc = 0.2

SS- 0
SS- 100
SS- 200
MB- 300
PB- 400
TP- 500
SD- 600
SD- 700
CB- 800
OS- 900
OS- 1000
PN-1100
PN-1200
PN-1300
PN-1400
SO-1500
SO-1600
SC-1700
DB-1800
DB-1900

RANGE LINES BY SUBCELL
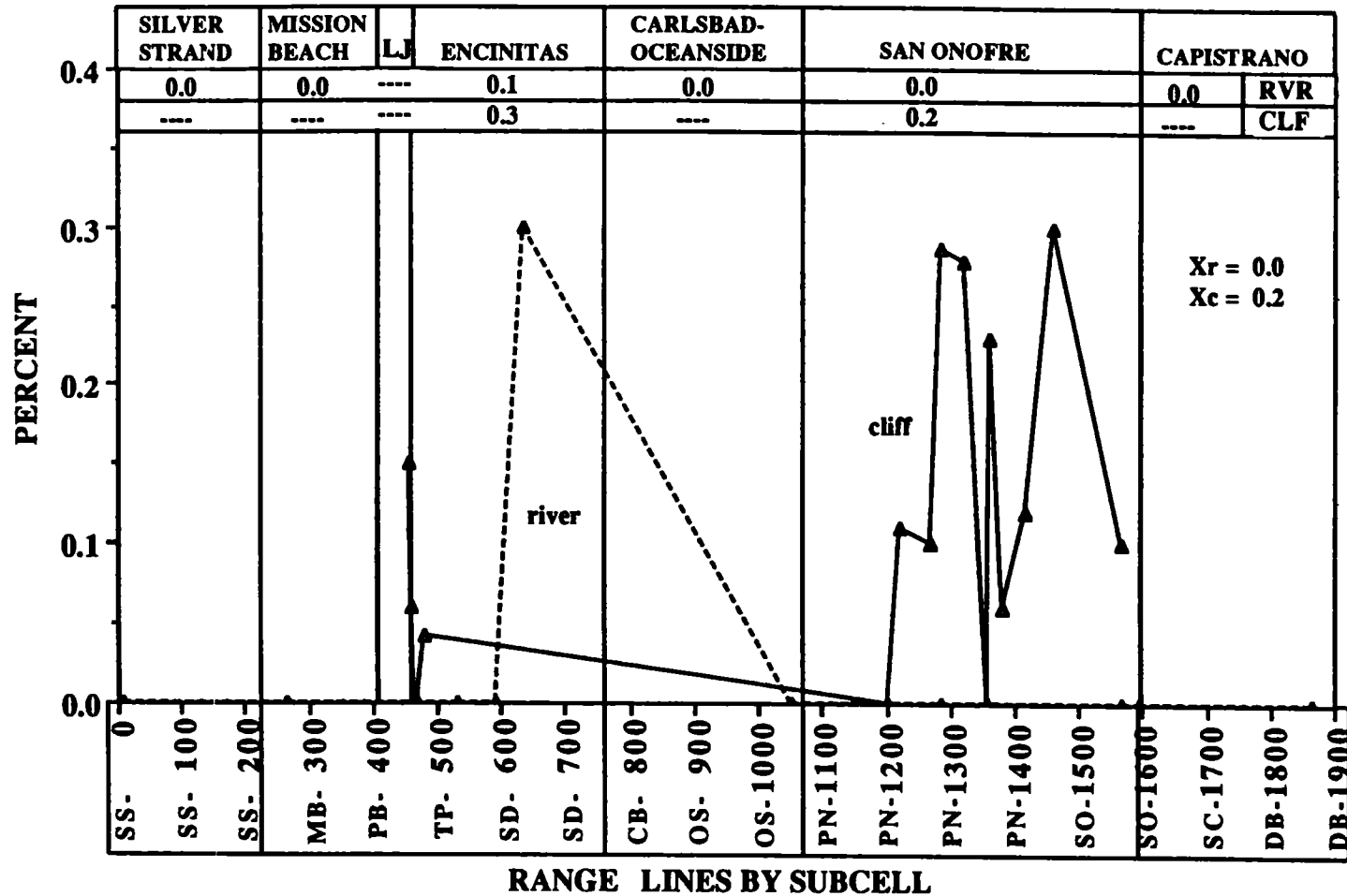
Figure 38. Line graph showing zoisite percentages for all 1986 upland area samples.

QUARTZ PERCENTAGES FOR 1986 BEACHES

SILVER STRAND	MISSION BEACH	LJ	ENCINITAS	CARLSBAD-OCEANSIDE	SAN ONOFRE	CAPISTRANO	
69.0	75.2	-	62.5	68.7	63.2	56.7	86W
65.9	74.2	-	65.2	66.7	58.3	65.7	86S

PERCENT (y-axis: 30, 40, 50, 60, 70, 80)

summer

winter

Xw = 63.6
Xs = 63.9

X-axis labels: SS-0, SS-100, SS-200, MB-300, PB-400, TP-500, SD-600, SD-700, CB-800, OS-900, OS-1000, PN-1100, PN-1200, PN-1300, PN-1400, SO-1500, SO-1600, SC-1700, DB-1800, DB-1900

RANGE LINES BY SUBCELL
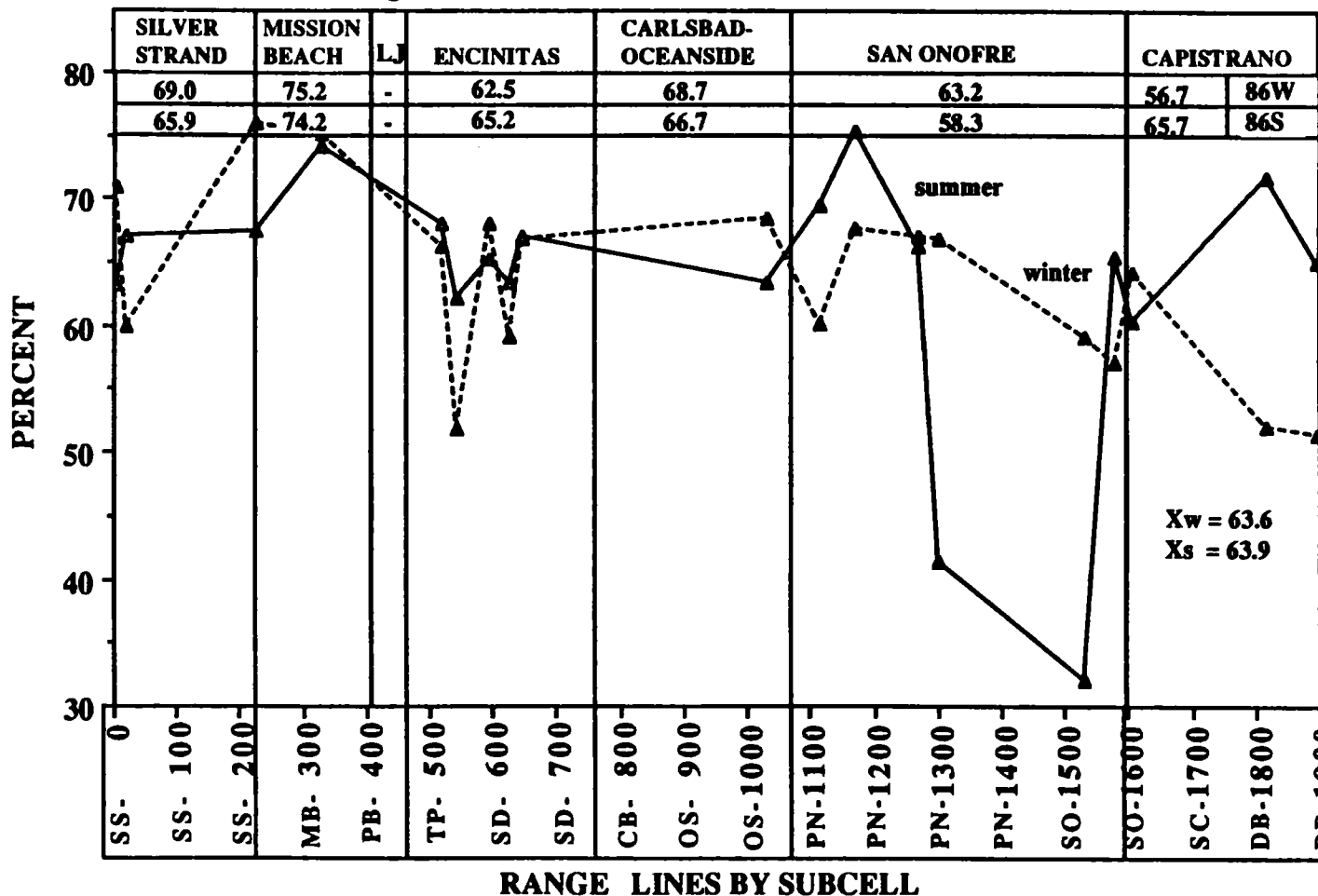
Figure 39.   Line graph showing quartz percentages for all 1986 beach samples.

PLAGIOCLASE PERCENTAGES FOR 1986 BEACHES

SILVER STRAND	MISSION BEACH	LJ	ENCINITAS	CARLSBAD-OCEANSIDE	SAN ONOFRE	CAPISTRANO	
15.0	9.2	-	15.6	10.6	13.7	12.9	86W
9.8	2.7	-	6.4	8.3	9.1	10.5	86S

winter

summer

Xw = 13.9
Xs = 8.3

PERCENT

RANGE LINES BY SUBCELL
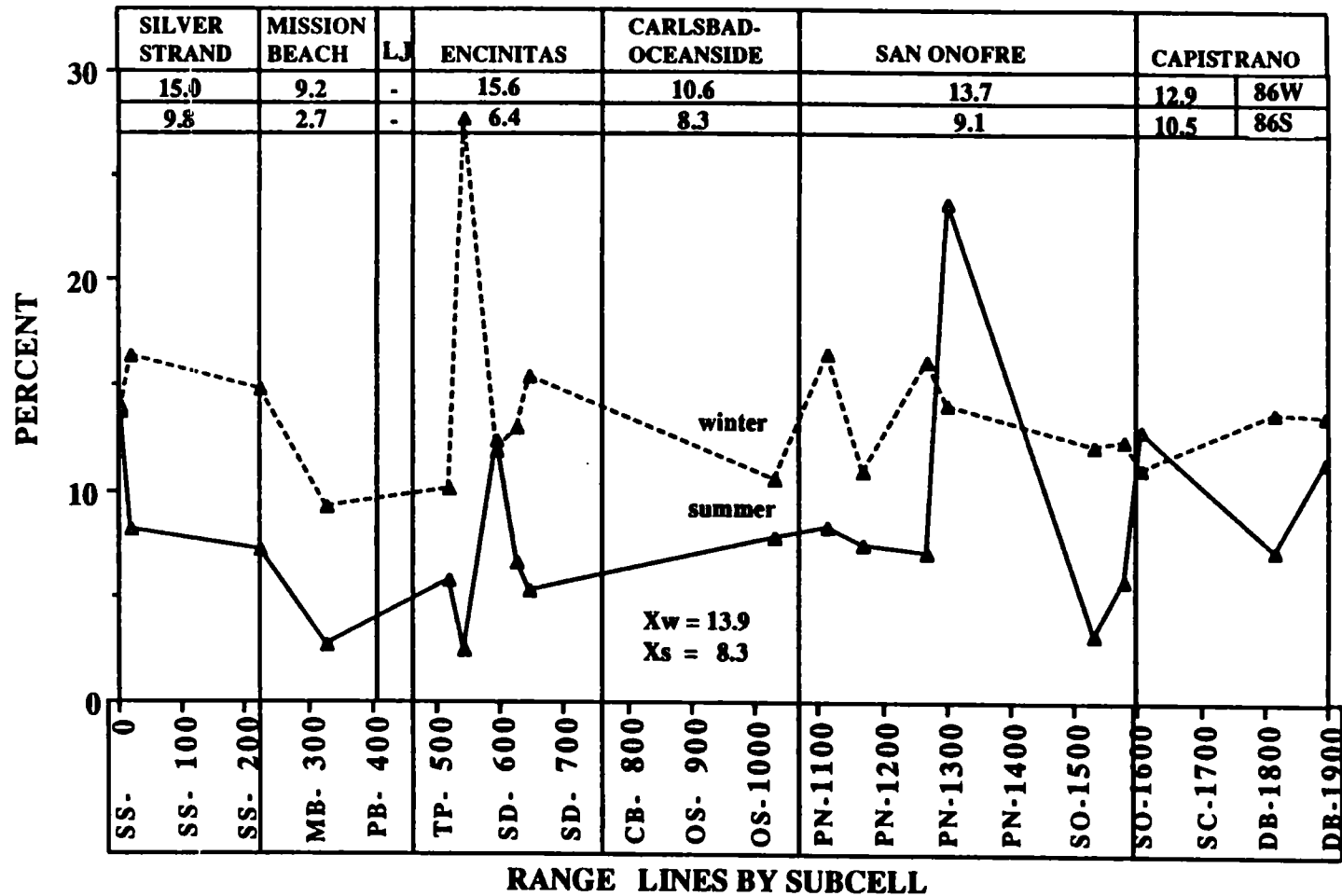
Figure 40. Line graph of plagioclase percentages for all 1986 beach samples.

78

K-FELDSPAR PERCENTAGES FOR 1986 BEACHES

SILVER STRAND	MISSION BEACH	LJ	ENCINITAS	CARLSBAD-OCEANSIDE	SAN ONOFRE	CAPISTRANO	
7.0	4.8	-	7.4	8.9	11.3	12.5	86W
12.7	11.8	-	9.4	9.1	10.4	11.6	86S

summer

winter

$X_w = 9.3$
$X_s = 10.7$

PERCENT

RANGE LINES BY SUBCELL

SS- 0, SS- 100, SS- 200, MB- 300, PB- 400, TP- 500, SD- 600, SD- 700, CB- 800, OS- 900, OS-1000, PN-1100, PN-1200, PN-1300, PN-1400, SO-1500, SO-1600, SC-1700, DB-1800, DB-1900
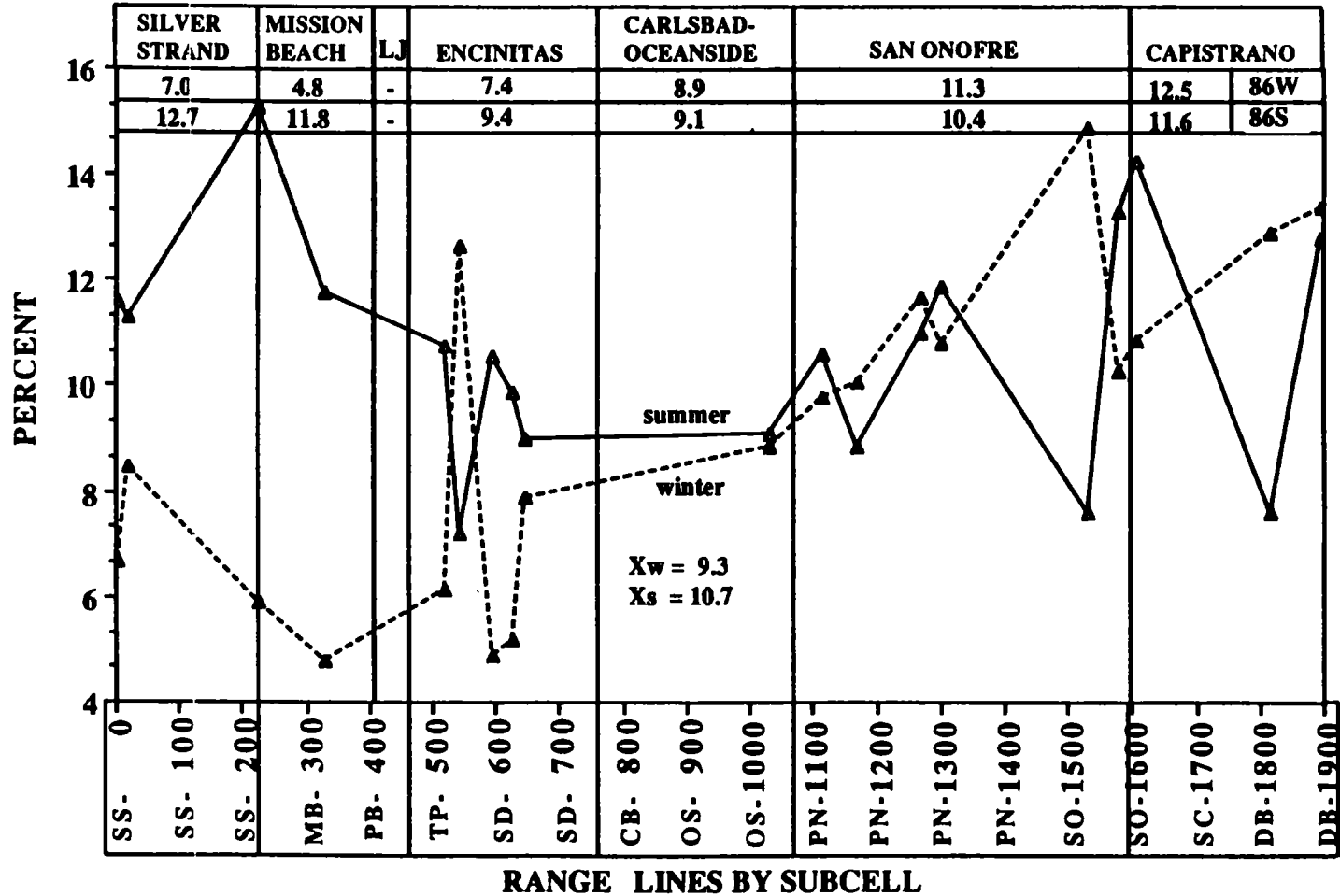
Figure 41. Line graph showing potassium feldspar percentages for all 1986 beach samples.

HEAVY MINERAL PERCENTAGES: 1986 BEACHES

SILVER STRAND	MISSION BEACH	LJ	ENCINITAS	CARLSBAD-OCEANSIDE	SAN ONOFRE	CAPISTRANO	
9.1	10.9	-	14.6	12.0	12.1	19.2	86W
11.8	11.4	-	18.6	16.1	21.7	12.4	86S

Xw = 13.3
Xs = 17.0

summer

winter

PERCENT

60
50
40
30
20
10
0

SS-0   SS-100   SS-200   MB-300   PB-400   TP-500   SD-600   SD-700   CB-800   OS-900   OS-1000   PN-1100   PN-1200   PN-1300   PN-1400   SO-1500   SO-1600   SC-1700   DB-1800   DB-1900

RANGE LINES BY SUBCELL

80
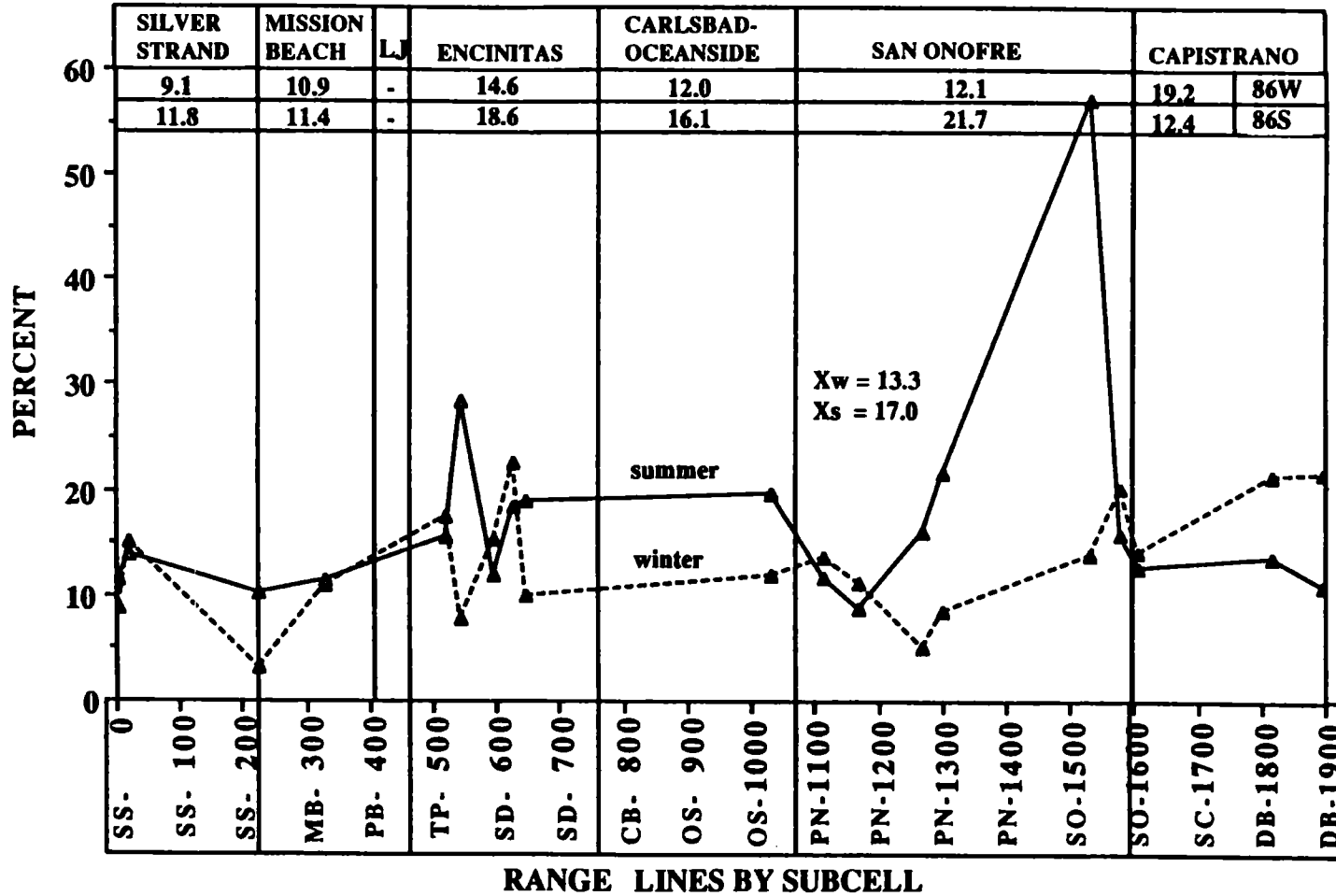
Figure 42. Line graph of heavy mineral percentages for all 1986 beach samples.

BIOTITE PERCENTAGES FOR 1986 BEACHES

SILVER STRAND	MISSION BEACH	LJ	ENCINITAS	CARLSBAD-OCEANSIDE	SAN ONOFRE	CAPISTRANO	
9.0	1.6	-	2.9	26.7	6.5	2.4	86W
4.2	4.0	-	1.1	4.7	3.2	1.8	86S

winter

summer

$X_w = 6.1$
$X_s = 2.8$

PERCENT

RANGE LINES BY SUBCELL

SS- 0, SS- 100, SS- 200, MB- 300, PB- 400, TP- 500, SD- 600, SD- 700, CB- 800, OS- 900, OS-1000, PN-1100, PN-1200, PN-1300, PN-1400, SO-1500, SO-1600, SC-1700, DB-1800, DB-1900
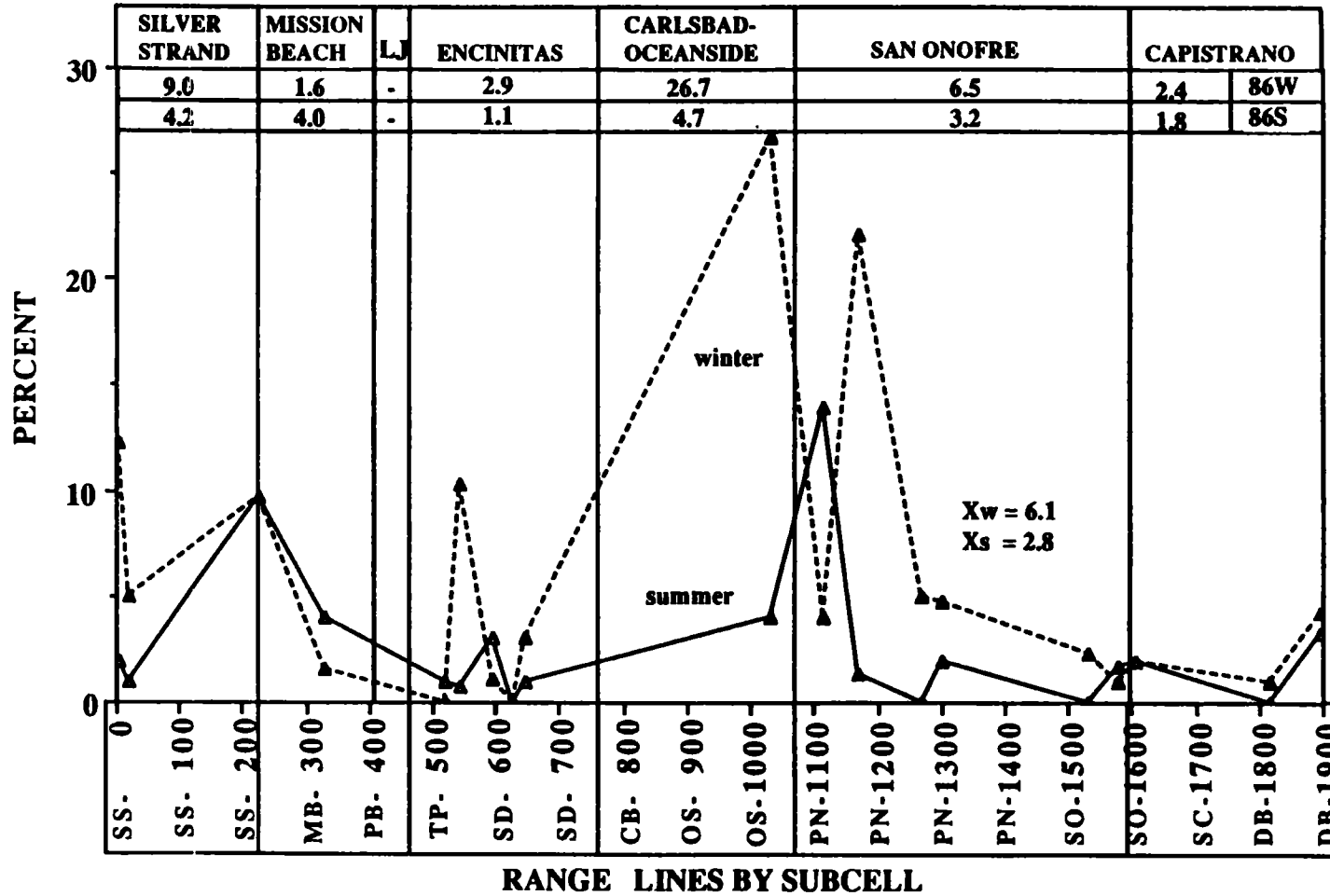
Figure 43. Line graph showing biotite percentages for all 1986 beach samples.

COMPOSITE PERCENTAGES FOR 1986 BEACHES

SILVER STRAND	MISSION BEACH	LJ	ENCINITAS	CARLSBAD-OCEANSIDE	SAN ONOFRE	CAPISTRANO	
2.2	1.7	-	5.5	2.3	12.1	8.9	86W
1.7	3.0	-	5.1	4.5	12.5	14.1	86S

$X_w = 7.2$
$X_s = 8.0$

winter

summer

PERCENT

RANGE LINES BY SUBCELL

Range lines: SS-0, SS-100, SS-200, MB-300, PB-400, TP-500, SD-600, SD-700, CB-800, OS-900, OS-1000, PN-1100, PN-1200, PN-1300, PN-1400, SO-1500, SO-1600, SC-1700, DB-1800, DB-1900
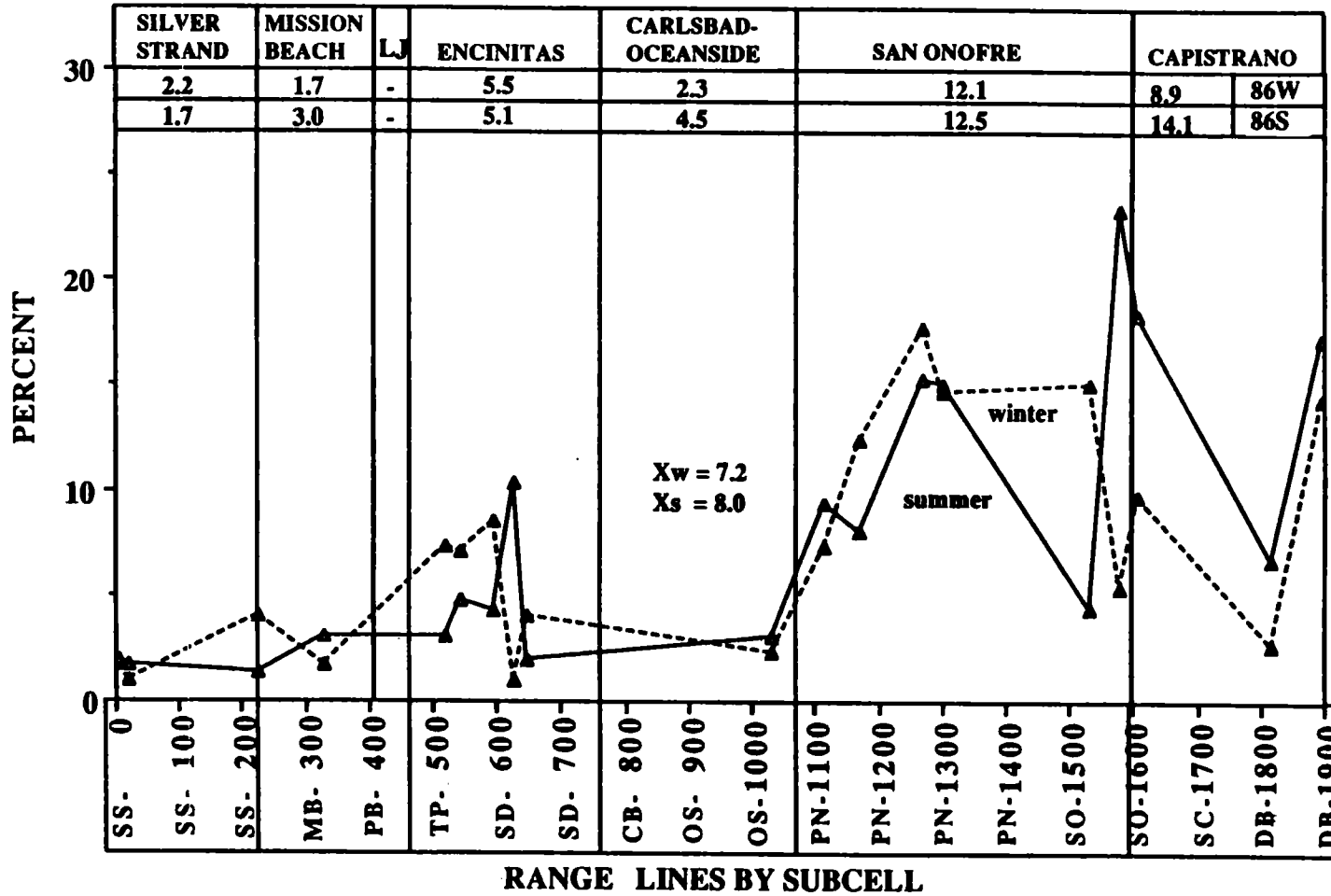
Figure 44. Line graph of composite particle percentages for all 1986 beach samples.

EPIDOTE PERCENTAGES FOR 1986

SILVER STRAND	MISSION BEACH	LJ	ENCINITAS	CARLSBAD-OCEANSIDE	SAN ONOFRE	CAPISTRANO	
3.3	2.0	-	13.4	2.7	22.1	15.8	86W
1.7	0.7	-	11.4	6.9	24.9	18.2	86S

PERCENT

60
50
40
30
20
10
0

summer
winter

$X_w = 13.8$
$X_s = 14.1$

SS- 0
SS- 100
SS- 200
MB- 300
PB- 400
TP- 500
SD- 600
SD- 700
CB- 800
OS- 900
OS-1000
PN-1100
PN-1200
PN-1300
PN-1400
SO-1500
SO-1600
SC-1700
DB-1800
DB-1900

RANGE LINES BY SUBCELL
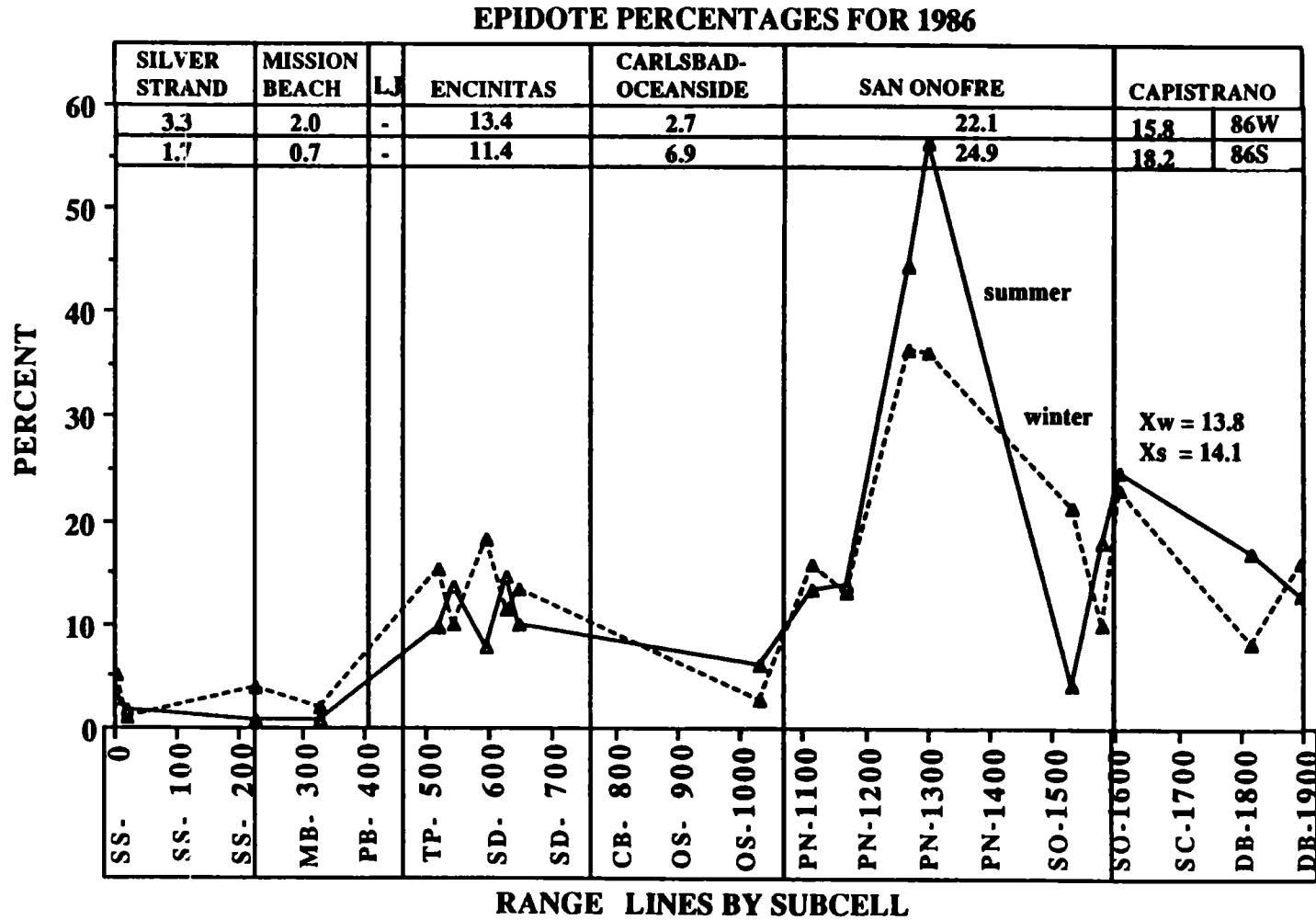
Figure 45. Line graph showing epidote percentages for all 1986 beach samples.

GARNET PERCENTAGES FOR 1986 BEACHES

SILVER STRAND	MISSION BEACH	LJ	ENCINITAS	CARLSBAD-OCEANSIDE	SAN ONOFRE	CAPISTRANO	
0.4	0.0	-	0.9	0.0	2.2	6.1	86W
0.2	0.7	-	0.9	0.8	4.2	2.7	86S

$Xw = 2.0$
$Xs = 2.0$

summer

winter

PERCENT

20

10

0

SS- 0 SS- 100 SS- 200 MB- 300 PB- 400 TP- 500 SD- 600 SD- 700 CB- 800 OS- 900 OS-1000 PN-1100 PN-1200 PN-1300 PN-1400 SO-1500 SO-1600 SC-1700 DB-1800 DB-1900

RANGE   LINES BY SUBCELL
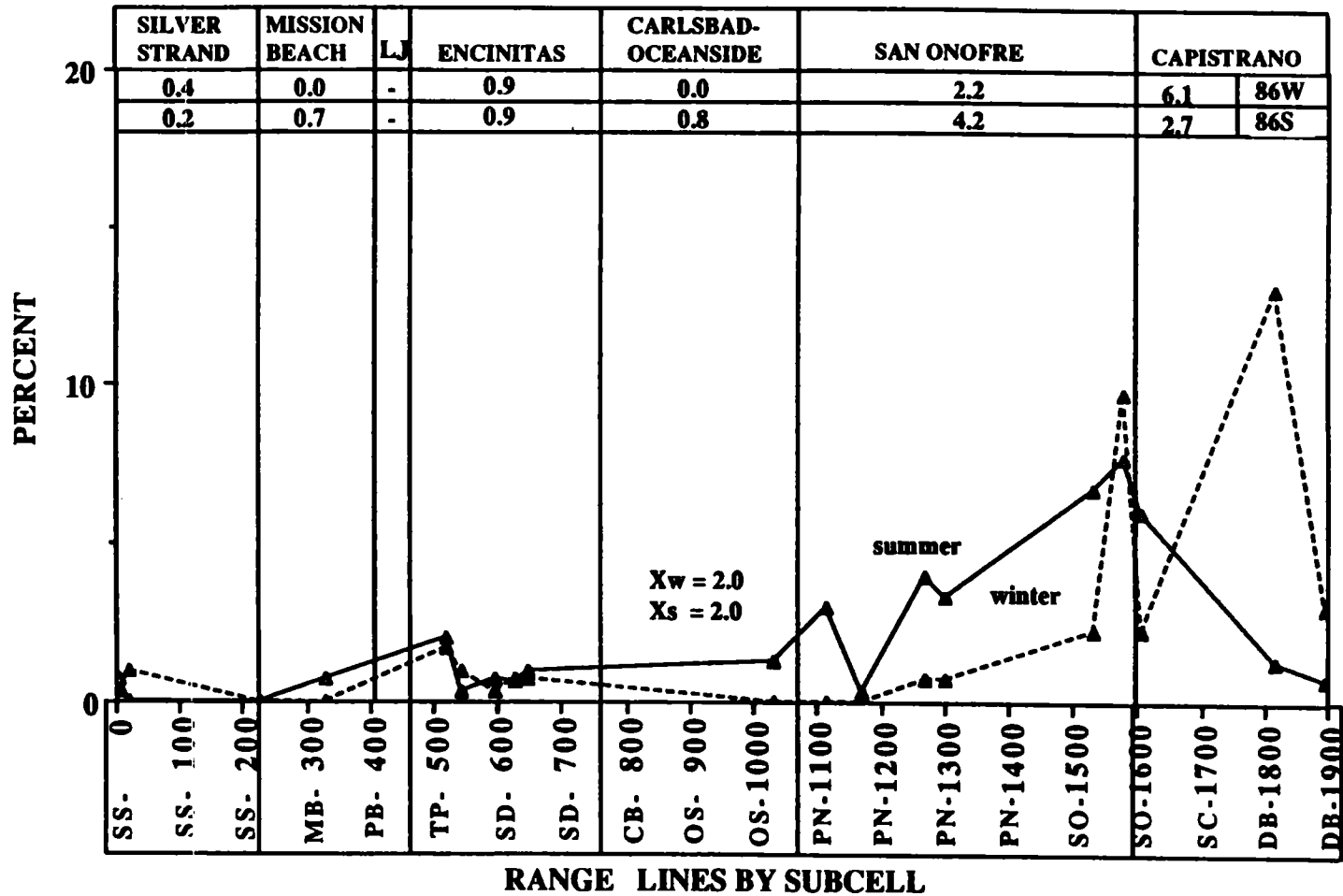
Figure 46.   Line graph showing garnet percentages for all 1986 beach samples.

84

GLAUCOPHANE PERCENTAGES: 1986 BEACHES

SILVER STRAND	MISSION BEACH	LJ	ENCINITAS	CARLSBAD-OCEANSIDE	SAN ONOFRE	CAPISTRANO	
0.4	0.0	-	1.7	1.0	4.2	0.7	86W
0.1	0.0	-	2.2	0.0	2.5	0.0	86S

PERCENT

winter

summer

$Xw = 2.0$
$Xs = 1.5$

RANGE LINES BY SUBCELL

SS- 0, SS- 100, SS- 200, MB- 300, PB- 400, TP- 500, SD- 600, SD- 700, CB- 800, OS- 900, OS- 1000, PN- 1100, PN- 1200, PN- 1300, PN- 1400, SO- 1500, SO- 1600, SC- 1700, DB- 1800, DB- 1900
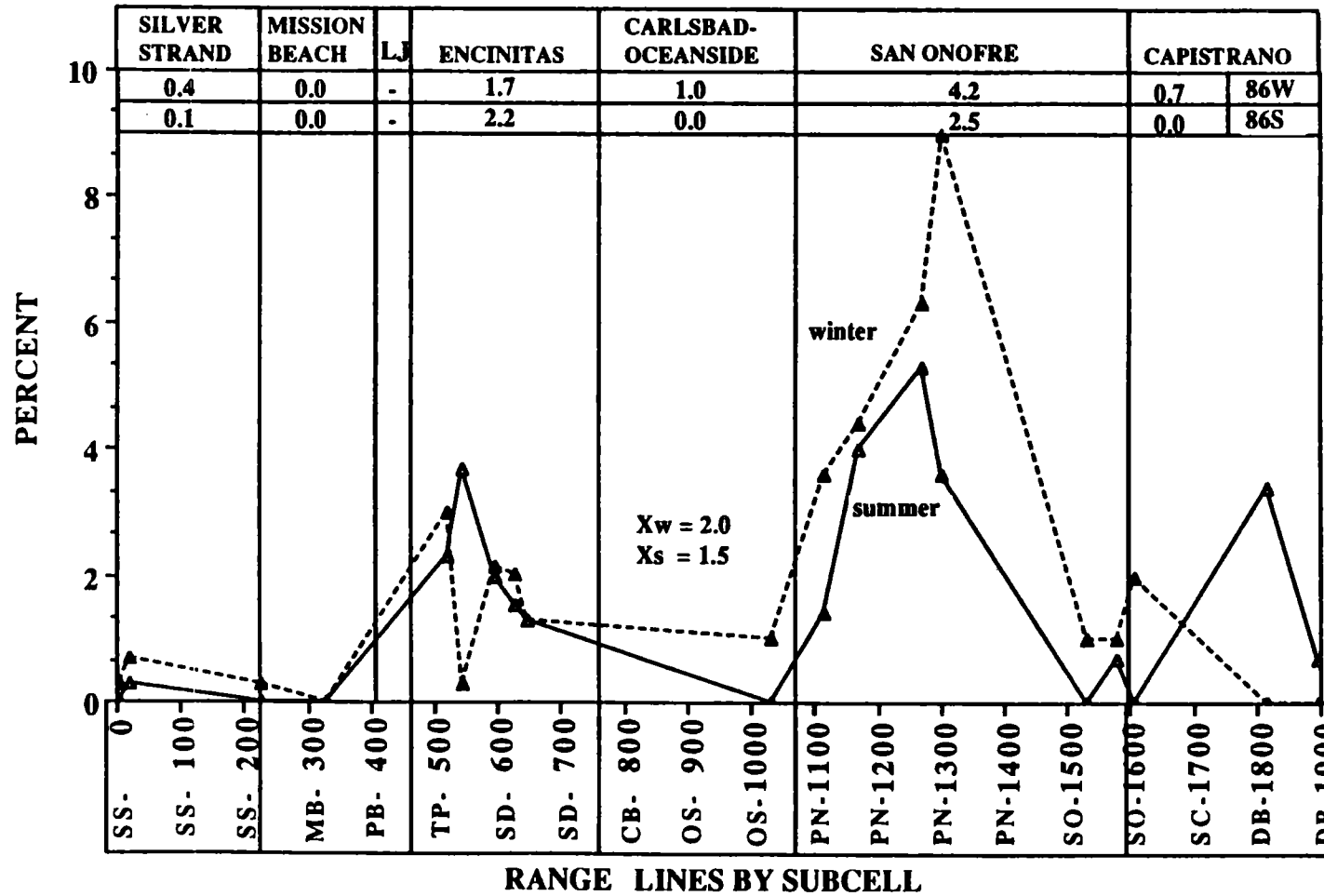
Figure 47. Line graph showing glaucophane percentages for all 1986 beach samples.

HORNBLENDE PERCENTAGES FOR 1986 BEACHES

SILVER STRAND	MISSION BEACH	LJ	ENCINITAS	CARLSBAD-OCEANSIDE	SAN ONOFRE	CAPISTRANO	
78.2	84.0	-	61.1	64.0	33.4	31.6	86W
87.2	83.7	-	74.4	74.0	24.4	47.4	86S

$X_w = 52.0$
$X_s = 57.7$
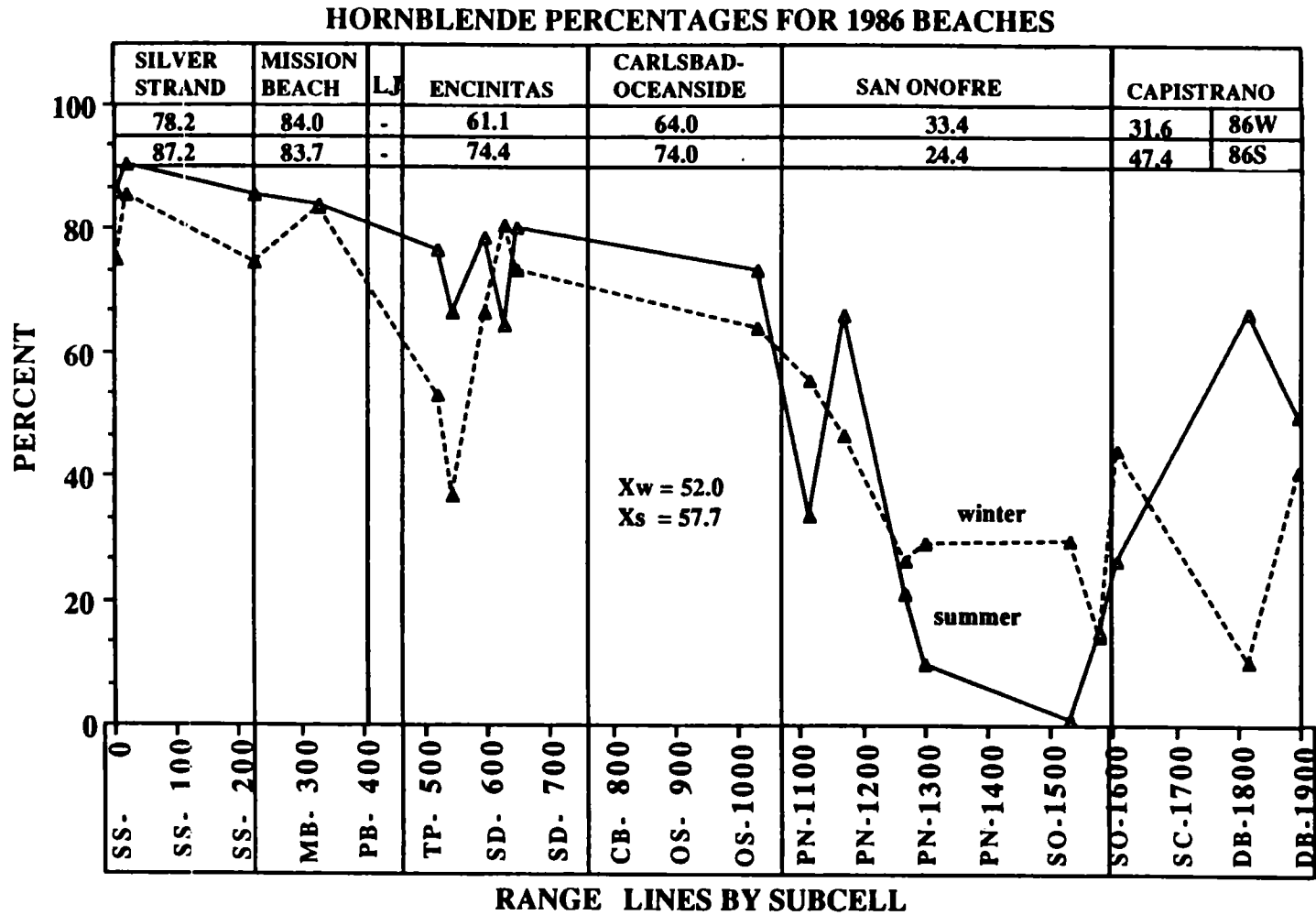
Figure 48. Line graph showing hornblende percentages for all 1986 beach samples.

HYPERSTHENE PERCENTAGES: 1986 BEACHES

SILVER STRAND	MISSION BEACH	LJ	ENCINITAS	CARLSBAD-OCEANSIDE	SAN ONOFRE	CAPISTRANO	
3.1	1.7	-	1.9	1.3	1.8	0.8	86W
1.5	2.0	-	1.3	1.2	0.9	1.7	86S

$X_w = 1.9$
$X_s = 1.3$

winter

summer

PERCENT

RANGE LINES BY SUBCELL
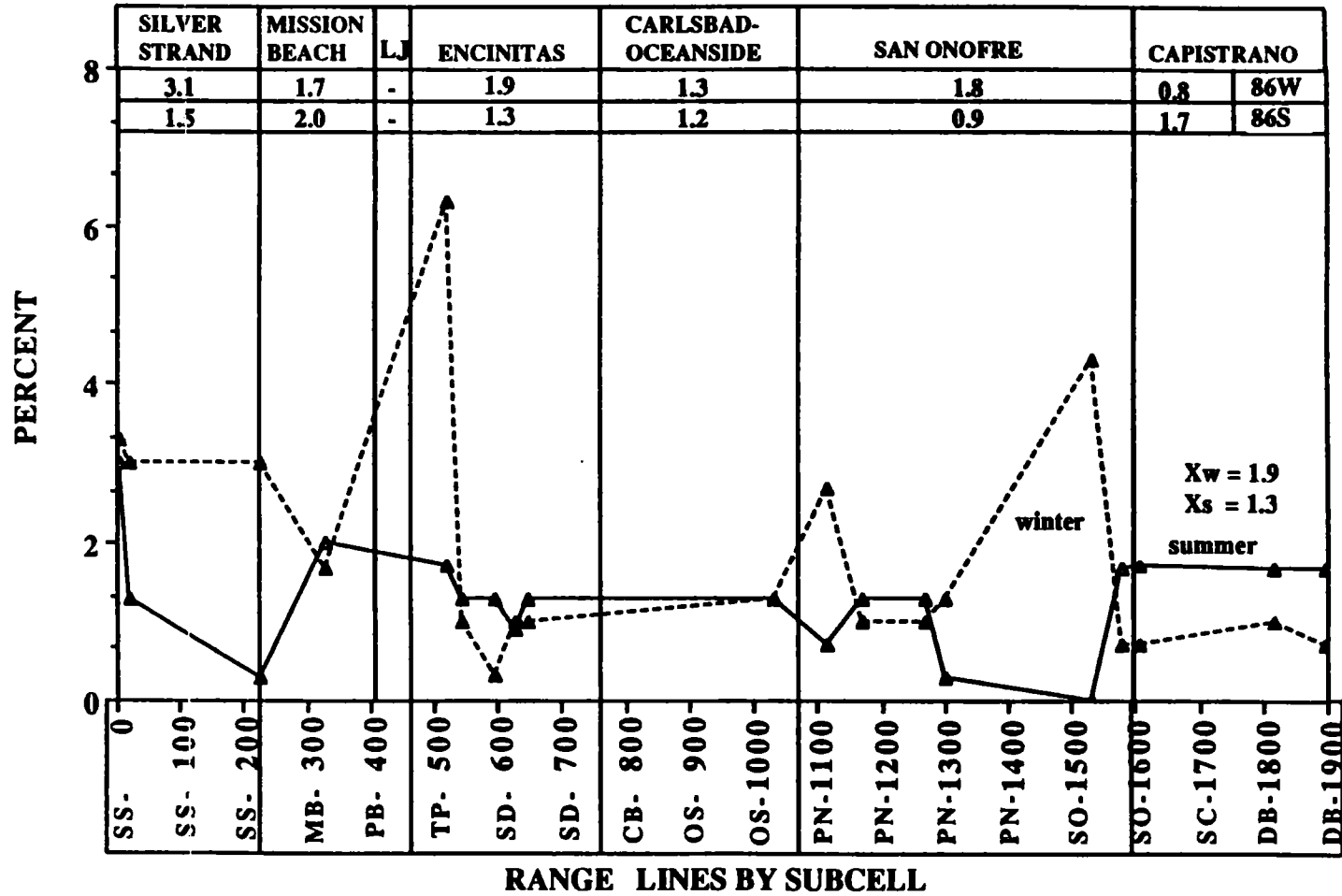
Figure 49. Line graph showing hypersthene percentages for all 1986 beach samples.

OPAQUE PERCENTAGES FOR 1986 BEACHES

SILVER STRAND	MISSION BEACH	LJ	ENCINITAS	CARLSBAD-OCEANSIDE	SAN ONOFRE	CAPISTRANO	
1.6	8.7	-	8.1	1.0	14.6	26.4	86W
1.2	4.3	-	2.8	6.4	19.9	7.7	86S
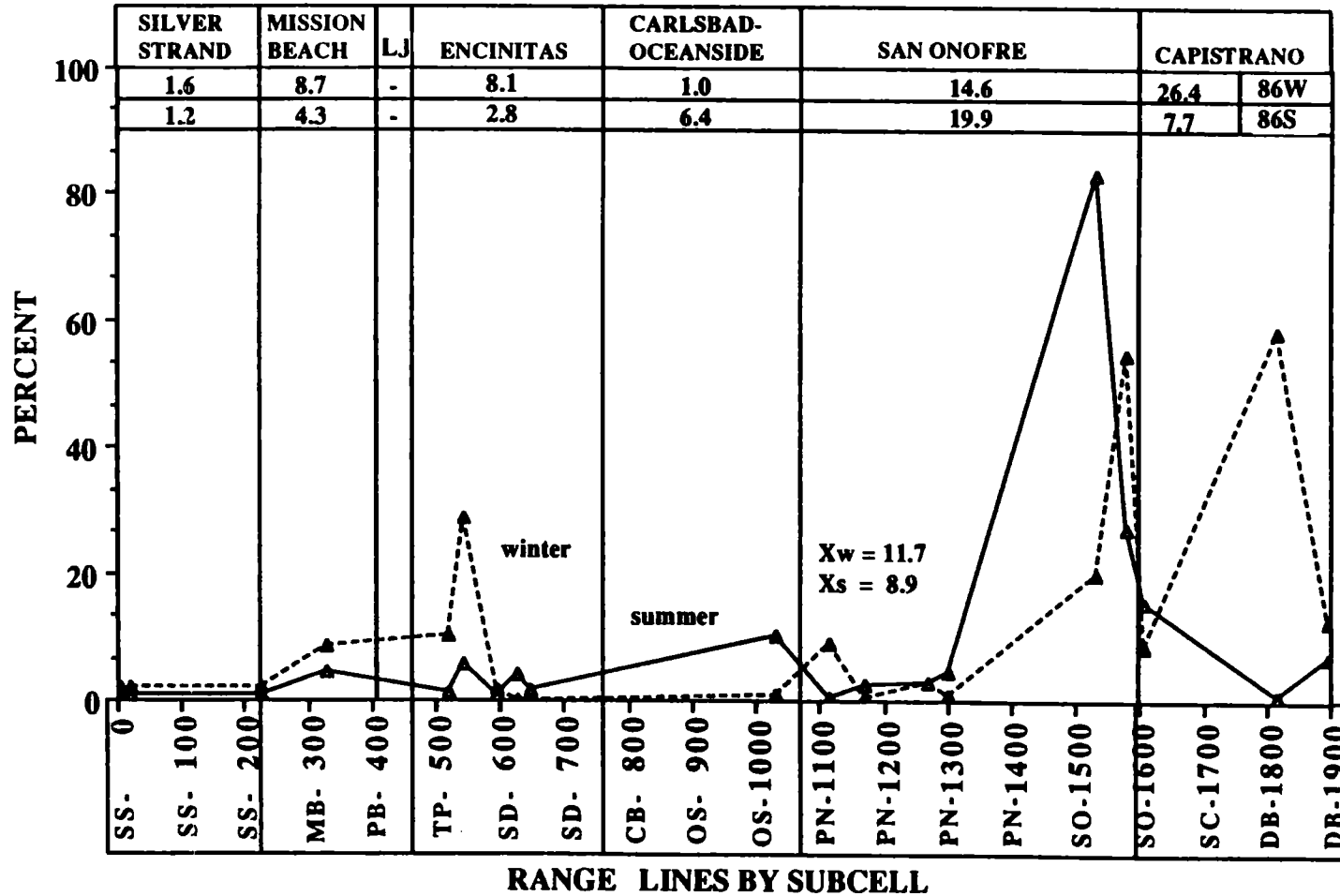
Figure 50. Line graph showing opaque percentages for all 1986 beach samples.

SPHENE PERCENTAGES FOR 1986 BEACHES

SILVER STRAND	MISSION BEACH	LJ	ENCINITAS	CARLSBAD-OCEANSIDE	SAN ONOFRE	CAPISTRANO	
1.3	0.3	-	2.3	0.3	2.3	5.9	86W
1.2	0.7	-	2.0	1.4	3.5	4.3	86S

PERCENT

summer

winter

$Xw = 2.5$
$Xs = 2.5$

RANGE LINES BY SUBCELL

SS-0 SS-100 SS-200 MB-300 PB-400 TP-500 SD-600 SD-700 CB-800 OS-900 OS-1000 PN-1100 PN-1200 PN-1300 PN-1400 SO-1500 SO-1600 SC-1700 DB-1800 DB-1900
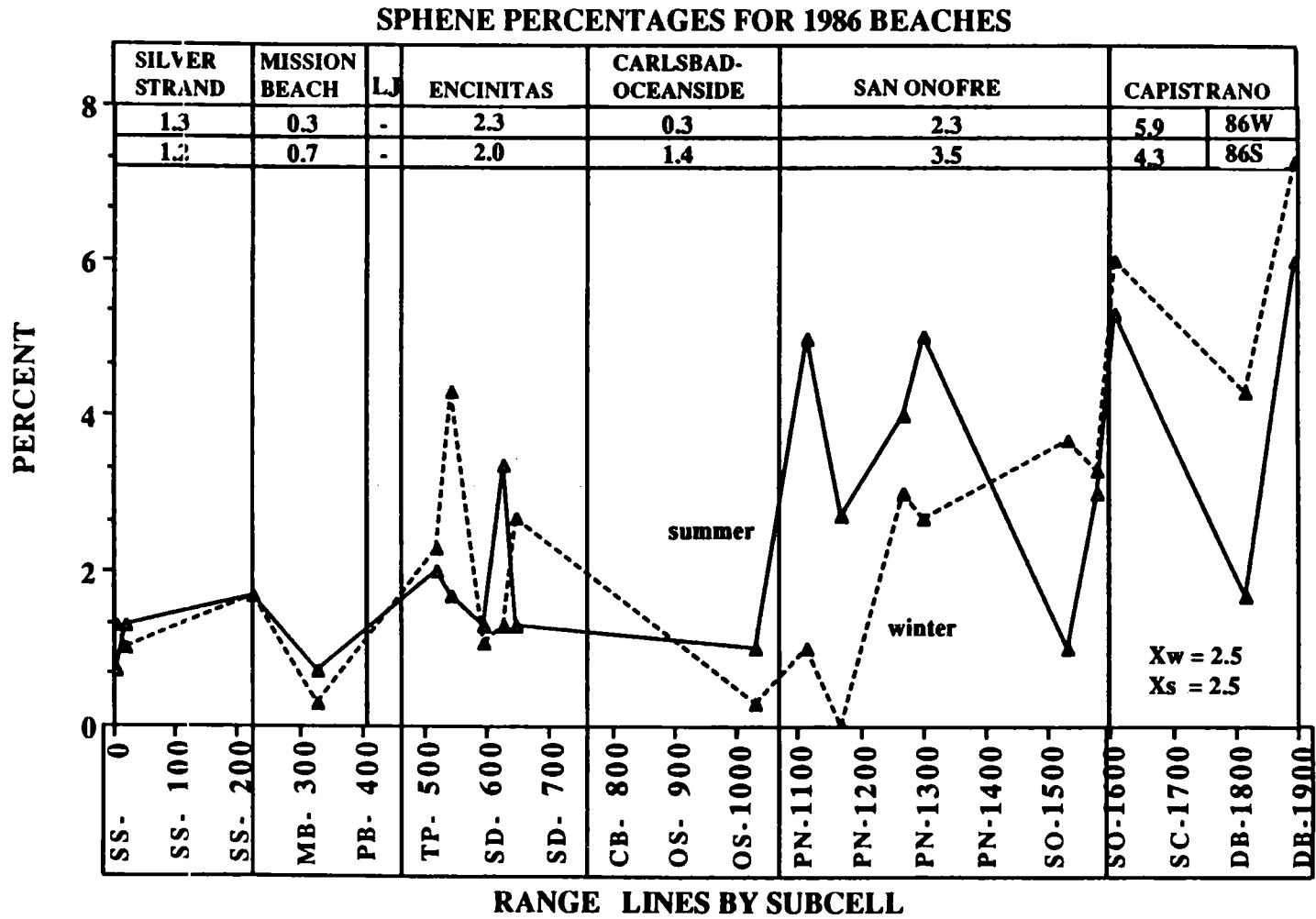
Figure 51. Line graph showing sphene percentages for all 1986 beach samples.

ACTINOLITE PERCENTAGES FOR 1986 BEACHES

SILVER STRAND	MISSION BEACH	LJ	ENCINITAS	CARLSBAD-OCEANSIDE	SAN ONOFRE	CAPISTRANO	
0.0	0.0	-	0.0	0.0	0.2	0.0	86W
0.1	0.0	-	0.1	0.0	0.0	0.1	86S

PERCENT

0.4

0.3

0.2

0.1

0.0

Xw = 0.05
Xs = 0.05

summer

winter

SS-0 SS-100 SS-200 MB-300 PB-400 TP-500 SD-600 SD-700 CB-800 OS-900 OS-1000 PN-1100 PN-1200 PN-1300 PN-1400 SO-1500 SO-1600 SC-1700 DB-1800 DB-1900

RANGE LINES BY SUBCELL
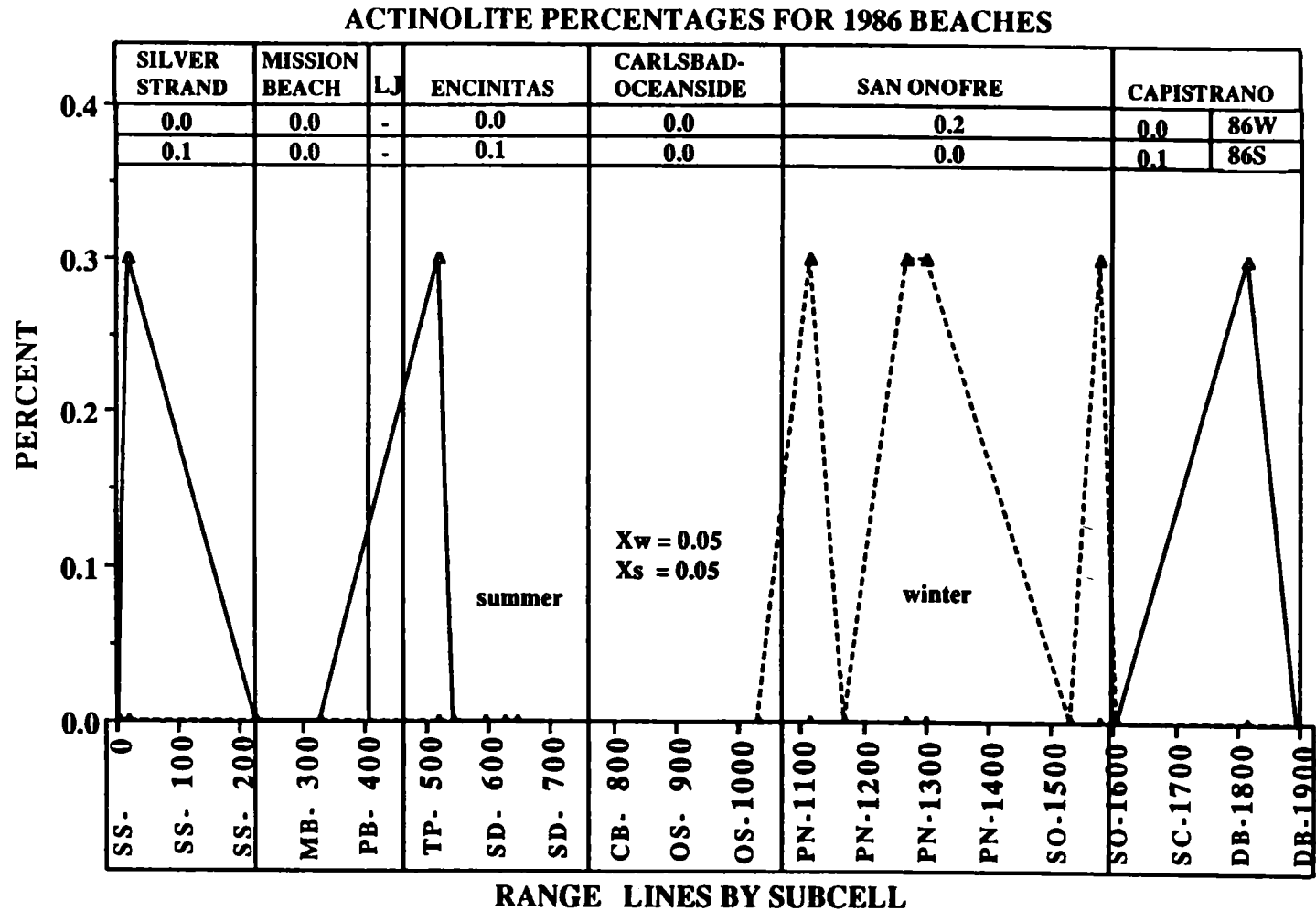
Figure 52. Line graph showing actinolite percentages for all 1986 beach samples.

APATITE PERCENTAGES FOR 1986 BEACHES

SILVER STRAND	MISSION BEACH	LJ	ENCINITAS	CARLSBAD-OCEANSIDE	SAN ONOFRE	CAPISTRANO	
0.0	0.0	-	0.0	0.0	0.05	0.23	86W
0.1	0.0	-	0.06	0.0	0.1	0.0	86S
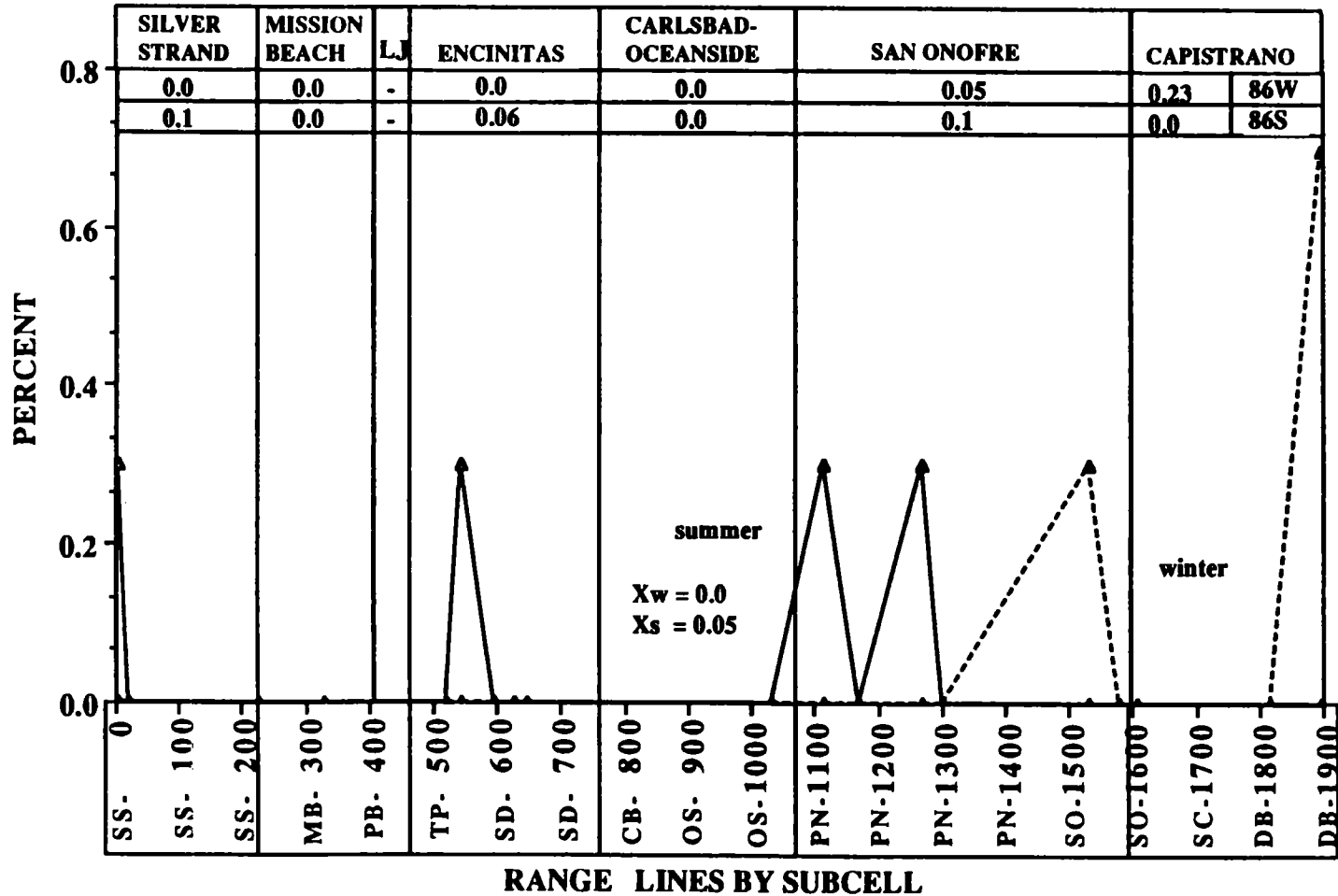
Figure 53. Line graph showing apatite percentages for all 1986 beach samples.

AUGITE PERCENTAGES FOR 1986 BEACHES

SILVER STRAND	MISSION BEACH	LJ	ENCINITAS	CARLSBAD-OCEANSIDE	SAN ONOFRE	CAPISTRANO	
0.2	0.7	-	0.2	0.7	0.4	0.7	86W
0.5	1.0	-	0.2	0.0	0.2	0.2	86S

PERCENT

winter

summer

Xw = 0.4
Xs = 0.3

SS- 0
SS- 100
SS- 200
MB- 300
PB- 400
TP- 500
SD- 600
SD- 700
CB- 800
OS- 900
OS-1000
PN-1100
PN-1200
PN-1300
PN-1400
SO-1500
SO-1600
SC-1700
DB-1800
DB-1900

RANGE LINES BY SUBCELL
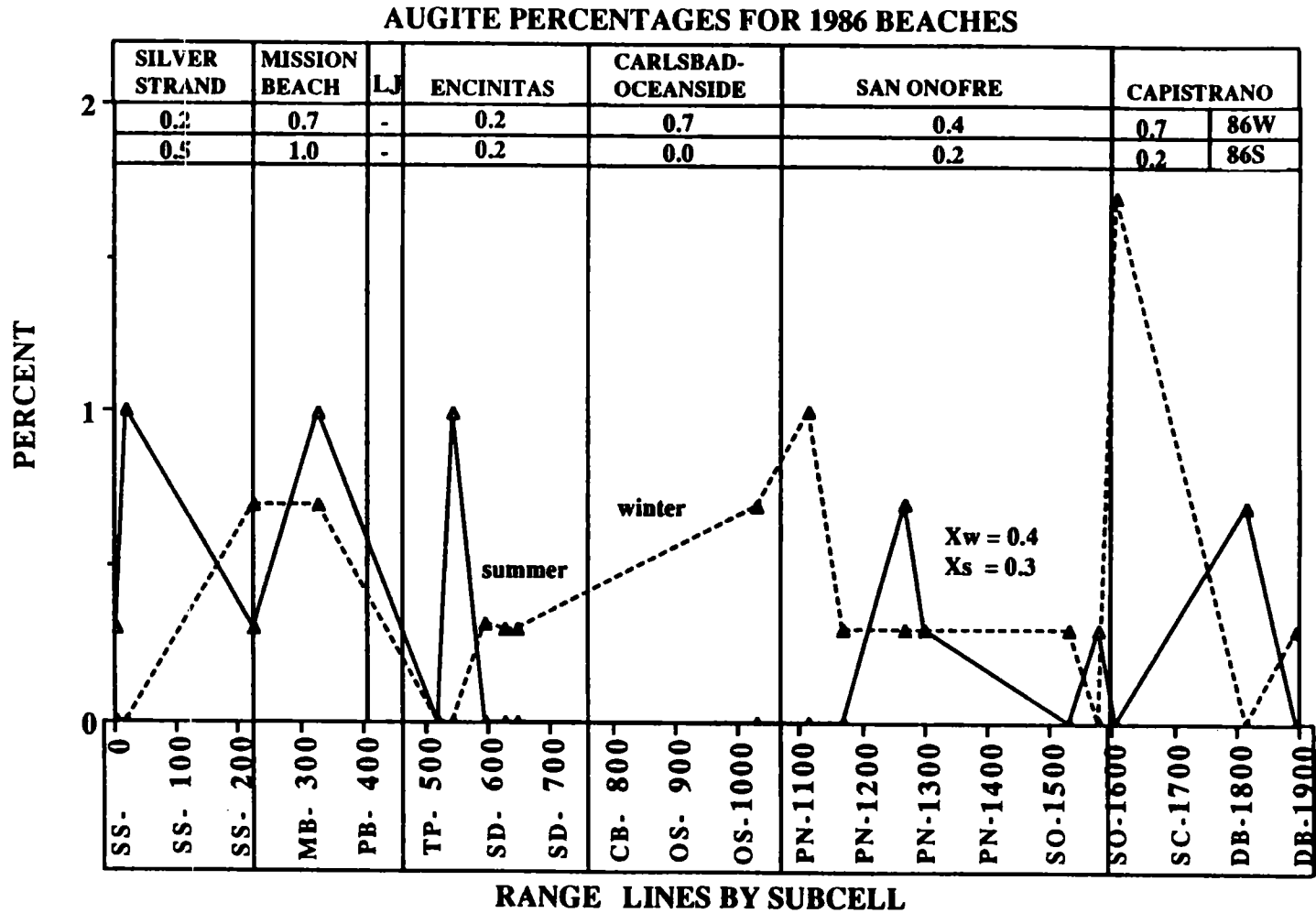
Figure 54. Line graph showing augite percentages for all 1986 beach samples.

OLIVINE PERCENTAGES FOR 1986 BEACHES

SILVER STRAND	MISSION BEACH	LJ	ENCINITAS	CARLSBAD-OCEANSIDE	SAN ONOFRE	CAPISTRANO	
0.0	0.0	-	0.3	0.0	0.0	0.0	86W
0.0	0.0	-	0.0	0.0	3.1	0.0	86S

PERCENT

summer

winter

Xw = 0.1
Xs = 0.9

SS- 0, SS- 100, SS- 200, MB- 300, PB- 400, TP- 500, SD- 600, SD- 700, CB- 800, OS- 900, OS-1000, PN-1100, PN-1200, PN-1300, PN-1400, SO-1500, SO-1600, SC-1700, DB-1800, DB-1900

RANGE LINES BY SUBCELL
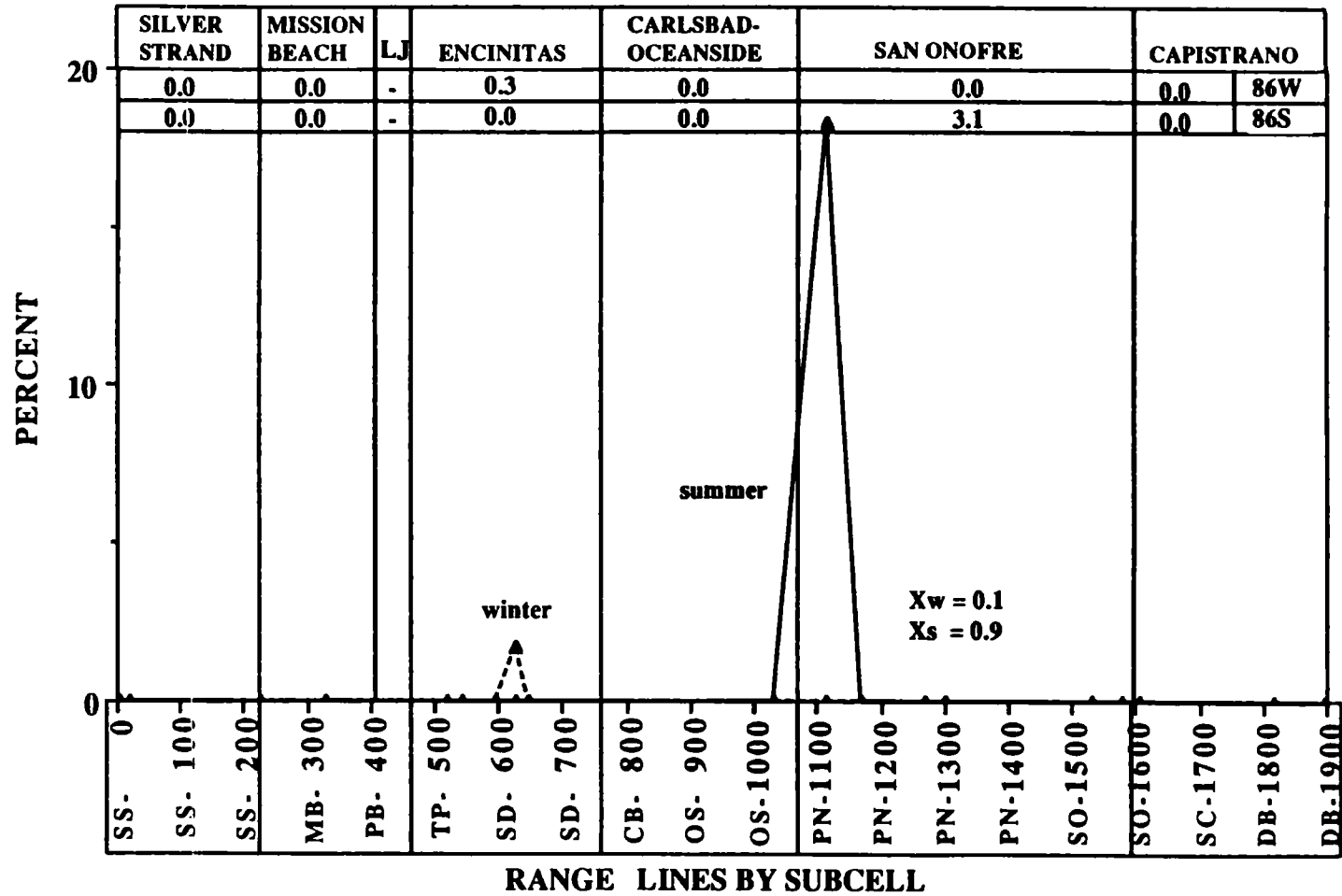
Figure 55. Line graph showing olivine percentages for all 1986 beach samples.

ZIRCON PERCENTAGES FOR 1986 BEACHES

SILVER STRAND	MISSION BEACH	LJ	ENCINITAS	CARLSBAD-OCEANSIDE	SAN ONOFRE	CAPISTRANO	
0.0	0.0	-	0.1	0.0	0.1	0.4	86W
0.0	0.0	-	0.3	0.0	0.2	0.2	86S

PERCENT

$X_w = 0.1$
$X_s = 0.2$

winter

summer

SS- 0 | SS- 100 | SS- 200 | MB- 300 | PB- 400 | TP- 500 | SD- 600 | SD- 700 | CB- 800 | OS- 900 | OS-1000 | PN-1100 | PN-1200 | PN-1300 | PN-1400 | SO-1500 | SO-1600 | SC-1700 | DB-1800 | DB-1900

RANGE LINES BY SUBCELL

Figure 56. Line graph sowing zircon percentages for all 1986 beach samples.

94

ZOISITE PERCENTAGES FOR 1986 BEACHES

SILVER STRAND	MISSION BEACH	LJ	ENCINITAS	CARLSBAD-OCEANSIDE	SAN ONOFRE	CAPISTRANO	
0.0	0.0	-	0.0	0.0	0.0	0.0	86W
0.0	0.0	-	0.0	0.0	0.1	0.0	86S

Xw = 0.0
Xs = 0.05

summer

winter

PERCENT

RANGE LINES BY SUBCELL

SS- 0, SS- 100, SS- 200, MB- 300, PB- 400, TP- 500, SD- 600, SD- 700, CB- 800, OS- 900, OS-1000, PN-1100, PN-1200, PN-1300, PN-1400, SO-1500, SO-1600, SC-1700, DB-1800, DB-1900

Figure 57. Line graph showing zoisite percentages for all 1986 beach samples.

variation within the Capistrano subcell, from DB-1900 to SO-1600 (Figure 50). The 1986 winter beach sample set has 26.4% opaque grains, which is more than double the 11.7% average for the combined beach samples (Table 14B). However, there are slightly fewer opaque grains in the 1986 end-of-summer beach samples within the Capistrano subcell.

4.20   Garnet (6.1% end-of-winter and 2.7% end-of-summer) and sphene (5.9% end-of-winter and 4.3% end-of-summer) comprise an appreciable proportion of the heavy minerals in the Capistrano subcell, from DB-1900 to SO-1600 (Figures 46 and 51). There is more garnet in the Capistrano subcell than the combined subcell beach averages for both the end-of-winter and end-of-summer sample sets (Table 14B). Garnet increases downcoast within the Capistrano subcell and persists into the San Onofre subcell (Figure 46). Glaucophane only occurs in the end-of-winter sample set (0.7%) of the Capistrano subcell (Figure 47).
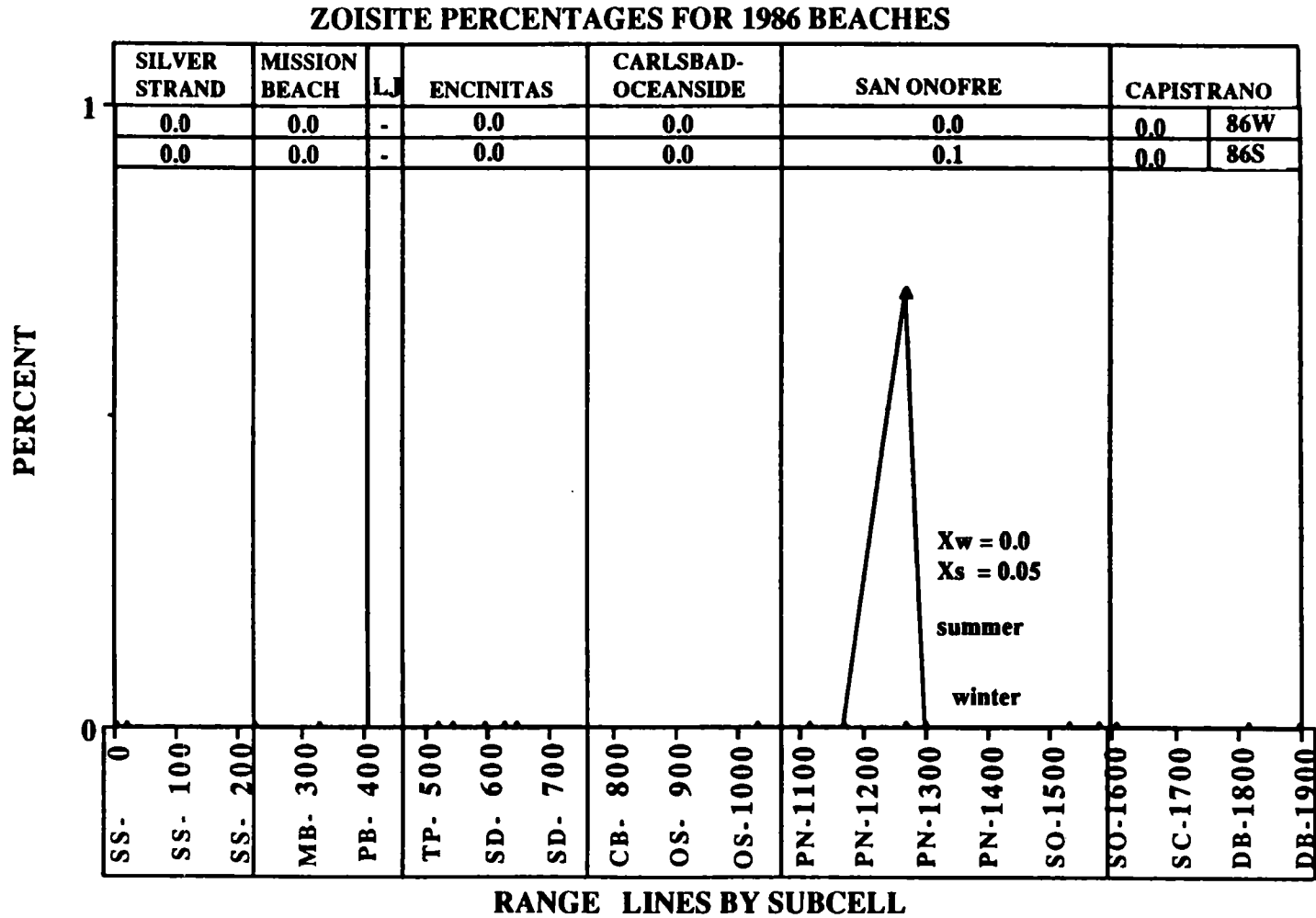
4.21   A sharp increase in glaucophane defines the boundary between the Capistrano and San Onofre subcells (Figure 47). The Capistrano subcell contains more epidote than all of the beaches combined for both the winter and summer sample sets. The San Onofre Creek (Figure 13) and the coastal cliffs cropping out from PN-1200 to SO-1460 in the San Onofre subcell (Figure 15) account for this glaucophane enrichment in the San Onofre subcell. This lithologic source change, which includes coastal cliffs along with the San Onofre and San Mateo Creeks, probably creates the sharp appearance for this subcell boundary. Therefore, San Mateo Point does not act as a physical barrier to prevent sediment transport within the littoral zone. Sediment exchange between the Capistrano and San Onofre subcells is best indicated by glaucophane. There is no source for glaucophane in the Capistrano subcell, so the presence of glaucophane on the Capistrano beaches from DB-1895 to SO-1610 (Figures 18 and 19) indicates littoral transport from the San Onofre to Capistrano subcell.

Oceanside Littoral Cell: San Onofre Subcell

Mineralogy of River Samples

4.22   Four rivers flow into the San Onofre subcell: San Mateo, San Onofre, and Las Flores Creek, and Santa Margarita River. San Mateo and San Onofre Creeks (SO-1595 and SO-1565) respectively discharge into the northern section of this subcell, whereas Las Flores Creek (PN-1285) and Santa Margarita River (PN-1150) flow into the southern end of the San Onofre subcell (Figure 11A). Quartz values increase from the Capistrano subcell to the San Onofre subcell whereas total heavy minerals decrease between these subcells. The average quartz content for the four rivers in the San Onofre subcell, from SO-1600 to PN-1100 (59.8%) includes 10% more quartz than the Capistrano subcell fluvial average (Figure 39). The rivers in the San Onofre subcell average 15% total heavy minerals, which is much less than the 25% heavy mineral average for the San Juan Creek draining into the Capistrano subcell (Figure 42). Both plagioclase and potassium feldspar percentages remain the same for the rivers draining into the San Onofre subcell as those fluvial mineral averages for the Capistrano subcell (Table 13A).

4.23   The most apparent mineralogic characteristic of the rivers flowing into the San Onofre subcell (San Mateo Creek, San Onofre Creek, Las Flores Creek, and Santa Margarita River) is the high degree of mineralogic variability between these four rivers

(Figure 13). Hypersthene, sphene, and opaque grains are the only major heavy minerals that maintain consistent amounts in all four rivers. Opaque grains decrease significantly from the Capistrano subcell rivers (30%) to the San Onofre subcell rivers (2.2%) from SO-1600 to OS-1080 (Figure 31). Less sphene occurs in the San Onofre subcell rivers (2.2%) from SO-1600 to OS-1080 than was available in the Capistrano fluvial discharge (6%) (Figure 32). Glaucophane demonstrates the most important single mineral change in the overall river mineral composition (Figure 28). Glaucophane is absent in the sample from San Juan Creek (DB-1865), and there are no coastal cliff samples within the Capistrano subcell. No source for glaucophane can be inferred for the Capistrano subcell (DB-1900 to SO-1600). The river average for the San Onofre subcell (SO-1600 to OS-1080) includes only 0.3% garnet, a large decrease from the 8% average contained in San Juan Creek (Figure 27). The rivers within the San Onofre subcell (SO-1600 to OS-1080) contain considerable amounts of hornblende (56.8%) and epidote (10.9%), but individual rivers show wide ranges for both minerals (Figures 26 and 29). Rivers draining into the San Onofre subcell generally have more epidote and hornblende than rivers draining into the Capistrano subcell.

Mineralogy of Cliff Samples

4.24   Quartz comprises more than 60% of each cliff sample collected in the Oceanside area, from PN-1400 to OS-1080 (Figure 20). The coastal cliffs in the northern section of the San Onofre subcell, from SO-1600 to PN-1400, include less quartz (Figure 20). The northern coastal cliff samples (SO-1600 to SO-1400) have more heavy minerals, ranging between 20% to 50%, than those cliffs exposed in southern San Onofre subcell (Figure 23). Plagioclase feldspar accounts for approximately 15% of each cliff sample in the San Onofre subcell, from SO-1600 to OS-1080 (Figure 21). Potassium feldspar typically comprises 10% of the total heavy mineral percentage in the cliffs of the San Onofre subcell (Figure 22). The northernmost cliff samples (PN-1450 to SO-1600) in the San Onofre subcell have up to 25% potassium feldspar.

4.25   The coastal cliffs within the San Onofre subcell (PN-1600 to PN-1200) contain hornblende, epidote, composite particles, and biotite as the major constituents of the heavy mineral fraction in this area. Hornblende remains in the same proportion for the cliffs in the San Onofre (SO-1600 to PN-1080) and the Encinitas subcells (22%) (Figure 12). Biotite is an important component of the coastal cliff heavy mineral assemblage. There is almost 30% biotite within the San Onofre cliffs, from PN-1450 to PN-1200, and slightly more biotite (36.9%) occurs in the southern cliffs of the Encinitas subcell, from TP-480 to LJ-455. Epidote forms a large proportion (20%) of the heavy minerals measured within the San Onofre subcell, SO-1600 to PN-1200. A large fraction of composite particles within this subcell are metamorphic rock fragments. Almost 6% of the total heavy mineral fraction is glaucophane. Garnet makes up 1.5% of the total heavy mineral content within the San Onofre cliffs. Only 2.5% sphene, 3.9% opaque grains occur in the San Onofre cliffs. Hypersthene averages only a small percent (0.6%) in the San Onofre cliffs.

Mineralogy of Beach Samples

4.26   Quartz continues to be the dominant mineral in the San Onofre subcell from SO-1600 to OS-1080 (63.2% end-of-winter; 58.3% end-of-summer), increasing downcoast (Figure 39). There are more heavy minerals (21.7%) within the end-of-summer sample set than in the end-of-winter set (12.1%) for the Capistrano subcell (DB-1900 to SO-1600),

which shows a reversed seasonal trend (Table 14A). No significant change can be described for either varieties of feldspar from the Capistrano to the San Onofre subcells. There is slightly more plagioclase than potassium feldspar in the end-of-winter sample set within the San Onofre subcell (SO-1600 to OS-1080). Plagioclase feldspar shows a seasonal trend, decreasing from winter to summer SO-1600 to OS-1080 (13.7% end-of-winter and 9.1% end-of-summer) (Figure 40). This seasonally related trend in plagioclase feldspar is documented for every littoral subcell and cell in the study area (Table 14a).

4.27   There is less hornblende in the San Onofre subcell (SO-1600 to OS-1080) for both the April and October 1986 sample sets than the Capistrano subcell (DB-1900 to SO-1600). Hornblende comprises only 33.4% of the total heavy minerals in the end-of-winter sample set and 24.4% for the end-of-summer sample set for the San Onofre subcell (Figure 48). Epidote increases significantly in the San Onofre subcell (SO-1600 to OS-1080) for both seasons from the proportionately large values in the Capistrano subcell (DB-1900 to SO-1600) (Figure 45). More epidote is present in the end-of-summer than the end-of-winter sample sets for both of these two northern subcells from DB-1900 to OS-1080 (Figure 45). There is slightly less sphene (2.3% at the end-of-winter and 3.5% at the end-of-summer) in the San Onofre subcell (SO-1600 to OS-1080) than along the beaches of the Capistrano subcell (DB-1900 to SO-1600) (Figure 51). The percentage of glaucophane shows the most significant mineral change within this subcell, increasing from the Capistrano (DB-1900 to SO-1600) to the San Onofre subcell sample sets, from SO-1450 to PN-1150 (0.7% to 4.2% for the end-of-winter and 0.0% to 2.5% for the end-of-summer sample set) (Figure 47).

4.28   Biotite peaks from PN-1300 to OS-1080 for both the end-of-winter and end-of-summer sample sets in the San Onofre subcells (Figure 43). The southern concentration of biotite suggests net downcoast sediment accumulation. Alternatively, biotite could be selectively transported offshore in the northern and central portions of this cell. Epidote increases from the Capistrano (DB-1900 to SO-1600) to the San Onofre subcell (SO-1600 to PN-1250) for both seasonal beach sample sets (Figure 45). Peak concentrations of epidote characterize the beach in the San Onofre from PN-1400 to PN-1200 subcell (22.1% end-of-winter; 24.9% end-of-summer) (Figure 45). Large peaks in the percentage of opaque grains occur in the northern section of the San Onofre subcell (Figure 50) at the mouths of the San Mateo (SO-1595) and San Onofre Creeks (SO-1565). The peak of opaque grains is more pronounced in the April 1986 sample set at SO-1585, between the river mouths. This mineral peak broadens and shifts toward the south, extending to PN-1300 in the end-of-summer sample set (Figures 18 and 19). This shift in the peak for opaque grains, primarily derived from these streams, suggests downcoast transport of heavy minerals in the San Onofre subcell during the summer of 1986. Overall, there is a higher percentage of opaque grains in the San Onofre subcell than the Capistrano subcell. Likewise, garnet trends support southward transport during the summer of 1986 in the San Onofre subcell. A peak of garnet occurs in the end-of-winter sample set at SO-1590, between San Mateo and San Onofre Creeks (Figure 46). This concentration occurs farther south in the end-of-summer sample set (Figure 46).

4.29   Glaucophane, biotite, garnet and opaque grains provide the best arguments describing a longer-term net downcoast sediment accumulation in the San Onofre subcell. Glaucophane accumulations demonstrate significant contribution from both adjacent river and cliff source areas into the littoral zone of San Onofre subcell. Since the San Onofre Creek sample contains appreciable amounts of glaucophane and seasonal peak concentrations occur to the south on the beaches at PN-1300, net downcoast sediment

accumulation can be inferred. Additionally, the occurrence of glaucophane illustrates the leaky nature of the boundary between the San Onofre and Capistrano subcells(Figure 47). Therefore, sediment has been transported northward around San Mateo Point at some time either as a single discharge event or, more likely, multiple events during an undefined time interval. A gradual decrease of glaucophane from the San Onofre subcell into the Oceanside-Carlsbad subcell shows that the defined subcell boundary may not be an effective sediment barrier. The petrofacies change occurs near Oceanside because the San Onofre Breccia ridge is no longer exposed. Coastal cliffs have been documented to contribute a large volume of sediment (Kuhn and others, 1988). The preservation of this petrofacies boundary indicates that the supply of sediment from the cliffs and rivers in this area exceeds the effects of mixing, homogenization and dilution due to littoral sediment transport and other coastal processes. The substantial decrease in hornblende makes the other heavy minerals more prominent in the San Onofre subcell (Figures 18 and 19).

4.30   An amount of 17% olivine is present at PN-1110 in the end-of-summer beach sample set, immediately south of the Santa Margarita River (Figure 55). The presence of very small amounts of olivine in the cliffs and rivers from PN-1200 to PN-1400 document net southward longshore transport over an unknown length of time (Figure 36). Actinolite is present on the beaches in trace amounts throughout the San Onofre subcell, but it is only present in measurable amounts within the end-of-winter beach sample set collected in April 1986 (Figure 52). The distribution of apatite supports southward transport during the summer of 1986 in the San Onofre subcell because small amounts of apatite occur between PN-1200 and SO-1600 in the cliffs, but the overall distribution shifts southward from PN-1300 to PN-1100 in the end-of-summer sample set.

Mineralogic Comparison of the Capistrano and San Onofre Subcells

4.31   The profile of the 1986 summer beach total mineralogy shows a sharp increase in the concentration of heavy minerals at the boundary between the Capistrano and San Onofre subcells SO-1600 (Figure 17). An increase in heavy mineral content also occurs between these two subcells in the end-of-winter sample set, but it is not as well-developed (Figure 16). Likewise, a decrease in potassium feldspar at the Capistrano-San Onofre subcell boundary SO-1600 in the end-of-summer beach sample set suggests the occurrence of a rather distinct cell boundary (Figure 17). Apparently, the cell boundary is better defined for the end-of-summer beach samples. There appears to be more leakage during the winter, since the boundary is more transitional.

4.32   A sharper cell boundary between the Capistrano and San Onofre subcells can be described by the individual heavy mineral species for both the end-of-winter and end-of-summer sample sets (Figures 18 and 19). Hornblende, epidote, opaque grains, garnet and sphene show abrupt percentage changes at the Capistrano-San Onofre subcell boundary SP-1600 (Figures 18 and 19). Glaucophane, hypersthene, and composite particles all increase substantially within the San Onofre subcell (SO-1600 to OS-1080), and these minerals make the beach sample sets of San Onofre subcell quite distinct from those of the Capistrano subcell (DB-1900 to SO-1600) (Figures 18 and 19). The mineralogic changes are much more exaggerated in the end-of-summer beach sample set, especially the large increase of opaque grains within the San Onofre subcell (SO-1600 to PN-1400) (Figure 19).

4.33 The heavy mineral assemblage changes abruptly at San Mateo Creek, which probably reflects the mineralogic variety of sediment input by the San Mateo (SO-1595) and San Onofre Creeks (SO-1565), immediately south of this subcell boundary, SO-1600. Epidote and glaucophane accumulate in the downcoast segment of the Capistrano subcell in the end-of-winter sample set (Figure 18). These trends indicate a net northward transport of sediment along the coast in the San Onofre subcell (SO-1600 to OS-1080). Apparently, San Mateo Point partially restricts the transport of sediment from the Capistrano to the San Onofre subcell.

4.34 The boundary from the Capistrano to the San Onofre subcell at SO-1600 appears mineralogically distinct, especially the area plot of major heavy minerals (Figures 18 and 19). This change reflects a decrease in hornblende and sphene, an increase in epidote and biotite, and the dominance of glaucophane in the San Onofre subcell. The localized abundance of garnet in San Juan Creek (DB-1865) and in the April 1986 beach sample set (DB-1900 to SO-1650) (Figure 46) demonstrates the occurrence of fluvial input into the littoral system within the Capistrano subcell, especially during the winter. It is difficult to ascertain the direction of net sediment transport within the Capistrano subcell, because garnet is present in San Onofre Creek (SO-1565) and could be transported northward into the Capistrano subcell (Figure 46).

Oceanside Littoral Cell: Oceanside-Carlsbad Subcell

Mineralogy of River Sampled

4.35 The San Luis Rey River is the only river draining into the Oceanside-Carlsbad subcell. Overall, there is an increase in the quartz content from the 60% San Onofre subcell river average to the 67.5% value for the San Luis Rey River (Figure 20). The river composition of the Oceanside-Carlsbad (OS-1080 to CB-765) subcell has considerably more plagioclase feldspar (23.8%) than the San Onofre subcell (from SO-1600 to OS-1080) which contains only 14.8% plagioclase feldspar (Figure 21). A threefold southward reduction in the concentration of total heavy minerals within rivers occurs from the 15% heavy mineral average for the rivers in the San Onofre subcell (SO-1600 to PN-1100) to only 5% total heavy minerals in the river composition of the Oceanside-Carlsbad (from OS-1080 to CB-765) subcell (Figure 23). Likewise, the potassium feldspar concentration in the average river composition is greatly reduced from the 10.5% value for the San Onofre subcell to less than 4% feldspar in the Oceanside-Carlsbad subcell average (Figure 22).

4.36 The most significant fluvial source changes from the San Onofre subcell (SO-1600 to OS-1080) to the Oceanside-Carlsbad (OS-1080 to CB-765) subcell are reflected by the paucity of glaucophane and garnet in the river sediment (Figures 27 and 28). Hornblende percentages remain stable among the rivers of the San Onofre and Oceanside-Carlsbad subcells. Every subcell river average contains at least 50% hornblende (Figure 29). The average composition for the San Luis Rey River flowing into the Oceanside-Carlsbad subcell (OS-1080 to CB-765) includes much more biotite (25.7%) than rivers in the San Onofre subcell (SO-1600 to PN-1100), which average only 4.6% biotite (Figure 24). The river composition of the Oceanside-Carlsbad subcell contains slightly less epidote (7.3%) than the adjacent northern rivers draining into the San Onofre subcell (10.9%). There is a large reduction in the percentage of composite particles from the 19.3% in the San Onofre subcell (SO-1600 to OS-1080) to the 7.3% Oceanside-Carlsbad subcell average from OS-1080 to CB-765 (Figure 25). Hypersthene diminishes slightly from the 2.3%

San Onofre subcell river average to the less than 1% Oceanside-Carlsbad subcell river average for OS-1080 to CB-765 (Figure 30).

<center>Mineralogy of Beach Samples</center>

4.37   Overall, the beach sediment from the Oceanside-Carlsbad subcell (OS-1080 to CB-765) contains slightly more quartz than the San Onofre subcell (SO-1600 to OS-1080) (Figure 39). Similar amounts of total heavy minerals and plagioclase feldspar persist from the beaches of the San Onofre subcell to those in the Oceanside-Carlsbad subcell (Figure 40 and 42). There is slightly less potassium feldspar in both sample sets of beach sediment from the Oceanside-Carlsbad subcell (OS-1080 to CB-765) as compared to that of the San Onofre subcell (SO-1600 to OS-1080) (Figure 42).

4.38   The average amount of hornblende on the beaches in the Oceanside-Carlsbad subcell (OS-1080 to CB-765) is more than twice the hornblende percentage in the adjacent San Onofre subcell (SO-1600 to OS-1080). Hornblende illustrates a well-developed, systematic downcoast enrichment in the San Onofre subcell beach sediment that continues into the Oceanside-Carlsbad subcell (Figure 48). Biotite increases substantially from the beaches in the San Onofre subcell to those within the Oceanside-Carlsbad subcell boundaries (OS-1080 to CB-765) (Figure 17). The prevalence of biotite on the beach, particularly at the end-of-winter storm season, indicates that the Oceanside-Carlsbad subcell (OS-1080 to CB-765) experienced an episode of comparatively low mechanical energy (Figure 43). Epidote ranks just below biotite and hornblende in decreasing order of heavy mineral abundance for the Oceanside-Carlsbad subcell (OS-1080 to CB-765) (Figure 45). Although epidote is the third dominant heavy mineral constituent, much less epidote occurs in Oceanside-Carlsbad beach sediment (2.7% at the end-of-winter and 6.9% at the end-of-summer) than in the over 20% epidote-enriched beach sediment from the San Onofre subcell (SO-1600 to OS-1080) (Figure 45). Fewer composite particles, opaque grains, garnet, glaucophane and sphene occur in the Oceanside-Carlsbad subcell sample set than the San Onofre subcell sample set (Table 14b). Hypersthene values maintain averages just below 2% for both Oceanside-Carlsbad subcell and San Onofre subcell beach sediment (SO-1600 to CB-765) (Figure 49).

<center>Mineralogic Comparison of the San Onofre and Oceanside-Carlsbad Subcells</center>

4.39   Overall, the San Onofre subcell (SO-1600 to OS-1080) appears distinct from the Oceanside-Carlsbad subcell (OS-1080 to CB-765) for both the end-of-winter and end-of-summer total mineralogic profiles (Figures 16 and 17). The Oceanside-Carlsbad subcell has more quartz and potassium feldspar than the San Onofre subcell, but these changes are quite gradational. The most distinguishable changes in the total mineralogic composition of both April and October sample sets occur at the mouth of the Las Flores Creek, PN-1285, implying the significance of fluvial input to identified petrofacies.

4.40   The San Onofre subcell includes important compositional differences within the subcell from SO-1600 to OS-1080; mineral composition changes at the boundary between the San Onofre and Oceanside-Carlsbad subcells, OS-1080. Epidote and glaucophane increase from San Mateo Creek (SO-1595) to the beach adjacent to Las Flores Creek, PN-1285 (Figures 18 and 19). This southward concentration is restricted to glaucophane and epidote (Figures 45 and 47), which probably reflects source compositional changes rather

<center>101</center>

than longshore transport processes. Moreover, Las Flores Creek (PN-1285) influences beach mineral composition because the petrofacies downcoast from this river are different from the upcoast beach composition (Figures 18 and 19). If the observed mineralogic trends are persistent, then the San Onofre subcell could be further divided at Las Flores Creek, PN-1285.

4.41   The subcell delineation of the San Onofre and Oceanside-Carlsbad at OS-1080 is quite distinct based upon the area plots of various heavy minerals for both beach sample sets (Figures 18 and 19). Systematic trends in compositional change within the Oceanside-Carlsbad subcell (OS-1080 to CB-765) are not recognizable; but the mineralogy is distinct from that of the San Onofre subcell (SO-1600 to OS-1080) (Figures 24 and 29). Much more hornblende and biotite characterizes the Oceanside-Carlsbad littoral subcell during both the winter and summer than the San Onofre subcell. Consequently, there is less epidote, composite particles, opaque grains, sphene, garnet and glaucophane in the Oceanside-Carlsbad subcell. The mineral composition of the Oceanside-Carlsbad subcell remains relatively consistent throughout the subcell.

Oceanside Littoral Cell: Encinitas Subcell

Mineralogy of River Samples

4.42   Hornblende makes up about half of the total heavy mineral content of the San Elijo (SD-635), San Dieguito (SD-590) and Los Penasquitos Rivers (TP-530) that drain into the Encinitas subcell (CB-765 to LJ-455). Approximately the same amount of composite particles occurs in the Encinitas subcell (CB-765 to LJ-455) (8%) as in the Oceanside-Carlsbad subcell (OS-1080 to CB-765). Sphene (5.8%) and opaque grains (5.2%) increase slightly from the Oceanside-Carlsbad subcell to the Encinitas subcell (Figures 31 and 32). The most important mineralogic change for the three rivers in this area is the presence of metamorphic minerals: namely, glaucophane (6.6%), garnet (1.3%), and epidote (16%) for the three rivers. The northernmost river within this subcell, San Elijo Lagoon (SD-635), appears anomalous from all the other rivers sampled (Figure 13). San Elijo Lagoon contains more major heavy minerals of the igneous plutonic facies (sphene, opaques, and composite particles), much less hornblende, and no glaucophane (Figure 13). Epidote cannot be used as a diagnostic tracer mineral because it is distributed throughout the Peninsular Ranges as a product of contact metamorphism. There is no glaucophane and little garnet in the San Elijo Lagoon sample, but the San Dieguito River and the Los Penasquitos Lagoon have an average of 1.6% glaucophane and 1.3% garnet in the fluvial sediment (Figure 46 and 47).

Mineralogy of Cliff Samples

4.43   Five samples were collected from Torrey Pine cliffs within the Encinitas subcell (Kuhn and others, 1987 and 1988). The stratigraphy of the exposed lithologic units in the Torrey Pines cliffs include the entire La Jolla Group: 1) Mount Soledad Formation 2) Delmar Formation 3) Torrey Sandstone 4) Ardath Shale 5) Scripps Formation and the 6) Friars Formation, following Kennedy and Moore's nomenclature (1971). These strata yield arkosic sediment.

102

4.44 The coastal cliffs in the Encinitas littoral subcell (CB-765 to LJ-455) contain slightly less quartz (56.5%) than the San Onofre (SO-1600 to OS-1080) cliff content (61.3%) (Figure 20). Only half the amount of the total heavy minerals for the San Onofre cliff strata occurs in the Encinitas subcell cliff samples (7.6%) (Table 13a). Cliff samples from the Encinitas subcell show a 5% increase in both plagioclase and potassium feldspar content compared to the feldspar values for the cliff strata from the San Onofre subcell.

4.45 Hornblende percentages in the cliffs decrease toward the south within the Encinitas subcell from CB-500 to LJ-455 (Figure 51). Overall, hornblende percentages remain about the same (22%) for this subcell as in the San Onofre subcell cliffs (Table 13A). Relatively high concentrations of biotite (36.9%) occur in the seacliffs within the Encinitas subcell from CB-500 to LJ-455 (Figure 28). Composite particles decrease slightly from the northern cliffs to the southern Torrey Pines cliffs. Opaque grains comprise a 12% average from CB-500 to LJ-455 for the Encinitas cliffs, increasing substantially from the 3.9% average of the northern San Onofre cliffs (SO-1460 to PN-1300). Little glaucophane or hypersthene occurs within the Encinitas cliff samples (Figures 28 and 30). Sphene occurs as a predominant accessory mineral (7%) in the cliffs at Torrey Pines (LJ-470), which is more than twice the sphene value for the San Onofre cliffs (SO-1460 to PN-1200) (Figure 32). Garnet occurs in small but consistent concentrations (1.1%) within four of the five cliff samples collected from the area. There is nearly as much garnet in the Encinitas cliffs (LJ-470) as in the San Onofre cliffs (SO-1460 to PN-1200) (Figure 27).

Mineralogy of Beach Samples

4.46 The Encinitas subcell (CB-765 to LJ-455) contains more quartz, heavy minerals and potassium feldspar in the end-of-summer beach sample set than the end-of-winter beach sample set (Figures 16 and 17). Plagioclase feldspar is the only light mineral that decreases significantly from the end-of winter (15.6%) to the end-of-summer (6.4%) sample sets in the Encinitas subcell (CB-765 to LJ-455) (Figure 41). Changes in the total mineral composition from the beaches of the Oceanside-Carlsbad subcell (OS-1080 to CB-765) to the Encinitas subcell (CB-765 to LJ-455) include a slight decrease in quartz (Figures 39). No overall differences in the feldspar content can be observed from the Oceanside-Carlsbad beaches to those of the Encinitas subcell (CB-765 to LJ-455) The seasonal differences of the feldspars have a wider range in the Encinitas subcell than in the Oceanside-Carlsbad subcell (Figure 41 and 42). The observed light mineral distribution indicates a great deal of sediment exchange between these two subcells.

4.47 Concentrations of heavy minerals in the Encinitas subcell (CB-765 to LJ-455) beach samples are not appreciably different from those of the Oceanside-Carlsbad (OS-1080 to CB-765) beaches. Hornblende concentrations remain virtually unchanged from the Oceanside-Carlsbad to the Encinitas subcell, suggesting considerable sediment exchange between these two subcells (Figure 51). Significantly more epidote is present in the Encinitas subcell (CB-765 to LJ-455) beach sample sets (13.4% end-of-winter; 11.4% end-of-summer) than those samples collected on the Oceanside-Carlsbad subcell (OS-1080 to CB-765)beaches (2.7% end-of-winter; 6.9% end-of-summer) (Figure 45). This increase of epidote on the beach within the Encinitas subcell does not necessarily indicate net southward sediment transport, but may reflect a major mineralogic change in the sediment source for these beaches. Both the cliffs (TP-480 to LJ-455) (Figure 16) and the rivers (SD-635 to TP-530) (Figure 13) show very high concentrations of epidote within the Encinitas subcell. The steep slopes and the shallow-headed La Jolla and Scripps submarine

103

canyons and La Jolla Point act as effective barriers to longshore sand transport. A slight increase in the amount of composite particles in the Encinitas subcell (CB-765 to LJ-455) beach sample set as compared with the Oceanside-Carlsbad subcell set (OS-1080 to CB-765) (Figure 44) reflects the increase of composite particles in the cliff and river sediment sources within the Encinitas subcell (Figure 25).

4.48   There is much less biotite in the Encinitas subcell (CB-765 to LJ-460) beach sample set (2.9% end-of-winter; 4.7% end-of-summer) than in the Oceanside-Carlsbad subcell (OS-1080 to CB-765) (Figure 43). Inasmuch as a large supply of biotite exists in the rivers and cliffs of both subcells, the reduction in the Encinitas subcell beach sediment may suggest an increase in depositional energy resulting in more offshore transport of this mineral. Slightly more sphene occurs in the beaches of the Encinitas subcell (CB-765 to LJ-455) (2.3% end-of-winter; 2.0% end-of-summer) than the beaches in the Oceanside-Carlsbad subcell (OS-1080 to CB-765) (0.3% end-of-winter; 1.4% end-of-summer) (Figure 51). More sphene occurs in the cliff (Figure 15) and river (Figure 13) samples of the Encinitas subcell than the Oceanside-Carlsbad subcell. Since there is a southward increase in sphene available for transport to the beach, southward increased sphene concentrations on the beach do not necessarily imply net southward longshore transport but may reflect local source contributions. Glaucophane increases slightly in the beach sediment of the Encinitas subcell (CB-765 to LJ-455) (1.1% end-of-winter; 2.2% end-of-summer) compared to that beach sediment from the Oceanside-Carlsbad subcell (OS-1080 to CB-765) (1.0% end-of-winter and none in the end-of-summer sample set). Glaucophane is present in both the San Dieguito River (SD-590) and the Penasquitos Lagoon (TP-530), and garnet is present both in the San Elijo Lagoon (SD-635) and San Dieguito River (SD-590) (Figure 13). However, no glaucophane or garnet occurred in the fluvial sample from the San Luis Rey River (OS-1050). Therefore, the compositional changes in the beaches of the Encinitas subcell reflect similar changes in source lithology and do not necessarily demonstrate downcoast concentration for any particular mineral. Opaque minerals (8.1% end-of-winter; 2.8% end-of-summer) in the Encinitas subcell (CB-765 to LJ-455) and hypersthene (1.9% end-of-winter; 1.3% end-of-summer) show no significant change from the Oceanside-Carlsbad subcell (OS-1080 to CB-765) (Figures 49 and 50).

4.49   Olivine is available in the southern section of the Encinitas subcell in the rivers and cliffs from TP-510 to LJ-455 (Figure 36). Approximately 2% of olivine is present at SO-620 in the end-of-winter beach sample set just south of San Elijo Creek (SD-635) (Figure 55). Olivine shows net northward transport within the Encinitas subcell. Actinolite occurs in very small amounts, less than 1% of both the rivers and cliffs in the northern segment of Encinitas subcell (Figure 33). For the end-of-summer sample set, 0.3% actinolite occurs at TP-535 (Figure 33) indicative of net southward transport of sand, during some undefined period of time. Because actinolite is only present in samples collected on the beach during October 1986, it probably represents a lag concentrate (Figure 52).

Mineralogic Comparison of Oceanside-Carlsbad and Encinitas Subcells

4.50   A gradational boundary occurs between the Oceanside-Carlsbad and Encinitas subcells. This transition suggests considerable sediment exchange between these subcells. Since little fluvial input occurs within the Oceanside-Carlsbad subcell during the recent past, this compositional consistency may indicate rather complete mixing across this boundary. The concentration of epidote, hornblende, hypersthene and sphene in the end-of-winter beach sample set (Figure 18) suggests net southward transport during the

104

winter. The end-of-summer sample set (Figure 19) does not show the same directional trends. Moreover, a northward increase in opaque grains implies some northward component of sediment transport during the summer. These homogeneities could indicate seasonally bidirectional vectors of littoral transport, sediment mixing, and/or onshore-offshore sediment transport.

4.51   A mineral suite for the Encinitas subcell (CB-765 to LJ-455) reflects compositional changes at the three river mouths: (San Elijo Lagoon (SD-635), San Dieguito River (SD-590), and Penasquitos Lagoon (PN-530). Opaque grains and composite particles increase south of the San Elijo Lagoon (Figures 18 and 19). The Penasquitos Lagoon, PN-530, marks most of the major changes in mineral assemblage that occur within this subcell. Garnet, glaucophane and hypersthene appear in appreciable quantities just south of Penasquitos Lagoon (Figures 18 and 19), and the concentrations taper off southward in both the end-of-winter and end-of-summer beach sample sets. Therefore, net sediment transport direction appears to be southward within this subcell. Inasmuch as no samples were collected for mineralogic analysis in the pocket beaches of the La Jolla Cove subcell, the transition zone at the Encinitas - La Jolla Cove subcell boundary cannot be evaluated. There is little reason to expect longshore sand transport around Point La Jolla.

Oceanside Littoral Cell: La Jolla Cove Subcell

4.52   No river, cliff or beach samples were collected from La Jolla Cove subcell (LJ-455 to SS-225), the smallest and southernmost subcell of the Oceanside Littoral Cell.

Mission Beach Littoral Cell
Mineralogy of River Sample

4.53   The quartz content of the San Diego River (MB-267)in the Mission Beach Littoral Cell (63.1%) is virtually the same as the values for the rivers in the Encinitas subcell (Table 13A). The Mission Beach river average for total heavy mineral content (23.3%) is more than twice that of rivers draining into the Encinitas subcell (9.1%) (Table 13A). Less plagioclase (9.8%) and potassium feldspar (7.0%) occurs in the San Diego River than those rivers draining into the Encinitas subcell (17.4% plagioclase and 10.8% potassium feldspar) (Table 13A). Figure 12 illustrates the major fluvial mineralogic differences between the rivers in the Encinitas subcell (CB-765 to LJ-455) and the Mission Beach Littoral Cell (PB-400 to SS-225). These percentages are given for a comparison of source lithology only; these subcells do not border each other. Sediment is not being transported around the steep cliffs of La Jolla Point or the La Jolla and Scripps submarine canyon heads.

4.54   The San Diego River, the only stream that discharges into the Mission Beach Cell, contains no glaucophane or garnet. Hornblende is the predominant heavy mineral within the fluvial sample set of the Mission Beach Littoral Cell (PB-400 to SS-225) (74%). Hornblende comprises half the total heavy mineral composition (Figure 48). Large quantities of biotite (17.7%) occur in the San Diego River (MB-267) (Figure 24). The remaining heavy mineral constituents diminish considerably in both abundance and variety from the Oceanside (DB-1900 to PB-400) to the Mission Beach Littoral Cell regions (PB-400 to SS-225). Composite particles (3.7%),   opaque grains (1.7%), hypersthene

105

(1.0%), epidote (0.7%), and sphene (0.7%) measured for the San Diego River sample show dramatic decreases from their relative abundance in the many rivers from San Juan Creek to Penasquitos Lagoon (Oceanside Littoral Cell).

Mineralogy of Beach Samples

4.55   Large amounts of quartz occur in the end-of-winter (75.2%) and end-of-summer (74.2%) beach sample sets. Relatively small amounts of heavy minerals occur in the Mission Beach Cell beach sample sets (PB-400 to SS-225) (10.9% end-of-winter, 11.4% end-of-summer). Much less plagioclase feldspar occurs in the Mission Beach Littoral Cell end-of-winter (9.2%) and end-of-summer (2.7%) sample sets. The relationship between the Mission Beach Littoral Cell (PB-400 to SS-225) and subcells in the Oceanside Littoral Cell (DB-1900 to LJ-455) can be evaluated on the area plots of total mineral concentrations for the end-of-winter and end-of-summer beach sample sets (Figures 18 and 19). The La Jolla Cove subcell contains the littoral cell boundary, but inadequate sampling does not permit a meaningful comparison.

4.56   Hornblende is the dominant heavy mineral on the beach in the Mission Beach littoral cell (PB-400 to SS-225) (84% for both the end-of-winter and end-of-summer sample sets) (Figure 48). Opaque grains remain in much the same concentration throughout the Mission Beach Littoral Cell (PB-400 to SS-225) beach samples without significant seasonal variation (8.7% end-of-winter, 4.3% end-of-summer). Much less epidote (2.0% end-of-winter, 0.7% end-of-summer) occurs in the Mission Beach Cell (PB-400 to SS-225) than Encinitas subcell (CB-765 to LJ-455) beach sediment. No systematic change in biotite or hypersthene concentrations can be observed between the beach sample sets within the Encinitas subcell (CB-765 to LJ-455) and those samples from the Mission Beach Littoral Cell (PB-400 to SS-225) (Figures 43 and 49). No glaucophane or garnet occurs in the beach sample sets from Mission Beach Littoral Cell, which is a reduction from Oceanside Littoral Cell. Overall, a much smaller variety of heavy minerals occurs in Mission Beach sediment (from PB-400 to SS-225) than in Oceanside Littoral Cell beach sand (DB-1900 to LJ-455).

Mineralogic Comparison of the Oceanside and Mission Beach Littoral Cells

4.57   The consideration of the Encinitas - Mission Beach cell boundary is not appropriate since these littoral zones are not adjacent; however, overall compositional differences can be discussed. The Mission Beach Littoral Cell beach sediment contains fewer heavy mineral species. Epidote, composite particles and opaque grains occur in smaller quantities than in the Oceanside Littoral Cell. Very little glaucophane, garnet or sphene occurs in the Mission Beach samples (Figures 18 and 19). Hornblende increases greatly for the Mission Beach samples in both sample sets. Hypersthene persists in similar abundances as in the Encinitas subcell (CB-765 to LJ-455). A gradational mineralogic change occurs north of the San Diego River at MB-330. This petrofacies may simply reflect the coastal processes in the Mission Bay area. The small percentage of heavy minerals in the Mission Beach Cell probably reflects the addition of inner shelf sediment as demonstrated by Fourier grain-shape analysis.

106

Silver Strand Littoral Cell

Mineralogy of River Sample

4.58   Only the Tijuana River (SS-008) drains into the Silver Strand Littoral Cell (SS-225 to SS-001). The total light mineral composition shows virtually no change from the San Diego River (MB-267) to the Tijuana River (SS-008) (Figure 12). Almost 90% of the total heavy mineral constituent is hornblende (Figure 13). Epidote, hypersthene and sphene increase slightly from the small amounts detected in the San Diego River (MB-267) (Figures 26, 30 and 32). Each of these heavy minerals comprise only about 2% of the total heavy mineral percentage. Composite particles decrease southward from the San Diego River to less than 2% in the Tijuana River (Figure 44). No garnet, glaucophane, and only negligible amounts of opaque grains occur in the Silver Strand Cell (SS-225 to SS-001). Heavy minerals are not nearly as varied or abundant as in the Oceanside Littoral cells.

Mineralogy of Beach Samples

4.59   Slightly less quartz is present in the Silver Strand (SS-225 to SS-001) beach (69.0% end-of-winter; 65.9% end-of-summer) than in the Mission Beach Littoral Cell (PB-400 to SS-225) (Figure 39). Much more plagioclase occurs in both beach sample sets from the Silver Strand Cell (SS-225 to SS-001) (15.0% end-of-winter; 9.8% end-of-summer) than in the Mission Beach Cell (PB-400 to SS-225) beach samples (9.2% end-of-winter; 2.7% end-of-summer) (Figure 40). Approximately 10% total heavy minerals occur in the beach sample sets for both the Silver Strand and the Mission Beach Littoral Cells (Figure 42). Potassium feldspar shows the same relative trends and concentrations in the Silver Strand Littoral Cell (SS-225 to SS-001) beach sample sets as the Mission Beach Littoral Cell (PB-400 to SS-225) (Figure 41).

4.60   For the Silver Strand (SS-225 to SS-001) beach averages, there is a slight seasonal decrease in the amount of quartz from winter to summer (69% end-of-winter and 66% end-of-summer) (Figure 39). Quartz makes up most of the beach sand in the Silver Strand Cell, followed by plagioclase feldspar (15% end-of-winter, 10% end-of-summer) (Figure 40). Both potassium feldspar (Figure 41) (7.0% end-of-winter, 12.7% end-of-summer) and heavy minerals (Figure 42) increase from winter to summer in the Silver Strand Cell (SS-225 to SS-001) (9.1% end-of-winter; 11.8% end-of-summer) within the Silver Strand Cell. A decrease in biotite present at the end-of-summer (from 9.0% to 4.2%) suggests an increase in depositional energy or dilution by other mineral grains.

4.61   Hornblende is the predominant major heavy mineral in the Silver Strand Cell (SS-225 to SS-001) beach sediment; 78.2% for the end-of-winter sample set and 87.2% for the end-of-summer sample set (Figure 48). No change in hornblende concentration occurs from the Mission Beach (PB-400 to SS-225) to the Silver Strand Littoral Cell (SS-225 to SS-001) beach samples (Figure 48). Biotite increases southward from the Mission Beach Littoral Cell beach sediment (1.65 end-of-winter; 4.0% end-of-summer) to the Silver Strand Littoral Cell (9.0% end-of-winter; 4.2% end-of-summer) (Figure 43). Epidote and hypersthene are present in subequal proportions within the Silver Strand Cell (SS-225 to SS-001); (3% at the end-of-winter beach samples and 1.5% in the end-of-summer sample set). (Figures 45 and 49). Opaque grains decrease slightly in the beach sample sets from the Mission Beach Cell (PB-400 to SS-225) to the Silver Strand Littoral Cell (SS-225 to SS-001) (Figure 50); whereas sphene increases southward from the Mission Beach Littoral

Cell (PB-400 to SS-225) to the Silver Strand Littoral Cell (SS-225 to SS-001) (0.3% to 1.3% end-of-winter; 0.7% to 1.2% end-of-summer) (Figure 51). Composite particles exist in similar concentrations for both Mission Beach and the Silver Strand Littoral Cells (Figure 44).

4.62   The presence of glaucophane and garnet even in small amounts (0.4%) suggests longshore sand transport. Garnet and glaucophane are not present in the samples from the Tijuana (SS-008) Rivers. Both garnet and glaucophane are present in both beach sample sets from the Silver Strand Littoral Cell (Figures 46 and 47). The appearance of actinolite at SS-008 in the end-of-summer 1986 beach samples (Figure 52), where none appeared at the end-of-winter indicates that actinolite was transported from the southern portion of the Silver Strand Littoral Cell. The Linda Vista and Bay Point Formations crop out in Mexico, providing blueschist metamorphic clasts to this southernmost segment of coast. Therefore, upcoast transport must predominate within the Silver Strand Littoral Cell. The occurrence of garnet, glaucophane and actinolite demonstrates net northward transport in the Silver Strand Cell. The increase in heavy mineral content from SS-008 to SS-225 may indicate net upcoast sediment during the summer of 1986 (Figures 16 and 17). Epidote increases within the northern segment (SS-225 to SS-100) for the end-of-winter sample set, providing additional evidence for northward sediment transport in the Silver Strand Cell.

Mineralogic Comparison of Mission Beach and Silver Strand Littoral Cell

4.63   San Diego Harbor together with steep submarine slopes off Point Loma form an effective barrier separating the Mission Beach from the Silver Strand Littoral Cell. Although Mission Beach samples appear mineralogically quite similar to those from the Silver Strand Cell, distinct differences in concentrations separate these two cells. Mineralogic trends reflective of net sediment accumulation form a sharp boundary (SS-225), particularly for the end-of-winter sample sets (Figures 16 and 18). A greater percentage of total heavy minerals accumulates on the beach in the southern portion of the Silver Strand Cell.

108

5. CONCLUSIONS

5.01 Fourier grain-shape analysis of medium sand-size quartz grains indicates the following average contributions from local sources for 1986 sample sets collected in the subcells of the Oceanside Littoral Cell as well as the Mission Beach and Silver Strand Littoral Cells.

Oceanside Littoral Cell:

Capistrano subcell (end-of-winter):

- San Juan Creek 12%;
- northern shelf 8%;
- southern shelf 12%;
- San Mateo Creek 28%; and
- downcoast beach (San Onofre subcell) 40%.

San Onofre subcell (end-of-winter):

- upcoast beaches (Capistrano subcell) 8%;
- San Mateo Creek 12%;
- northern shelf 5%;
- cliff 13%;
- Santa Margarita River 27%; and
- southern shelf 35%.

San Onofre subcell (end-of-summer):
- upcoast beach (Capistrano subcell) 8%;
- San Mateo Creek 11%;
- northern shelf 3%;
- cliff 14%;
- Santa Margarita River 33%; and
- southern shelf 32%.

Oceanside-Carlsbad subcell (end-of-winter)
- upcoast beach (San Onofre subcell) 11%;
- northern shelf 28%;
- San Luis Rey River 6%;
- southern shelf 9%; and

- downcoast beach (Encinitas subcell) 46%.

Encinitas subcell (end-of-winter)
- upcoast beach (Oceanside-Carlsbad subcell) 41%;
- San Dieguito River 5%;
- northern shelf 22%;
- cliff 12%;
- downcoast beach (La Jolla Cove subcell) 8%; and
- southern shelf 11%.

Encinitas subcell (end-of-summer):
- upcoast beach (Oceanside-Carlsbad subcell) 41%;
- San Dieguito River 5%;
- northern shelf 26%;
- cliff 12%;
- downcoast beach (La Jolla Cove subcell) 4%; and
- southern shelf 12%.

La Jolla Cove Subcell:
- inadequate sample control

Mission Beach Littoral Cell:
- San Diego River 24%; and
- inner shelf 76%.

Silver Strand Littoral Cell:
- northern shelf 11%;
- Tijuana River 40%;
- downcoast beach (south of Tijuana River) 38%; and
- cliff (northernmost extension of Playas de Tijuana) 11%.

5.02 An important result of the Fourier grain-shape analysis is the identification of the littoral contribution from inner shelf sources, which range from 11 to 76 percent and average approximately 35 percent.

5.03 The boundaries between the Oceanside, Mission Beach and Silver Strand Littoral Cells are known to be effective barriers to littoral sand transport. The results obtained by

Fourier grain-shape analysis for the 1986 beach sample sets indicate there is sand exchange between the Capistrano and San Onofre subcells and considerable exchange between the Oceanside-Carlsbad and Encinitas subcells. Except for beach nourishment projects, Oceanside Harbor is a littoral sediment sink, therefore little sand is exchanged naturally between the San Onofre and Oceanside-Carlsbad subcells. Sampling in the La Jolla Cove subcell was inadequate to examine the littoral exchange between the Encinitas and La Jolla Cove subcells.

5.04   Whereas the quartz populations in the Encinitas subcell were homogeneous from April to October 1986, samples from the San Onofre subcell indicated net upcoast transport during this time interval. Seasonal data were not available for the other littoral subcells or cells. Samples from the Silver Strand Littoral Cell also indicated net upcoast transport during a relatively recent time interval.

5.05   One of the most interesting results of the Fourier grain-shape analysis is the compositional homogeneity of the quartz grain populations within the subcells and cells. This condition presumably has resulted from thorough mixing of quartz sand populations from cross shore and bidirectional longshore transport, presumably during a relatively recent period of time.

5.06   A mineralogic change occurs at the boundary between the Capistrano and San Onofre subcells. It is interesting to note that for the 1986 beach samples, the boundary is somewhat transitional for the end-of-winter sample set and more distinct for the end-of-summer set. Inasmuch as the mouths of both San Onofre and San Mateo Creeks occur south of San Mateo Point, it appears that sediment discharged from these rivers was transported upcoast and concentrated south of San Mateo Point during the summer of 1986 to produce a more distinct boundary. This, in turn, suggests that San Mateo Point partially restricts longshore sand transport. However, mineralogic similarities of the Capistrano and San Onofre subcells indicate that substantive sediment exchange has occurred across this subcell boundary during an undefined time interval.

5.07   The mineralogic composition of the San Onofre subcell is distinct from that of the Oceanside-Carlsbad subcell. These two subcells are separated by Oceanside Harbor and associated structures, therefore, except for beach nourishment programs, little sand is exchanged between these subcells.

5.08   The gradational mineralogic boundary between the Oceanside-Carlsbad and Encinitas subcells indicates considerable sediment exchange across the boundary (the onshore projection of the head of Carlsbad Submarine Canyon). The sediment exchange and mixing across this boundary presumably is due to bidirectional longshore transport.

5.09   The character of the boundary between the Encinitas and La Jolla Cove subcells cannot be evaluated, because no mineralogical analysis was performed on La Jolla Cove samples.

5.10   There is little reason to believe littoral sand is being transported across the heads of La Jolla and Scripps submarine canyons and around the steep submarine slopes off

Point La Jolla to the Mission Beach Cell. Likewise, the steep submarine slopes off Point Loma and San Diego Harbor form an effective sediment barrier between the Mission Beach and Silver Strand Littoral Cells.

5.11   An isolated peak of glaucophane in the 1986 sample set from the Capistrano subcell was derived from San Mateo Creek and/or the coastal cliffs extending from stations SO-1460 to PN-1200. The occurrence of this peak indicates upcoast littoral transport from the San Onofre to the Capistrano subcell.

5.12   In the San Onofre subcell, San Mateo and San Onofre Creeks and the coastal cliffs from stations SO-1460 to PN-1200 are a source for glaucophane and actinolite. Small percentages of olivine occur in the cliffs and rivers between stations PN-1400 and PN-1200. The concentrations of glaucophane, actinolite and olivine in the southern portion of the San Onofre subcell suggest net downcoast longshore transport.

5.13   The mineral composition of the Oceanside-Carlsbad subcell is relatively constant throughout for the 1986 sample set. However, the concentration of epidote, hornblende, hypersthene and sphene in the southern portions of this subcell for the end-of-winter set suggests southward transport during the winter months. A northward increase in opaque grains for the end-of-summer sample set may imply some upcoast transport during the summer months. The observed compositional uniformity does suggest rather thorough sediment mixing, which presumably is the result of bidirectional longshore transport.

5.14   The principal mineralogic changes in the Encinitas subcell occur near the mouths of the San Elijo Lagoon, San Dieguito River and Penasquito Lagoon. Opaque grains and composite particles increase south of San Elijo Lagoon. Garnet, glaucophane and hypersthene occur in appreciable quantities south of Penasquitos Lagoon and the concentrations decrease downcoast for both the end-of-winter and end-of-summer sample sets. Although little longshore transport appears to have occurred from April to October 1986, the net transport direction appears to have been downcoast.

5.15   No mineralogic data were obtained for the La Jolla Cove subcell.

5.16   Only two samples were taken from the Mission Beach Littoral Cell, and the mineralogic consistency of these two samples does not permit any inferences to be made regarding sediment transport within this cell.

5.17   Garnet, glaucophane and actinolite are present in the 1986 beach samples from the Silver Strand Littoral Cell. These minerals were not present in the sample from the Tijuana River, but do occur in the Linda Vista and Bay Point Formations which crop out in the bluffs along the southern part of the Silver Strand Cell in Mexico. The occurrence of these minerals throughout the Silver Strand Cell suggests net upcoast longshore transport. This assertion is supported by the increase in heavy mineral content, including epidote, from Stations SS-008 to SS-225.

6. GLOSSARY

Centroid- The point whose coordinates are the mean values of the coordinates of the points in the set. For example, the center is the centroid of a circle; the centroid of a triangle is the point of intersection of its medians.

Cosine-Theta Similarity Coefficients - Cosine-theta may be thought of as expressing similarity as an angular relationship between two samples or variables represented in a multidimensional coordinate system; the similarity between two samples p and q being represented by the angle between their respective vectors in the coordinate system.

Covariance- The arithmetic mean or the expected mean value of the product of the deviations of two variables from their respective mean values.

Eigenvalue- The algebraic roots of a characteristic equation of the coefficient matrix.

Facies- A distinctive rock type, broadly corresponding to a certain depositional environment or mode of origin.

Fourier Analysis- A method for representing a periodic mathematic function as an infinite series of summed sine and cosine terms.

Kurtosis- The quality, state, or condition of peakedness or flatness of the graphic representation of a statistical distribution.

Orthogonal- In its mathematical sense as meaning perpendicular, e.g. in relation to a pair of orthogonal coordinate axes.

Q-Mode- Comparisons between or among objects or samples.

R-Mode- Comparisons between or among variables.

Skewness- The quality, state, or condition of being distorted or lacking symmetry; especially the quality or state of asymmetry shown by a frequency distribution that is bunched on one side of the average and tails out on the other side.

Standard Deviation- The square root of the average of the squares of deviation about the mean of a set of data. It is a statistical measure of dispersion.   ·

Variance- The square of the standard deviation.

Wave Number (or Harmonic)- The number of wave cycles per unit of distance in a given direction.
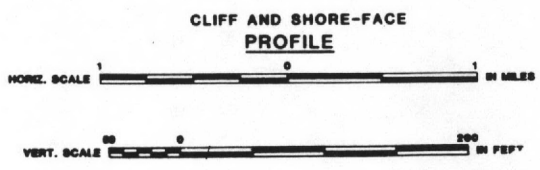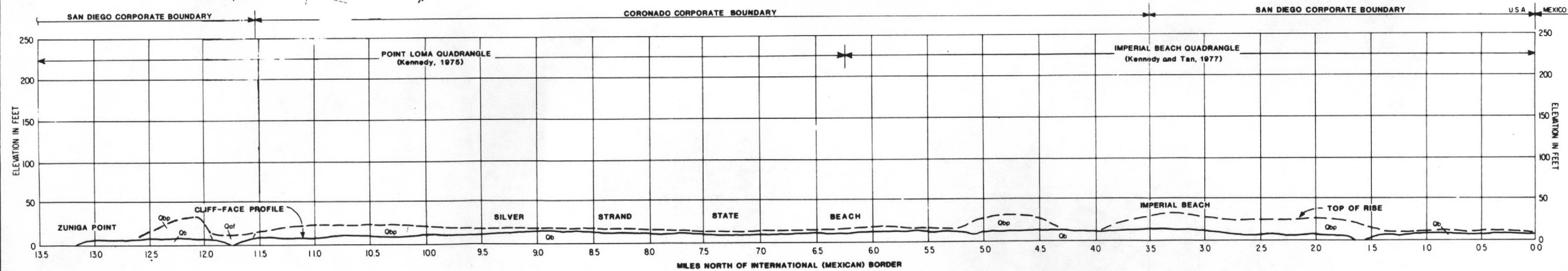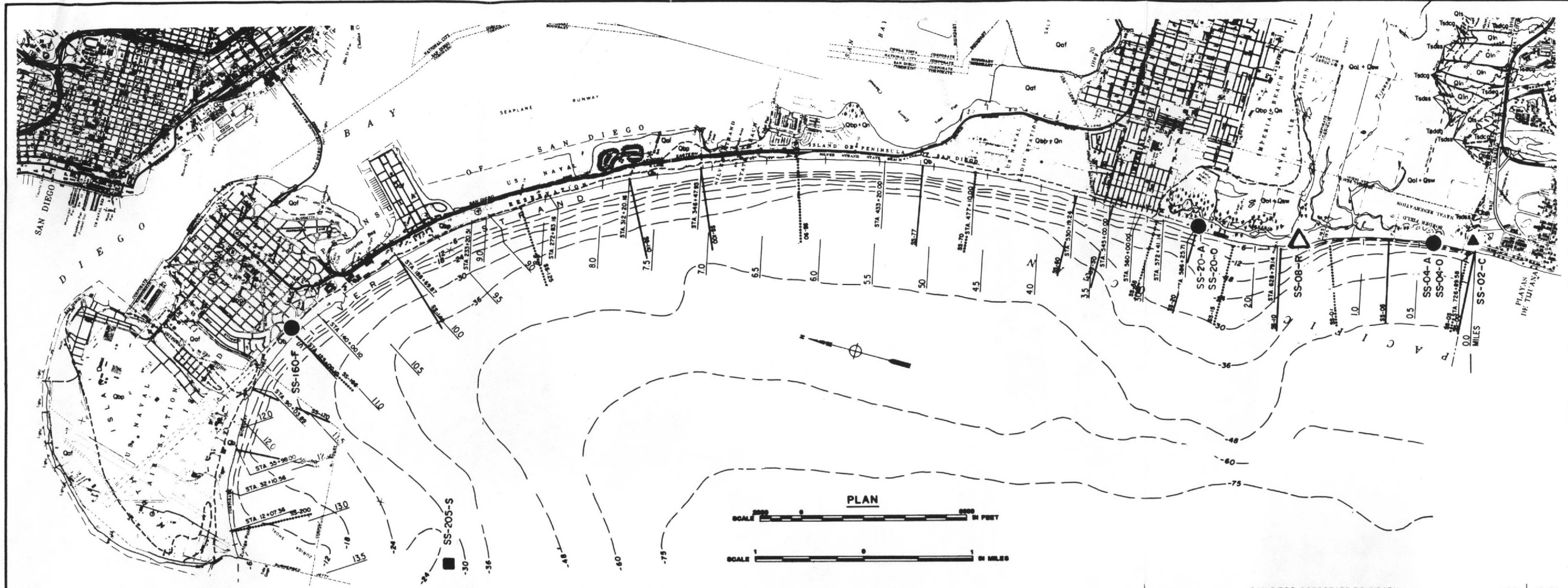
7. REFERENCES

Ahlschwede, K. S., 1988, Sources and net littoral transport of sand in San Diego and southern Orange Counties, southern California: Fourier grain-shape analysis: Unpublished M.S. thesis, University of Southern California, Los Angeles, California, 135 p.

Bendat, J. S., and Piersol, A. G., 1971, Random data: Analysis and measurement procedures: Wiley-Interscience, Inc., New York, 407 p.

Blatt, H. Middleton, G.V., and Murray, 1972, Origin of sedimentary rocks: Englewood Cliffs, New Jersey, Prentice-Hall, Inc., 634 p.

Bloom, L., 1979, Th relationships among river, beach and submarine canyon sands in the southern Santa Barbara littoral cell, Ventura County, California: Fourier grain-shape analysis: unpubl. Master's thesis, Univ. of Southern California, Los Angeles, California, 115 p.

Bloomfield, P., 1976, Fourier analysis of time series: An introduction: Wiley-Interscience Inc., New York, 258 p.

Bomer, E. J., 1985, Quartz grain-shape modification in high-gradient fluvial environments: Fourier grain-shape analysis: Unpublished M.S. thesis, University of Southern California, Los Angeles, California, 139 p.

Brigham, E.O., 1974, The fast Fourier transform: Englewood Cliffs, New Jersey, Prentice-Hall, Inc. 252 p.

Broadhead, S. D., 1988, Fourier grain-shape analysis of the sources and littoral transport of sand, San Elijo Lagoon to Point La Jolla: Unpublished M.S. Thesis, University of Southern California, Los Angeles, California, 235 p.

Brown, P.J., Ehrlich, R., and Colquhoun, D.J., 1980, Origin of patterns of quartz sand types on the southwestern United States continental shelf and implications on contemporary shelf sedimentation - Fourier grain shape analysis: Jour Sed. Petrology, v. 50, p. 1095-1100.

Carver, R.E., 1971, Procedures in sedimentary petrology: New York, Wiley-Interscience, 653 p.

Cho, K. H., 1989, Sedimentology of a composite inner-shelf sand body resulting from the resuspension of nearshore sediment by episodic, storm-generated currents, Oceanside California: unpublished M.S. thesis, University of Southern California, Los Angeles, 104 p.

Clark, R. A., and Osborne, R.H., 1982, Contribution of Salinas River sand to the beaches of Monterey Bay, California, during the 1978 flood period: Fourier grain-shape analysis: Jour. Sed. Petrology, v. 52, p. 807-822.

Darigo, N.J., 1984, Quarternary stratigraphy and sedimentation of the mainland shelf of San Diego County, California: Unpublished M.S. thesis, University of Southern California, Los Angeles, California, 2 vols., 447 p.

Darigo, N.J., and Osborne, R.H., 1986, Quaternary stratigraphy and sedimentation of the inner continental shelf, San Diego, California: in Knight, R.J., and McLean, J.R., eds., Shelf sands and sandstones: Canadian Society of Petroleum Geologists, Memoir 11, p. 73-98.

Davis, J.C., 1986, Statistics and data analysis in geology: John Wiley & Sons, New York, 646 p.

Ehrlich, R., and Weinberg, B., 1970, An exact method for characterization of grain shape: Jour. Sed. Petrology, v. 40, p. 205-212.

Ehrlich, R., Orzeck, J.J., and Weinberg, B., 1974, Dentrital quartz as a natural tracer - Fourier grain shape analysis: Jour. Sed. Petrology, v. 44, p. 145-150.

Ehrlich, R., and Chin, M., 1980, Fourier grain-shape analysis: A new tool for sourcing and tracking abyssal silts: Marine Geol., v. 38, p. 219-232.

Ehrlich, R., Brown, P.J., Yarus, J.M., and Przygocki, R., 1980, The origin of shape frequency distributions and the relationship between size and shape: Jour. Sed. Petrology, v. 50, p. 475-484.

Emery, K.O., 1960,. The sea off southern California: A modern habitat of petroleum: New York, John Wiley and Sons, 366 p.

Gaylor, J.M., 1984, Sources and transport of sand in the littoral zone of Lake Tahoe, California and Nevada: Fourier grain-shape analysis: unpubl. Master's thesis, University of Southern California, Los Angeles California, 112 p.

Hudson, C.B., and Ehrlich, R., 1980, Determination of relative provenance contributions in samples of quartz sand using Q-mode factor analysis of Fourier grain shape data: Jour. Sed. Petrology, v. 50, p. 1101-1110.

Inman, D.L., 1981, Evaluation of the budget of waves and sand, Oceanside littoral cell and recommendations for monitoring and sand bypassing: Technical Report, U.S. Army Corps of Engineers, Los Angeles District, 24 p.

Inman, D. L., and Chamberlain, T.K., 1960, Littoral sand budget along the southern California coast: Report of the Twenty-first International Geological Congress, Copenhagen, Volume of Abstracts, p. 245-246.

Kuhn, G. G., and Shepard, F.P., 1984, Sea cliffs, beaches and coastal valleys of San Diego County: Berkeley, University of Califonia Press, 193 p.

Kuhn, G.G., Osborne, R.H., Ahlschwede, K.S., and Compton,E.A., 1987, Processes, locations and rates of coastal cliff erosion from 1947 to present, Dana Point to the United States-Mexico border and the stratigraphy of contributing cliffs and bluffs at San Onofre, Camp Pendleton, and Torrey Pines: Technical Report, Los Angeles District, U.S. Army Corps of Engineers, 298 p., 11 plates.

Kuhn, G. G., Osborne, R. H., Compton, E. A., and Fogarty, T., 1988, Processes, locations and rates of coastal cliff erosion from 1887 to 1947, Dana Point to the Mexican Border: Technical Report, Los Angeles District, U.S. Army Corps of Engineers, Ref. No. CCSTW 88-8, 300 p.

Larsen, E. S., 1948, Batholith of Corona, Elsinore and San Luis Rey quadrangles, southern California: Geological Society of America Memoir 29, 182 p.

Mazzullo, J. M., and Ehrlich, R., 1980, A vertical variation in the St. Peter Sandstone - Fourier grain shape analysis: Jour. Sed. Petrology, v. 50, p. 63-70.

Mazzullo, J.M., and Ehrlich, R., 1983, Grain shape variation in the St. Peter Sandstone: A record of eolian and fluvial sedimentation of an early Paleozoic cratonic sheet sand: Jour. Sed. Petrology, v. 53, p. 105-119.

Mrakovitch, J., Ehrlich, R., and Weinberg, B., 1976, New technique for stratigraphic analysis and correlation - Fourier grain-shape analysis, Louisiana offshore Pliocene: Jour. Sed. Petrology, v. 46, p. 226-233.

Osborne, R. H., Edelman, M.C. Gaylor, J. M., and Waldron, J. M., 1985, Sedimentology of the littoral zone in Lake Tahoe, California-Nevada: Technical Report, California State Lands Commission, 88 p.

Osborne, R.H., Darigo, N.J., and Scheidemann, R.C., Jr., 1983, Potential offshore sand and gravel resources of the inner continental shelf of southern California: State of California, Dept. of Boating and Waterways, 302 p.

Porter, G.A., Ehrlich, R., Osborne, R.H., and Combellick, R.A., 1979, Sources and nonsources of beach sand along southern Monterey Bay, California - Fourier shape analysis: Jour. Sed. Petrology, v. 49, p. 727-732.

Riester, D.D., Shipp, R.C., and Ehrlich, R., 1982, Patterns of quartz sand shape variation, Long Island Littoral and shelf: Jour. Sed. Petrology, v. 52, p. 1307-1314.

Schultz, D.J., 1980, The effects of hydrofluoric acid on quartz grain shape - Fourier grain shape analysis: Jour. Sedimentary Petrology, v. 50, p. 644-645.

Simon, Li & Associates, Inc., 1988, River sediment discharge study San Diego region: Technical Report, Los Angeles District, U.S. Army Corps of Engineers, Ref. No. CCSTW 88-3, 95 p.

Stuart, C.J., 1979, Lithofacies and origin of the San Onofre Breccia, coastal southern California, in Stuart, C.J., ed., A guidebook to Miocene lithofacies and depositional environments, southern California and northwestern Baja California: Los Angeles, Pacific Section of the Society of Economic Paleontologists and Mineralogists, p. 25-42.

Tekmarine, Inc., 1987, Oceanside Littoral Cell Preliminary Sediment Budget Report: Technical Report, Los Angeles District, U.S. Army Corps of Engineers, Ref. No. CCSTW 87-4, 158 p.

Van Nieuwenhuise, R, Yarus, J. M., Przxygocki, R. S., and Ehrlich, R., 1978, Sources of shoaling in Charleston Harbor: Fourier grain shape analysis: Jour. Sed. Petrology, v. 48, p. 373-384.

Young, K., 1980, Fourier analysis of quartz grains, a new method of interpreting sediment movement: Marine Resource Bull., v. 12, no. 2, p. 4-5.

PLAN

SCALE | IN FEET

SCALE | IN MILES

SAN DIEGO CORPORATE BOUNDARY | CORONADO CORPORATE BOUNDARY | SAN DIEGO CORPORATE BOUNDARY | U.S.A | MEXICO

POINT LOMA QUADRANGLE
(Kennedy, 1975)

IMPERIAL BEACH QUADRANGLE
(Kennedy and Tan, 1977)

ZUNIGA POINT — CLIFF-FACE PROFILE — SILVER STRAND STATE BEACH — IMPERIAL BEACH — TOP OF RISE

ELEVATION IN FEET

MILES NORTH OF INTERNATIONAL (MEXICAN) BORDER

CLIFF AND SHORE-FACE
PROFILE

HORIZ. SCALE | IN MILES

VERT. SCALE | IN FEET

LEGEND

———	BEACH PROFILE ONLY
·········	BEACH PROFILE PLUS SEDIMENT SAMPLING
×	OFFSHORE SEDIMENT STAKE
⊙	WAVE GAGE
▲	CLIFF OR BLUFF SAMPLE
△	RIVER SAMPLE
●	BEACH SAMPLE
■	SHELF SAMPLE

NOTE:
SEE PLATE 7 (SHEETS 1 AND 2) FOR EXPLANATION
OF GEOLOGICAL SYMBOLS, AND NOMENCLATURE

COAST OF CALIFORNIA STORM AND TIDAL WAVES STUDY

DANA POINT TO MEXICAN BORDER

GEOLOGY
OF THE
COASTAL ZONE

MEXICAN BORDER (MI. 0.0) TO ZUNIGA JETTY (MI. 13.2)
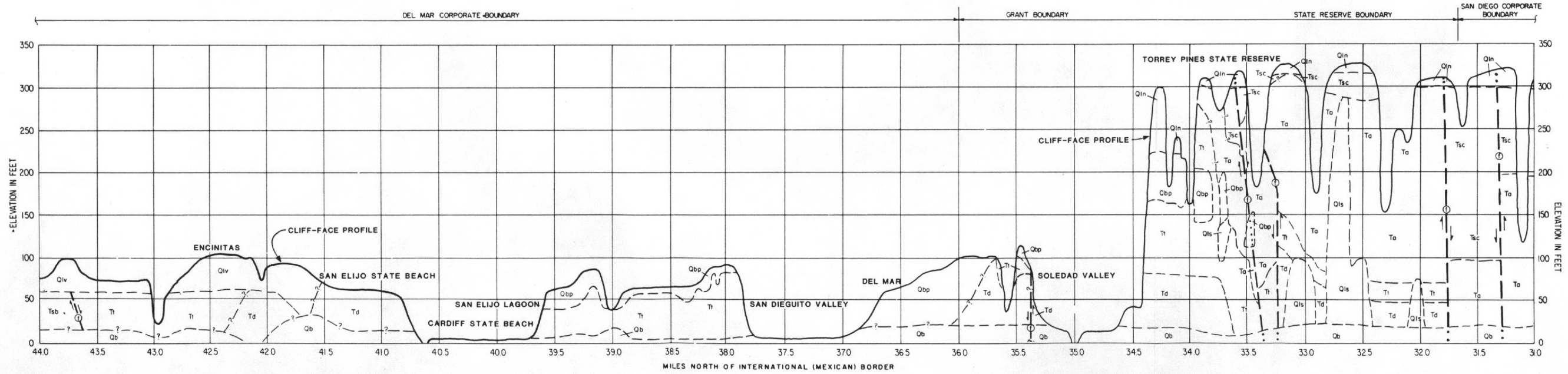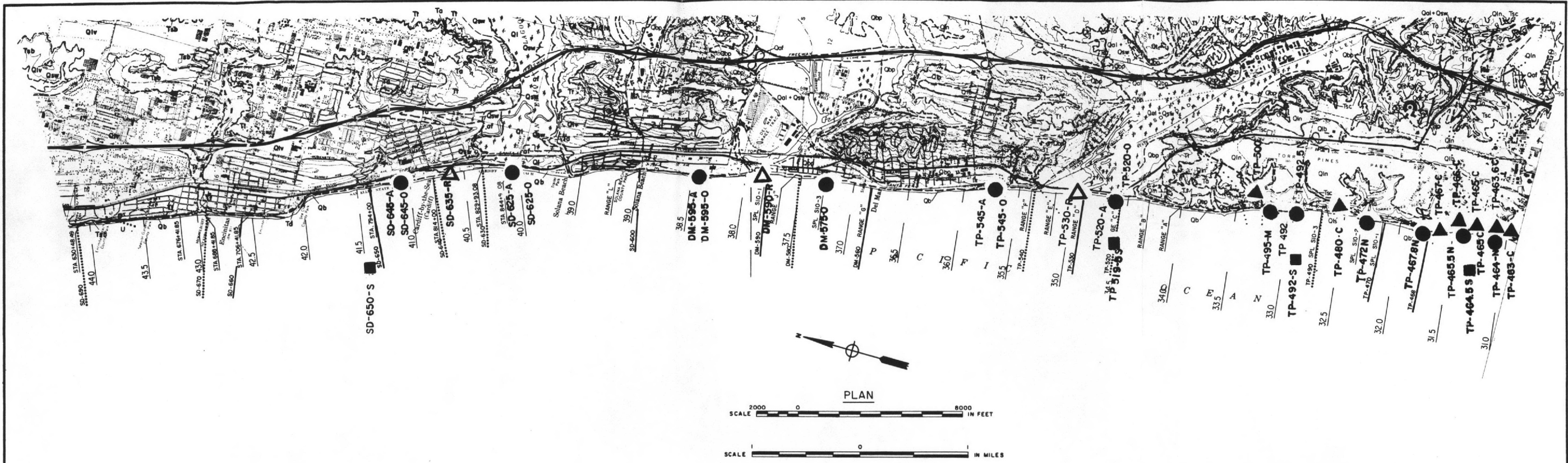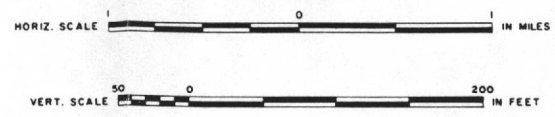
U. S. ARMY CORPS OF ENGINEERS
LOS ANGELES DISTRICT

PLATE 1

PLAN

SCALE [2000 ... 0 ... 8000] IN FEET

SCALE [1 ... 0 ...] IN MILES

CLIFF AND SHORE-FACE
PROFILE

HORIZ. SCALE [1 ... 0 ... 1] IN MILES

VERT. SCALE [50 ... 0 ... 200] IN FEET

LEGEND

——	BEACH PROFILE ONLY
······	BEACH PROFILE PLUS SEDIMENT SAMPLE
✕	OFFSHORE SEDIMENT STAKE
⊕	WAVE GAGE
▲	CLIFF OR BLUFF SAMPLE
△	RIVER SAMPLE
●	BEACH SAMPLE
■	SHELF SAMPLE

NOTE:
SEE PLATE 8 (SHEETS 1 AND 2) FOR EXPLANATION
OF GEOLOGIC SYMBOLS, AND NOMENCLATURE.

COAST OF CALIFORNIA STORM AND TIDAL WAVES STUDY

DANA POINT TO MEXICAN BORDER

GEOLOGY
OF THE
COASTAL ZONE

POINT LOMA (MI. 14.0) TO LA JOLLA (MI. 31.0)

U.S. ARMY CORPS OF ENGINEERS
LOS ANGELES DISTRICT

PLATE 2

PLAN

SCALE 2000 0 8000 IN FEET

SCALE 1 0 1 IN MILES

CLIFF AND SHORE-FACE
PROFILE

HORIZ. SCALE 1 0 1 IN MILES

VERT. SCALE 50 0 200 IN FEET

NOTE:
SEE PLATE 7 (SHEETS 1 AND 2) FOR
EXPLANATION OF GEOLOGIC SYMBOLS,
AND NOMENCLATURE.

LEGEND

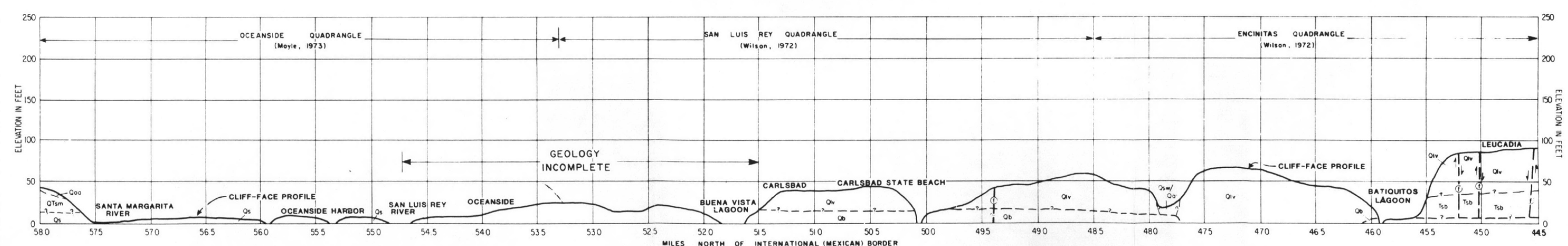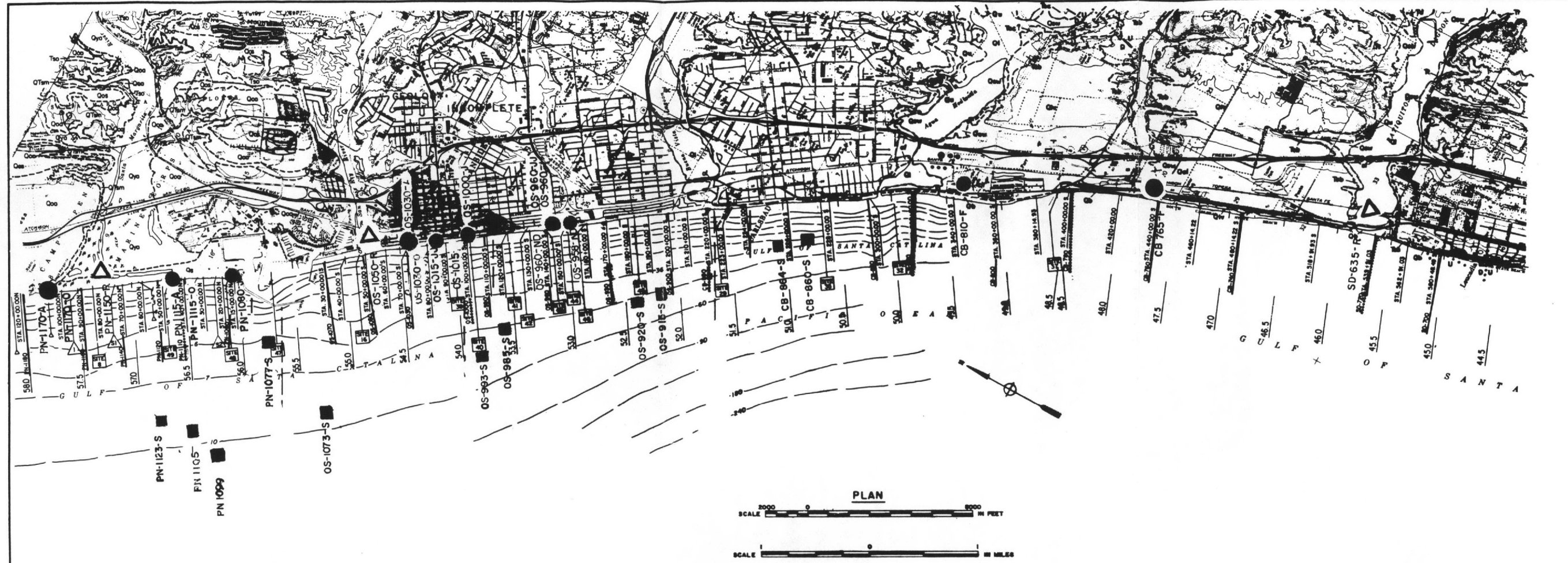|	
——	BEACH PROFILE ONLY
··········	BEACH PROFILE PLUS SEDIMENT SAMPLING
X	OFFSHORE SEDIMENT STAKE
⊕	WAVE GAGE
▲	CLIFF OR BLUFF SAMPLE
△	RIVER SAMPLE
●	BEACH SAMPLE
■	SHELF SAMPLE

COAST CALIFORNIA STORM AND TIDAL WAVES STUDY

DANA POINT TO MEXICAN BORDER

GEOLOGY

OF THE

COASTAL ZONE

LA JOLLA (MI. 31.0) TO LEUCADIA (MI. 44.0)
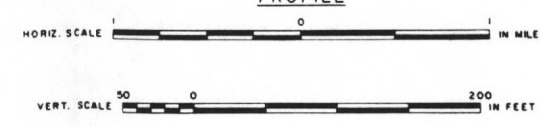
U. S. ARMY CORPS OF ENGINEERS
LOS ANGELES DISTRICT

PLATE 3

PLAN

SCALE ___ 2000 ___ 0 ___ 6000 ___ IN FEET

SCALE ___ 0 ___ IN MILES

CLIFF AND SHORE-FACE PROFILE

HORIZ. SCALE ___ 0 ___ IN MILES

VERT. SCALE ___ 50 ___ 0 ___ 200 ___ IN FEET

OCEANSIDE QUADRANGLE
(Moyle, 1973)

SAN LUIS REY QUADRANGLE
(Wilson, 1972)

ENCINITAS QUADRANGLE
(Wilson, 1972)

ELEVATION IN FEET — 250, 200, 150, 100, 50

GEOLOGY INCOMPLETE

CARLSBAD   CARLSBAD STATE BEACH   LEUCADIA

SANTA MARGARITA RIVER   CLIFF-FACE PROFILE   BUENA VISTA LAGOON   CLIFF-FACE PROFILE   BATIQUITOS LAGOON

OCEANSIDE HARBOR   SAN LUIS REY RIVER   OCEANSIDE

MILES NORTH OF INTERNATIONAL (MEXICAN) BORDER

580 575 570 565 560 555 550 545 540 535 530 525 520 515 510 505 500 495 490 485 480 475 470 465 460 455 450 445
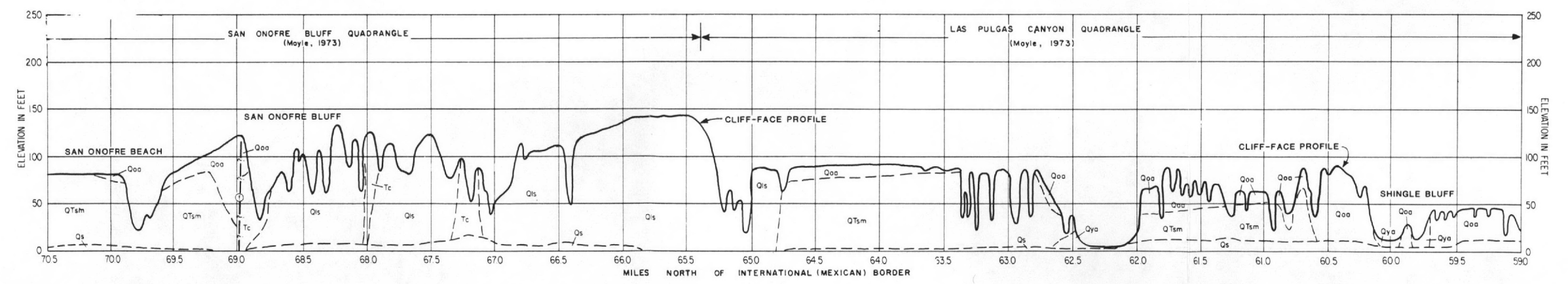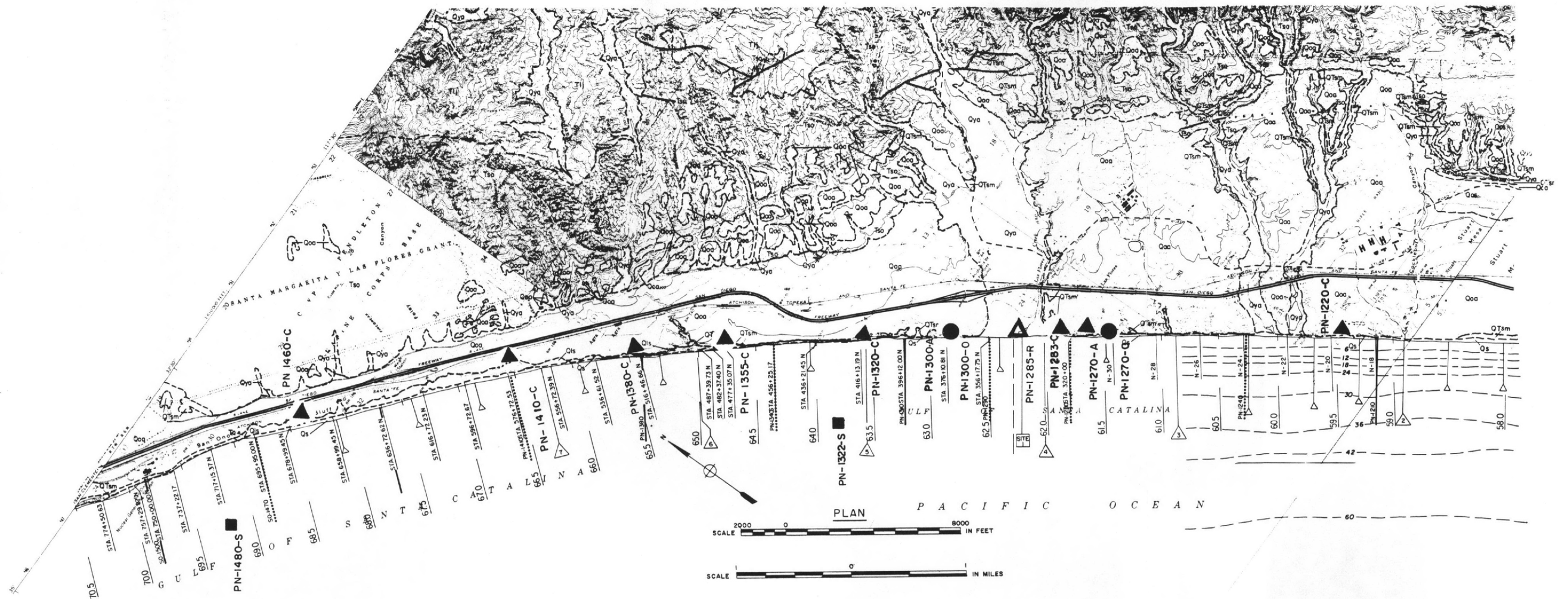
NOTES:
1. SEE PLATE 7 (SHEETS 1 AND 2) FOR EXPLANATION OF GEOLOGIC SYMBOLS AND NOMENCLATURE.
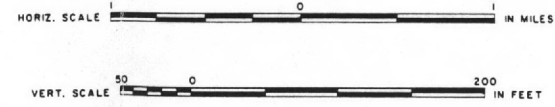2. GEOLOGY INCOMPLETE FOR SOUTH OCEANSIDE AREA (APPROXIMATELY MI 51.8 TO MI 55.2).

LEGEND

———	BEACH PROFILE ONLY
··········	BEACH PROFILE PLUS SEDIMENT SAMPLING
×	OFFSHORE SEDIMENT STAKE
⊙	WAVE GAGE
▲	CLIFF OR BLUFF SAMPLE
△	RIVER SAMPLE
●	BEACH SAMPLE
■	SHELF SAMPLE

COAST OF CALIFORNIA STORM AND TIDAL WAVES STUDY

DANA POINT TO MEXICAN BORDER

GEOLOGY
OF THE
COASTAL ZONE

LEUCADIA (MI. 44.0) TO SANTA MARGARITA RIVER (MI. 58.0)

U. S. ARMY CORPS OF ENGINEERS
LOS ANGELES DISTRICT

PLATE 4

PLAN

PACIFIC OCEAN

SCALE 2000 0 8000 IN FEET

SCALE 0 IN MILES

CLIFF AND SHORE-FACE
PROFILE

HORIZ. SCALE 0 IN MILES

VERT. SCALE 50 0 200 IN FEET

LEGEND

BEACH PROFILE ONLY
BEACH PROFILE PLUS SEDIMENT
SAMPLING
X OFFSHORE SEDIMENT STAKE
WAVE GAGE
▲ CLIFF OR BLUFF SAMPLE
△ RIVER SAMPLE
● BEACH SAMPLE
■ SHELF SAMPLE

NOTE:
SEE PLATE 7 (SHEETS 1 AND 2) FOR EXPLANATION
OF GEOLOGIC SYMBOLS AND NOMENCLATURE.

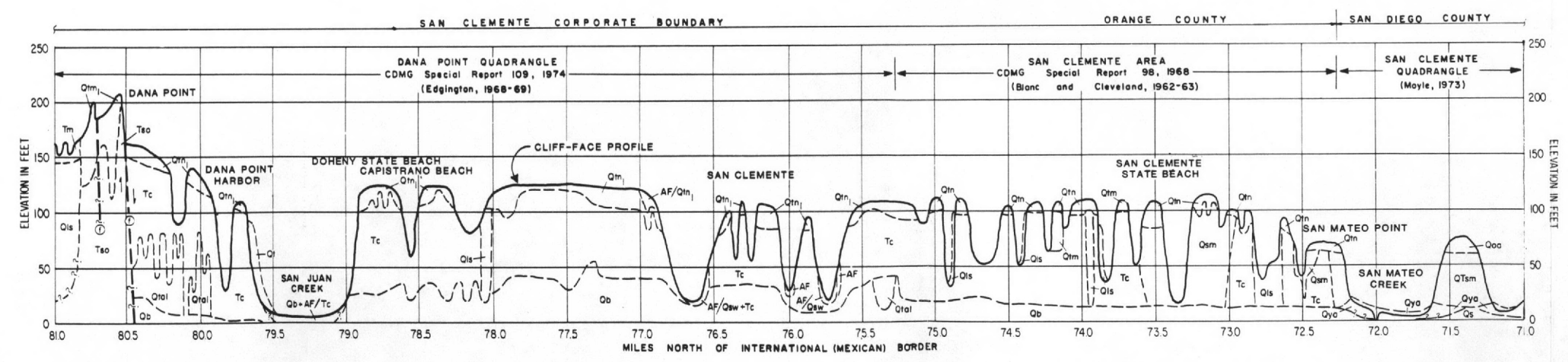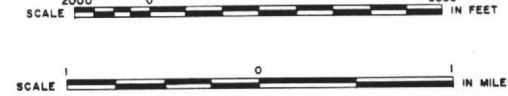COAST OF CALIFORNIA STORM AND TIDAL WAVES STUDY

DANA POINT TO MEXICAN BORDER

GEOLOGY
OF THE
COASTAL ZONE
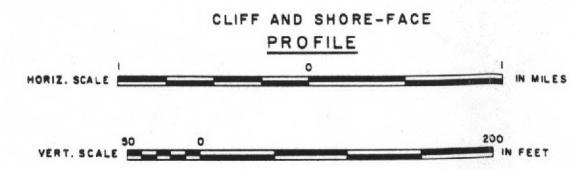
SANTA MARGARITA RIVER (MI. 58.0) TO SAN ONOFRE (MI. 70.5)

U. S. ARMY CORPS OF ENGINEERS
LOS ANGELES DISTRICT

PLATE 5

PLAN

SCALE 2000 0 8000 IN FEET

SCALE 1 0 IN MILES

SAN CLEMENTE CORPORATE BOUNDARY   ORANGE COUNTY   SAN DIEGO COUNTY

DANA POINT QUADRANGLE
CDMG Special Report 109, 1974
(Edgington, 1968-69)

SAN CLEMENTE AREA
CDMG Special Report 98, 1968
(Blanc and Cleveland, 1962-63)

SAN CLEMENTE
QUADRANGLE
(Moyle, 1973)

MILES NORTH OF INTERNATIONAL (MEXICAN) BORDER

LEGEND

——— BEACH PROFILE ONLY

········· BEACH PROFILE PLUS SEDIMENT SAMPLING

× OFFSHORE SEDIMENT STAKE

⊕ WAVE GAGE

△ RIVER SAMPLE

● BEACH SAMPLE

■ SHELF SAMPLE

CLIFF AND SHORE-FACE
PROFILE

HORIZ. SCALE 1 0 IN MILES

VERT. SCALE 50 0 200 IN FEET

NOTE:
SEE PLATE 7 (SHEETS 1 AND 2) FOR EXPLANATION
OF GEOLOGIC SYMBOLS AND NOMENCLATURE.

COAST OF CALIFORNIA STORM AND TIDAL WAVES STUDY

DANA POINT TO MEXICAN BORDER

GEOLOGY
OF THE
COASTAL ZONE

SAN ONOFRE (MI. 70.5) TO DANA POINT (MI. 80.5)

U. S. ARMY CORPS OF ENGINEERS
LOS ANGELES DISTRICT

PLATE 8